

**Efforts towards the Macrocyclic Core of Marineosin A and
Development of Pyrrolidine-Based Scaffolds for Diversity-Oriented Synthesis**

by

Rachel A. Perez

Bachelor of Science, Azusa Pacific University, 2006

Submitted to the Graduate Faculty of
The Kenneth P. Dietrich School of
Arts and Sciences in partial fulfillment
of the requirements for the degree of
Doctor of Philosophy

University of Pittsburgh

2015

UNIVERSITY OF PITTSBURGH

Dietrich School of Arts and Sciences

This dissertation was presented

by

Rachel A. Perez

It was defended on

May 13th, 2015

and approved by

Craig S. Wilcox, Professor, Department of Chemistry

W. Seth Horne, Assistant Professor, Department of Chemistry

Barry Gold, Professor and Chair, Department of Pharmaceutical Sciences

Dissertation Advisor: Scott G. Nelson, Professor, Department of Chemistry

Copyright © by Rachel A. Perez

2015

**Efforts towards the Macrocyclic Core of Marineosin A and
Development of Pyrrolidine-Based Scaffolds for Diversity-Oriented Synthesis**

Rachel A. Perez, PhD

University of Pittsburgh, 2015

The total synthesis of marineosin A, a unique spiroaminal with selective cytotoxicity, has been under investigation in our laboratory. A ruthenium-catalyzed enolate allylic alkylation methodology and azafulvene dimer-derived metathesis strategy have been considered as potential routes, towards the synthesis of the macrocyclic core of marineosin A.

A novel route to the synthesis of diverse pyrrolidine scaffolds, for diversity-oriented synthesis has additionally been under investigation in our laboratory. The synthetic route encompasses a series of reductive amination, iodocyclization, azide substitution, and reductive deprotection to deliver the target diamine scaffolds in 14-16% yield. In addition, an asymmetric approach to the synthesis of (2*S*,3*R*,4*R*)- β -iodo amine has been presented, which takes advantage of selective Ru(II)-catalyzed Claisen rearrangement methodology.

TABLE OF CONTENTS

1.0	INTRODUCTION.....	1
1.1	BIOLOGICAL ACTIVITY AND STRUCTURAL FEATURES.....	1
1.2	PREVIOUS EFFORTS DIRECTED TOWARDS THE TOTAL SYNTHESIS OF MARINEOSINS A AND B	3
	1.2.1 Evaluation of Proposed Biosyntheses	4
	1.2.2 Synthetic Strategies of Modeled Compounds	9
2.0	EFFORTS DIRECTED TOWARDS THE MACROCYCLIC CORE OF MARINEOSIN A	14
	2.1 LIMITATIONS OF PREVIOUS STRATEGIES.....	14
	2.2 EFFORTS UTILIZING ENOLATE ALLYLIC ALKYLATION	14
	2.2.1 Retrosynthetic Analysis.....	14
	2.2.2 Ruthenium-Catalyzed Enolate Allylic Alkylation	15
	2.3 EFFORTS UTILIZING AZAFULVENE DIMER METATHESIS.....	22
	2.3.1 Retrosynthetic Analysis.....	22
	2.3.2 Azafulvene Dimer Derived Metathesis	23
	2.4 CONCLUSIONS	29
3.0	INTRODUCTION.....	30

3.1	DIVERSITY-ORIENTED SYNTHESIS OF NATURAL PRODUCT-LIKE STRUCTURES	30
3.2	PREVIOUS APPLICATIONS OF 1, 3-CYCLOADDITION REACTIONS FOR REGIO- AND STEREO-SPECIFIC FORMATION OF PYRROLIDINES.....	32
3.3	SYNTHESIS OF FUSED PYRROLIDINE-HYBRID LIBRARIES	36
4.0	DEVELOPMENT OF PYRROLIDINE SCAFFOLDS FOR DIVERSITY-ORIENTED SYNTHESIS BY CLAISEN REARRANGEMENT OF ALLYL VINYL ETHERS	40
4.1	LIMITATIONS OF PREVIOUS STRATEGIES	40
4.2	RETROSYNTHETIC ANALYSIS OF FUNCTIONALIZED PYRROLIDINE SCAFFOLDS	41
4.3	SYNTHESIS OF A GENERAL PYRROLIDINE SCAFFOLD FOR DIVERSIFICATION	42
4.3.1	Formation of Claisen Products from Simple Allyl Vinyl Ethers.....	42
4.3.2	Formation of Pyrrolidines from Claisen Products	43
4.4	DIVERSITY BY INCORPORATION OF C ₃ SUBSTITUTION.....	48
4.5	ASYMMETRIC SYNTHESIS OF β -IODO PYRROLIDINE SCAFFOLD	53
4.6	CONCLUSIONS	55
5.0	EXPERIMENTAL	56
5.1	EFFORTS TOWARDS THE SYNTHESIS OF MARINEOSIN A	57
5.2	DEVELOPMENT OF PYRROLIDINE SCAFFOLDS FOR DIVERSITY-ORIENTED SYNTHESIS	65
	APPENDIX A	91

APPENDIX B	98
BIBLIOGRAPHY	107

LIST OF TABLES

Table 1. Enyne metathesis approach to marineosin macrocycle	26
Table 2. Relay-ring closing metathesis approach	27
Table 3. Exploration of dipolarophile reactivity with Schreiber's catalyst	37
Table 4. Cyclization conditions with various electrophilic iodine sources	45
Table 5. Iridium catalyzed isomerization of bis(allyl) ethers 211-216.....	51
Table 6. Synthesis of C ₃ substituted diamines	53
Table 7. Crystallographic Information for Compound 89	92
Table 8. Atomic coordinates and equivalent isotropic displacement parameters (Å ²) for 89	92
Table 9. Bond lengths [Å] and angles [°] for 89.....	93
Table 10. Anisotropic atomic displacement parameters (Å ²) for 89	96
Table 11. Hydrogen atomic coordinates and isotropic atomic displacement parameters (Å ²) for 89.....	97
Table 12. Crystallographic Information for Compound 194	99
Table 13. Atomic coordinates and equivalent isotropic displacement parameters (Å ²) for 194	100
Table 14. Bond lengths [Å] and angles [°] for 194.....	101
Table 15. Anisotropic atomic displacement parameters (Å ²) for 194	105

Table 16. Hydrogen atomic coordinates and isotropic atomic displacement parameters (\AA^2) for 194.....	106
---	-----

LIST OF FIGURES

Figure 1. Representative structures of natural products isolated from marine actinomycetes	2
Figure 2. Structures of marineosins A (4) and B (5) and undecylprodigiosin (6)	3
Figure 3. Fenical's proposed biosynthesis	5
Figure 4. Synthesized spiroiminal stereoisomers.....	10
Figure 5. Lindsley's key retrosynthetic fragments	11
Figure 6. X-ray crystal structure of 89.....	20
Figure 7. Sources of skeletally diverse small molecules	30
Figure 8. Proposed transition state of Co (II)/ephedrine ligand.....	33
Figure 9. Application of Jørgensen's $Zn(OTf)_2/t\text{-BuBOX}^a$ and Zhang's $AgOAc/xylyl\text{-FAP}^b$ systems to development of pyrrolidine libraries	36
Figure 10. Proposed transition state of Ag(I)/QUINAP catalyst	38
Figure 11. Thermal Claisen rearrangement of general allyl vinyl ether (174)	43
Figure 12. X-ray crystal structure of aziridinium 194	48
Figure 13. Asymmetric Ru (II)-catalyzed [3,3]-sigmatropic rearrangement of general allyl vinyl ether (174).....	54
Figure 14. X-ray crystal structure of 89.....	91

Figure 15. X-ray crystal structure of 194..... 98

LIST OF SCHEMES

Scheme 1. Lindsley's retrosynthetic analysis	5
Scheme 2. Synthesis of C ₁₀ -C ₂₃ fragment.....	6
Scheme 3. Failed synthesis of spiro-tetrahydropyran-dihydropyrrole aminal core 10.....	7
Scheme 4. Snider's retrosynthetic analysis.....	8
Scheme 5. Synthesis of model spiroiminals	8
Scheme 6. Shi's retrosynthetic analysis of spiroiminal fragment.....	9
Scheme 7. Synthesis of model spiroaminal lactam.....	10
Scheme 8. Synthesis of key intermediate 39	12
Scheme 9. Synthesis of model spiroiminal and macrocyclic fragments.....	13
Scheme 10. Proposed retrosynthetic analyses of marineosin A	15
Scheme 11. Ruthenium-catalyzed enolate alkylation of 56 and 61	16
Scheme 12. Forward synthetic route to model substrate 68	18
Scheme 13. Synthesis of diacetates 80 and 84.....	19
Scheme 14. Possible mechanism for the formation of 89.....	21
Scheme 15. Proposed retrosynthetic analyses of marineosin A	22
Scheme 16. Retrosynthetic analysis using azafulvene dimer	23
Scheme 17. Optimized synthesis of iodoalkyne 108	24

Scheme 18. Synthesis of enyne substrate 114	25
Scheme 19. Synthesis of relay-ring closing substrate 122.....	27
Scheme 20. Ring-closing metathesis approach.....	28
Scheme 21. [3+2] cycloaddition of N-metalated azomethine ylide with electron deficient alkenes	32
Scheme 22. Synthesis of fused-pyrrolidine hybrid libraries	39
Scheme 23. Retrosynthetic analysis of racemic pyrrolidine scaffolds	42
Scheme 24. Synthesis of γ,δ -unsaturated aldehyde	43
Scheme 25. Synthesis of γ,δ -unsaturated amides and amines	44
Scheme 26. Proposed mechanism of iodoamination of 185	46
Scheme 27. Synthesis β -azido amine 192 and diamine 196.....	47
Scheme 28. Preparation of allylic alcohols.....	49
Scheme 29. Iridium-catalyzed deallylation.....	51
Scheme 30. Synthesis of β -iodo amine 253	55

LIST OF ABBREVIATIONS

Acac	Acetylacetonate
BICP	Bis(diphenylphosphino)-dicyclopentane
BINAP	2,2'-Bis(diphenylphosphino)-1,1'-binaphthyl
Boc	<i>tert</i> -Butoxycarbonyl
BOX	Bisoxazoline
Cbz	Carboxybenzyl
CDI	1,1'-Carbonyldiimidazole
COE	Cyclooctene
Cp	Cyclopentadienyl
Cp*	Pentamethylcyclopentadienyl
DBFOX	Dibenzofuranyl-2,2'-bisoxazoline
DBU	1,8-Diazabicyclo[5.4.0]undec-7-ene
DDQ	2,3-Dichloro-5,6-dicyano-1,4-benzoquinone
DIBAL	Diisobutylaluminium hydride
DIC	<i>N,N'</i> -Diisopropylcarbodiimide
DMAP	4-Dimethylaminopyridine
DMP	Dess–Martin periodinane

DMS Dimethyl sulfide
 DOS Diversity-oriented synthesis
 EDC 1-Ethyl-3-(3-dimethylaminopropyl)carbodiimide
 HMDS Hexamethyldisilazane
 HOBt *N*-Hydroxybenzotriazole
 ImH Imidazole
 MDM2 Murine double minute oncogene
 NIS *N*-iodosuccinimide
 NMO *N*-Methylmorpholine *N*-oxide
 NMP *N*-Methyl-2-pyrrolidone
 Piv Pivalate
 PyBOP Benzotriazol-1-yl-oxytripyrrolidinophosphonium hexafluorophosphate
 QUINAP 1-(2-Diphenylphosphino-1-naphthyl)isoquinoline
 TBHP *tert*-Butyl hydroperoxide
 TBS *tert*-Butyldimethylsilyl
 TES Triethylsilyl
 TFA Trifluoroacetic acid
 TIPS Triisopropylsilyl
 TMS Trimethylsilyl
 TMS_q (Trimethylsilyl)quinine
 TPAP Tetrapropylammonium perruthenate
 Ts Tosyl
 xylyl-FAP 3,5-Dimethylphenyl bis-ferrocenyl amide phosphine

1.0 INTRODUCTION

1.1 BIOLOGICAL ACTIVITY AND STRUCTURAL FEATURES

Terrestrial bacteria within the order Actinomycetales have historically demonstrated a prolific ability to generate thousands of small molecule natural products. These compounds from terrestrial sources have included clinically useful antibiotics, anticancer agents and immunosuppressive agents.¹ Amongst the most useful soil-derived genera, *Streptomyces* and *Micromonospora* account for the vast majority of microbial antibiotics discovered.² Although the genus *Streptomyces* is generally associated with terrestrial soils, marine soil bacteria that require seawater for growth have become increasingly important sources of novel secondary metabolites. These marine actinomycetes that display distinct phylotypes, are unrelated to strains previously discovered on land or in the sea. Targeted screening has revealed secondary metabolites such as marinomycin A (**1**), marinone (**2**) and salinosporamide C (**3**) with substantial activities against selected human tumors and drug-resistant bacterial pathogens (Figure 1).^{3,4,5}

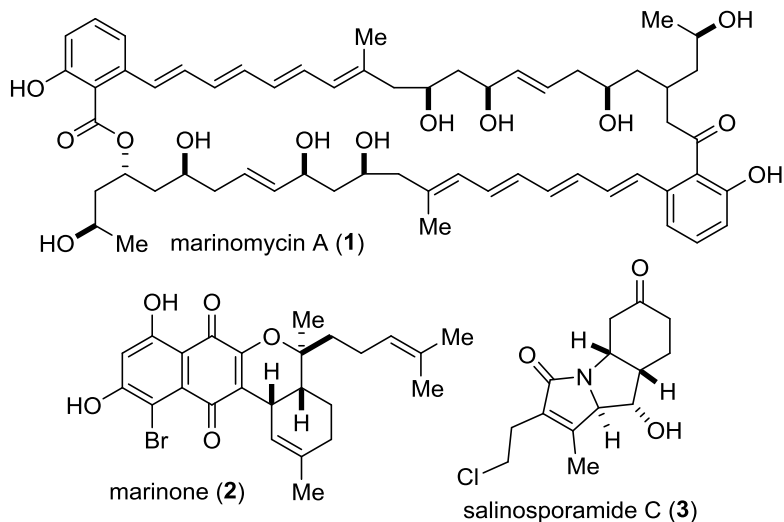


Figure 1. Representative structures of natural products isolated from marine actinomycetes

Marineosins A and B (**4, 5**), are two novel compounds originally isolated from cultures of sediment-derived marine actinomycetes, related to the genus *Streptomyces* (Figure 2).⁶ These unique spiroaminals were first identified by Fenical and coworkers in 2008. Biosynthetically, **4** and **5** are thought to have derived from a prodigiosin-like class of bacterial pigments. These features are highlighted by the presence of a bis-pyrrole functionality typified by undecylprodigiosin (**6**). However, the spiro-tetrahydropyran-dihydropyrrole aminal ring systems of the marineosins is unprecedented and believed to arise from a modification within the pigment pathway.⁷ Structurally, marineosin A (**4**) and B (**5**) differ at both C₇ and C₈ stereocenters, a feature which results in substantially different cytotoxic activities. The major isomer, marineosin A (**4**) displayed inhibition of human colon carcinoma HCT-116 with an IC₅₀ of 0.5 μM. In contrast, marineosin B (**5**) displays considerably weaker cytotoxicity with an IC₅₀ of 46 μM. Furthermore, testing of marineosin A (**4**) in a NCI 60 cell line panel indicated a broad cytotoxicity with selectivity against melanoma and leukemia cell lines (Figure 2).^{6,8,9}

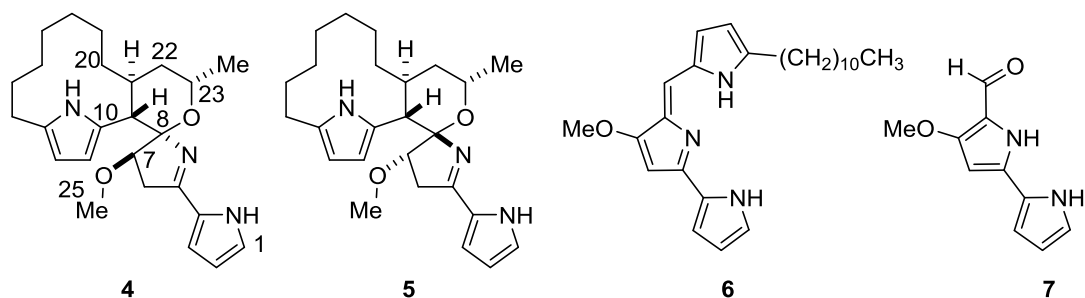


Figure 2. Structures of marineosins A (**4**) and B (**5**) and undecylprodigiosin (**6**)

Fenical and co-workers have also proposed a possible biosynthesis of **4** and **5**. The envisioned route involves known 4-methoxy-2,2'-bipyrrole-5-carbaldehyde (**7**), a key intermediate in the biosynthetic pathway of prodigiosin-like pigments, and relies on a potential inverse-electron-demand hetero-Diels-Alder cycloaddition to deliver the core marineosin structure (Figure 3).⁶ An alternative biosynthesis of the marineosins has additionally been proposed by Snider based on sequencing data of the gene cluster responsible for the biosynthesis of undecylprodigiosin (**6**) in *Streptomyces coelicolor*.¹⁰ The alternative route takes advantage of nonheme iron-dependent dioxygenases to initiate and sequester radicals throughout the pathway (Figure 2).⁹

1.2 PREVIOUS EFFORTS DIRECTED TOWARDS THE TOTAL SYNTHESIS OF MARINEOSINS A AND B

The biomimetic syntheses initially proposed by Fenical and Snider, have recently been evaluated. These preliminary efforts have focused primarily on key transformations en route to marineosins A (**4**) and B (**5**). More recently, Lindsley and Shi have investigated synthetic

strategies based upon model systems of the 12-membered macrocyclic core and spiroiminal fragments of these natural products.^{11,12,13}

1.2.1 Evaluation of Proposed Biosyntheses

Fenical's proposal shown in Figure 3, centers on the conversion of **9** to **10** via an intramolecular hetero-Diels-Alder reaction to simultaneously form both the dihydropyran ring and spiroaminal functionality. The hypothesized biosynthetic C₁-C₂₅ Diels-Alder substrate (**9**) was thought to result from a direct condensation of C₁-C₉ 4-methoxy-2, 2'-bipyrrole-5-carbaldehyde (**7**) and the enone containing C₁₀- C₂₄ pyrrole **8**. Common to the biosynthetic pathway of prodigiosins, bipyrrole **7** has previously been demonstrated through feeding studies to be derived from proline, serine, glycine and several additional acetate subunits. Similar to Fenical's proposal the known biosynthesis of prodigiosins is convergent often involving late-stage condensation with substituted pyrroles. A diastereomeric mixture of **4** and **5** can therefore be explained by visualizing the ensuing cyclization occurring from above and below the plane of enone **9**.⁶ A detailed account of subsequent steps towards the total synthesis of marineosin A and B have not been previously reported.

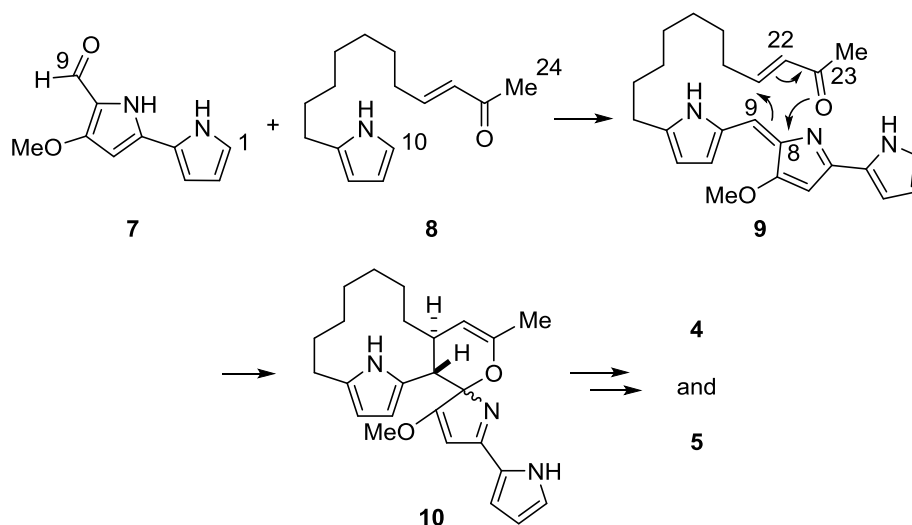
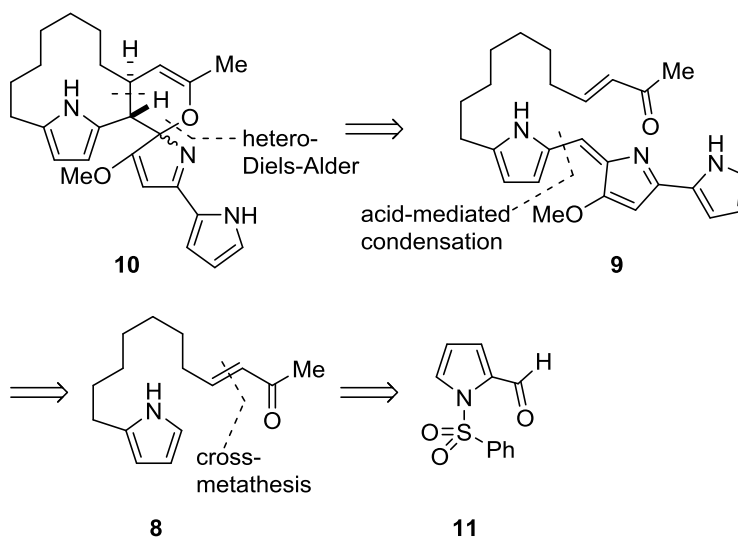


Figure 3. Fenical's proposed biosynthesis

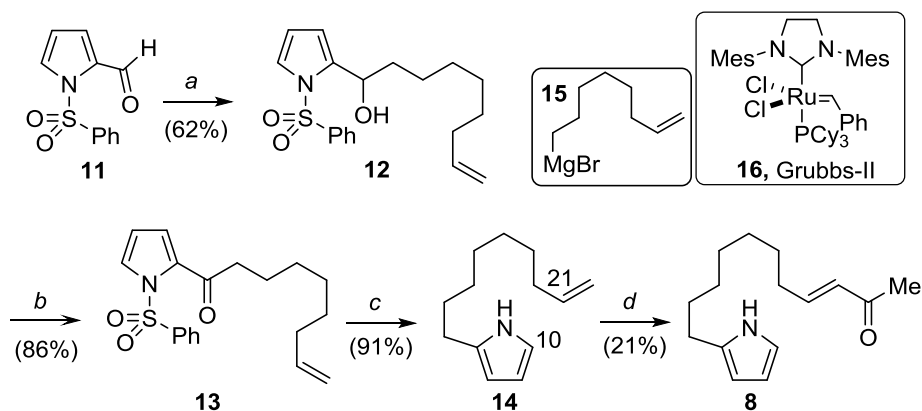
In order to investigate this proposed biosynthesis, Lindsley and coworkers further developed a retrosynthetic analysis based upon Fenical's design. The analysis commences with a hetero-Diels-Alder cycloaddition to generate **10**, followed by acid-mediated condensation of bipyrrole **7** with enone **8**.^{14, 15} Cross metathesis with methyl vinyl ketone provides enone **8**, previously synthesized directly from pyrrole-2-carboxaldehyde **11** (Scheme 1).¹⁶

Scheme 1. Lindsley's retrosynthetic analysis



The three step sequence to enone **8**, as detailed in Scheme 2, involved Grignard **15** addition to 1-(phenylsulfonyl)-1H-pyrrole-2-carbaldehyde (**11**), providing secondary alcohol **12**. Ley oxidation to ketone **13** followed by a one-pot addition, rearrangement, deoxygenation and elimination cascade developed by Muchowski afforded intermediate **14**.¹⁶ Notably, application of Muchowski's one-pot cascade was only pursued after preliminary disconnection pathways involving both sp^2 - sp^3 Suzuki couplings and S_N^2 reactions with 2-pyrrole organometallics (Li or $B(OH)_2$) failed to provide **14**. Similarly, S_N^2 disconnection pathways involving organometallic reagents and primary bromo- or mesyl- substituted pyrroles failed.⁸

Scheme 2. Synthesis of C_{10} - C_{23} fragment



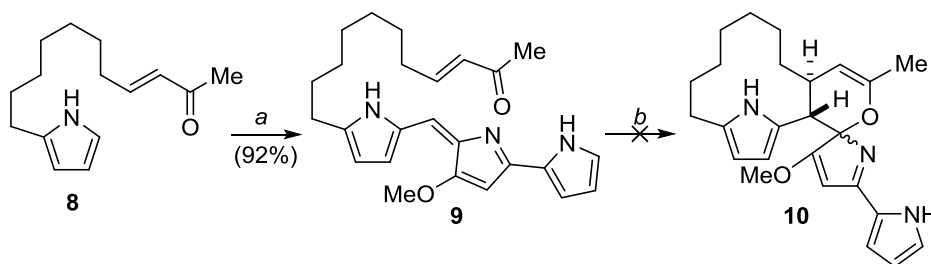
a) **15**, THF, 0 °C to rt. b) TPAP, NMO, CH_2Cl_2 , 4 h, rt. c) $NaBH_4$, *i*-PrOH, 24 h, 82 °C. d) 0.5 mol % Grubbs-II (**16**), CH_2Cl_2 , 12 h, 25 °C. NMO = *N*-methylmorpholine-*N*-oxide, TPAP = tetrapropylammonium perruthenate.

Completion of the enone fragment under standard cross-metathesis conditions with 0.5 mol % Grubbs-II (**16**) and methyl vinyl ketone provided **8** as a minor product in 21% yield. Interestingly, the major reaction pathway underwent Grubbs-II (**16**) catalyzed nucleophilic conjugate addition of **14** (at C_{10}) with methyl vinyl ketone. Further experimentation revealed the reaction to be general with respect to both electron rich pyrroles and acyclic Michael acceptors.

However, increasing catalyst loading from 0.5 to 30 mol % and reducing reaction temperature permitted the further isolation of cross-metathesis product **8** in 40% yield.⁸

Acid-mediated condensation of the resulting enone **8** with bipyrrole **7**, previously synthesized via literature protocol, generated the acyclic Diels-Alder substrate **9**. As shown in Scheme 3, the proposed biomimetic Diels-Alder reaction of **9** to deliver the desired spiro-fused aminal core (**10**) was unsuccessful despite the exploration of various reaction conditions. Further molecular modeling studies revealed a large degree of flexibility present in the alkyl linker moiety, indicating an intramolecular Diels-Alder mechanism is likely energetically disfavored.⁸

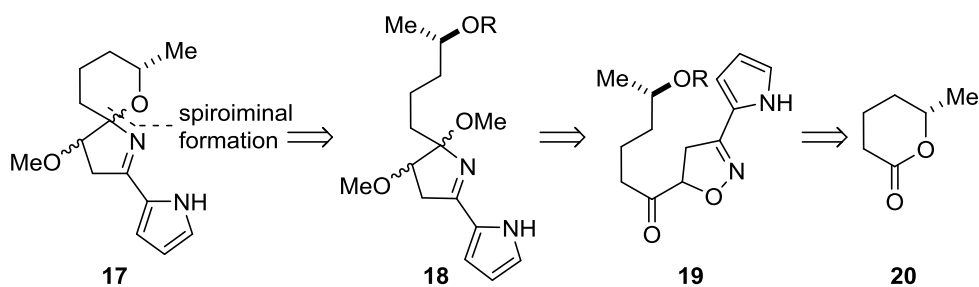
Scheme 3. Failed synthesis of spiro-tetrahydropyran-dihydropyrrole aminal core **10**



a) **7**, 0.87 M HCl, MeOH than NH₄OH. b) Reaction conditions = heat, microwave, photochemical, Lewis acid catalysis, mineral acid catalysis, solvent, and additives.

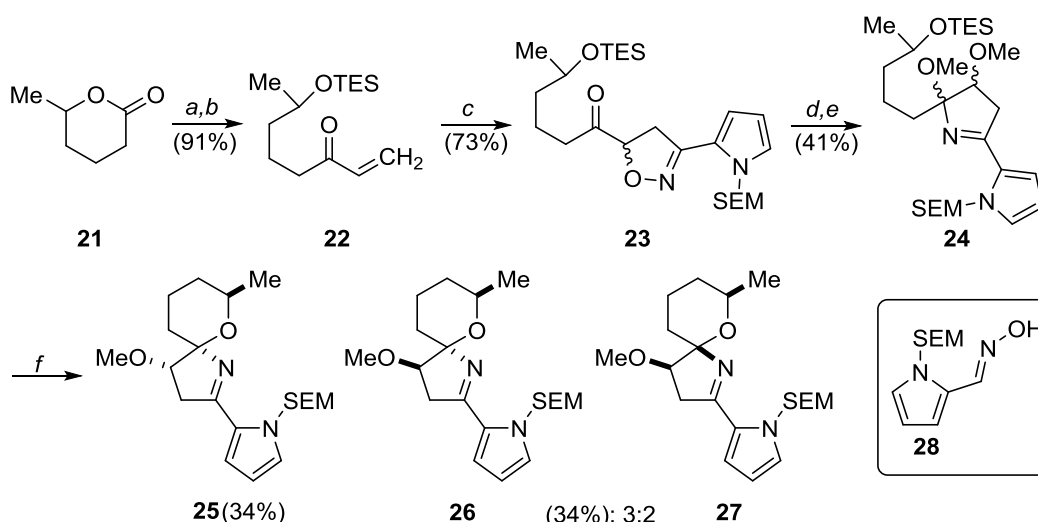
Snider's biosynthetic efforts have focused mainly on the generation of a model system for the unprecedented spiroiminal fragment. The retrosynthetic analysis attempts to mimic an alternative biological pathway, previously suggested to involve the participation of several nonheme iron-dependent dioxygenases. As displayed in Scheme 4, the key disconnection results from simultaneous spiroiminal and tetrahydropyran ring formation from intermediate **18**. Synthesis of intermediate **18** was believed to proceed via stepwise hydrogenolysis of the N-O bond followed by *O*-methylation of isoxazoline **19**. Furthermore, the synthesis of **19** was envisioned to proceed through a series of addition, protection, and *N*-oxide cycloaddition of lactone **20**.⁹

Scheme 4. Snider's retrosynthetic analysis



To investigate this sequence, model lactone **21** which lacks the macrocyclic ring of **4** was selected (Scheme 5). A series of vinyl addition, secondary alcohol protection, followed by *N*-oxide cycloaddition with the derivative of 1-SEM-pyrrole-2-carboxaldehyde oxime (**28**) resulted in the formation of isoxazoline **23**. Hydrogenolysis of the N-O bond over Raney nickel followed by methylation produced the spiroiminal precursor **24**. Treatment of **24** with 2 M aqueous hydrochloric acid hydrolyzed the triethylsilyl ether with a net loss of methanol, forming **25** in 35% yield, along with an inseparable 3:2 mixture of **26** and **27**.⁹

Scheme 5. Synthesis of model spiroiminals

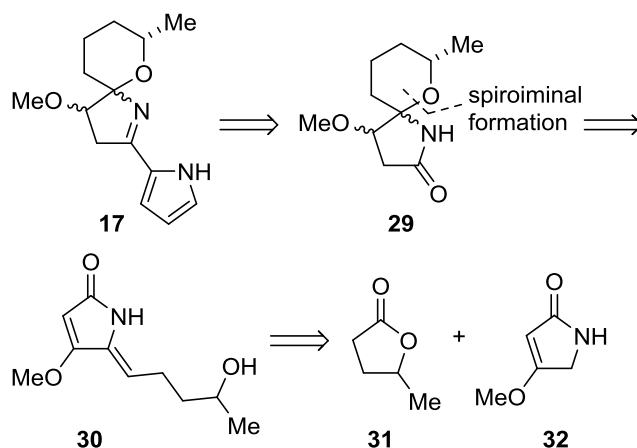


a) vinylmagnesium bromide, THF. b) TESCl, Et₃N, DMAP, THF. c) **28**, 5% aqueous NaOCl, CH₂Cl₂. d) Raney Ni 2800, H₂, MeOH. e) NaH, MeI, THF, 25 °C. f) 2 M aqueous HCl, 1:3 THF/CH₃CN. TESCl = chlorotriethylsilane, DMAP = 4-(dimethylamino)pyridine.

1.2.2 Synthetic Strategies of Modeled Compounds

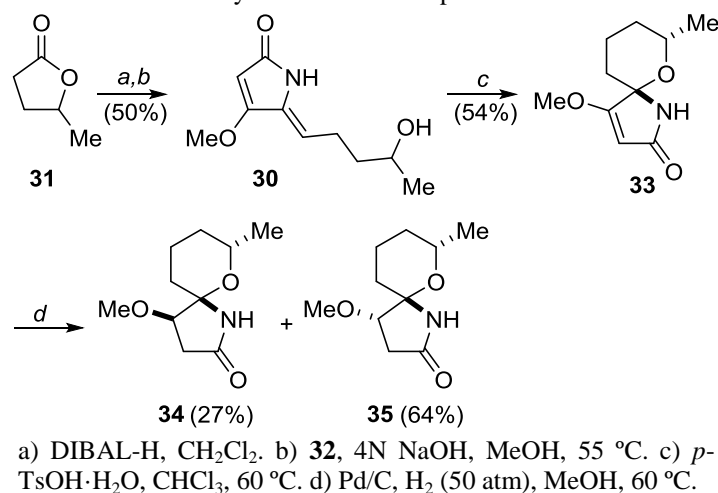
Synthetic approaches based on the formation of model systems of the macrocyclic core and spiroiminal fragments of marineosins A and B (**4**, **5**), have recently been reported by Lindsley and Shi.^{13,12} Shi's retrosynthetic analysis indicated in Scheme 6, targets the spiroiminal fragment of marineosins A and B (**4**, **5**). This approach relies on the late installation of the sensitive pyrrole ring via a Vilsmeier-Haack type reaction to afford **17**. Spiroiminal formation was envisioned to occur through acid-catalyzed *N*-acyliminium ion cyclization of **30**, prepared from commercially available reagents **31** and **32**.¹³

Scheme 6. Shi's retrosynthetic analysis of spiroiminal fragment



A finalized synthesis of spiroaminal lactams **34** and **35** is displayed in Scheme 7. The route commences with DIBAL-H reduction of γ -valerolactone (**31**), followed by treatment of the resulting hemiacetal with 4-methoxy-3-pyrrolin-2-one (**32**) and 4N NaOH in MeOH to give **30**. Cyclization was achieved utilizing *p*-TsOH·H₂O to afford **33**, followed by hydrogenation to yield isomers **34** and **35** in 27% and 64% yield respectively.¹³

Scheme 7. Synthesis of model spiroaminal lactam



Final installation of the pyrrole ring involving a Tf₂O mediated Vilsmeier-Haack type reaction, resulted in the formation of three spiroiminal stereoisomers (Figure 4). Unfortunately, the stereochemistry of both synthetic targets was unrealized. In the case of marineosin B (**5**), isomer **37** reflects the desired stereochemistry, however **36** and **38** are unnatural products. However, the authors contribute a degree of stability to the presence of the fused macrocyclic ring in the natural product, making the desired stereochemistry of marineosin A (**4**) more favorable.¹³

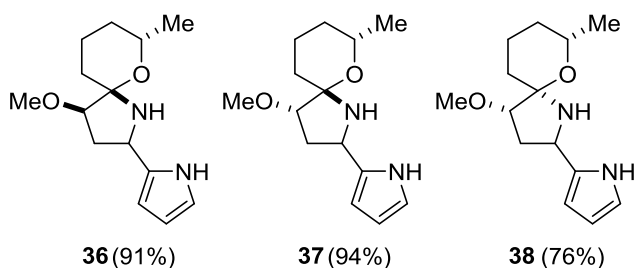


Figure 4. Synthesized spiroiminal stereoisomers

Similarly, Lindsley has recently focused on the synthesis of the model spiroiminal structure **41** and macrocyclic fragment **40** (Figure 5). The retrosynthetic analysis hinges on the formation of **39**, which is utilized as an intermediate en route to **40** and **41**. Synthesis of key

intermediate **39** commenced with an aldol reaction under Crimmins' conditions to deliver Evans' *syn* product **44**, from aldehyde **42** and **43**. Hydrolysis of the auxiliary followed by TIPS protection, hydroxyl-directed epoxidation, benzyl protection of the secondary alcohol, and PMB deprotection resulted in the formation of **45** in 14% yield over 5 steps. Finally, directed opening of the epoxide with Red-Al, protection of the primary hydroxyl group and conversion of the secondary alcohol to methyl ether afforded key intermediate **39** (Scheme 8).¹²

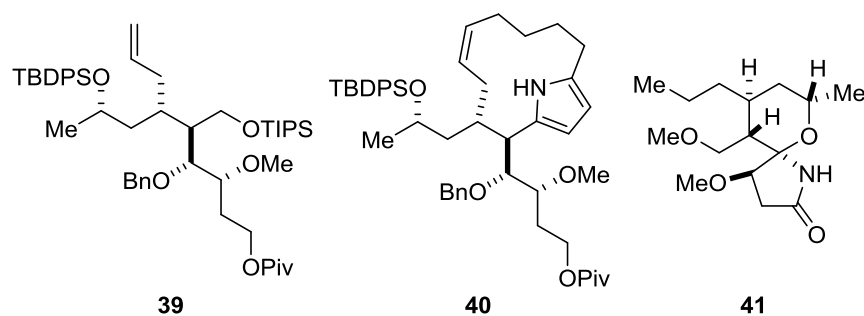
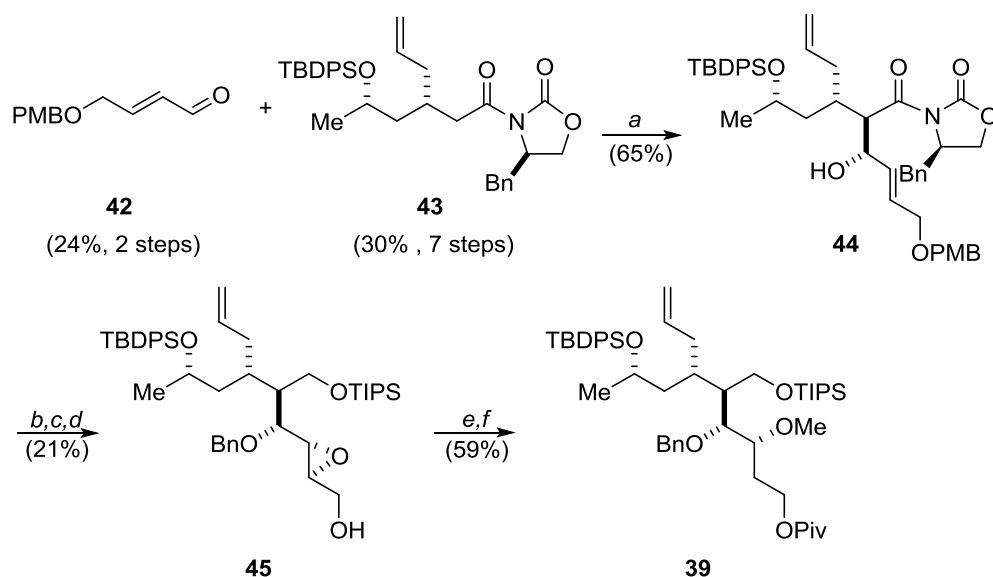


Figure 5. Lindsley's key retrosynthetic fragments

Access to the model spiroiminal of marineosins A and B (**4**, **5**) from intermediate **39** was initiated by a sequence of reductive deprotection of pivalate followed by oxidation of the resulting alcohol to aldehyde, Pinnick oxidation to the corresponding carboxylic acid and final coupling with ammonium chloride to provide amide **47**. Hydrogenolysis of the benzyl ether and hydrogenation of the olefin, followed by oxidation of the resulting secondary alcohol and acid mediated cyclization resulted in the formation of **41** (Scheme 9, part a).¹²

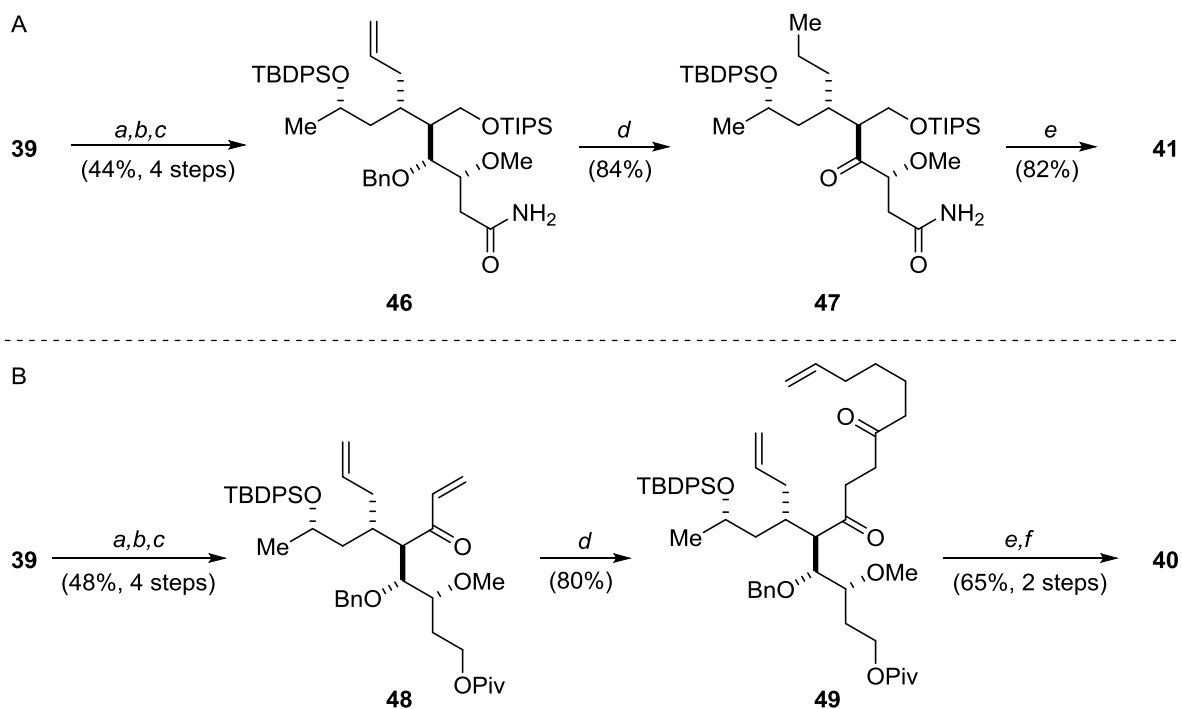
Scheme 8. Synthesis of key intermediate **39**



a) 1. TiCl_4 , DIPEA, NMP, CH_2Cl_2 ; 2. **42**, CH_2Cl_2 . b) 1. LiBH_4 , MeOH, THF; 2. TIPSCl, ImH, CH_2Cl_2 . c) $\text{VO}(\text{acac})_2$, TBHP, CH_2Cl_2 . d) 1. BnBr, NaH, TBAI, THF; 2. DDQ, CH_2Cl_2 , pH 7 phosphate buffer. e) Red-Al, THF. f) 1. PivCl, pyr, CH_2Cl_2 ; 2. Me_3OBF_4 , CH_2Cl_2 .

A synthesis of the macrocyclic fragment **40** commences with a sequence of TIPS deprotection, oxidation, vinyl Grignard addition and second oxidation to afford α , β -unsaturated ketone **48** (Scheme 9, part b). Stetter reaction of **48** with 6-heptenal afforded the RCM substrate **49**. A final ring closing metathesis of **49**, followed by microwave assisted pyrrole construction afforded target macrocycle **40** in 5.1% overall yield from (*S*)-propylene oxide.¹²

Scheme 9. Synthesis of model spiroiminal and macrocyclic fragments



Part A. a) DIBAL-H, CH₂Cl₂. b) SO₃-pyr, Et₃N, DMSO. c) 1. NaO₂Cl, NaH₂PO₄, 2-methyl-2-butene; 2. EDC, HOBt, NH₄Cl, DMF. d) 1. Pd/C, H₂, EtOAc; 2. TPAP, NMO, CH₂Cl₂. e) 0.01M HCl, MeOH. Part B. a) BF₃·OEt₂, CH₂Cl₂. b) SO₃-pyr, Et₃N, DMSO. c) 1. vinylmagnesium bromide, THF; 2. Dess-Martin periodinane, CH₂Cl₂. d) 6-Heptenal, Et₃N, thiazolium hydrochloride, 1, 4-dioxane. e) Grubbs I catalyst (30 mol %), CH₂Cl₂ (0.0005 M). f) NH₄OAc, MeOH, microwave irradiation.

2.0 EFFORTS DIRECTED TOWARDS THE MACROCYCLIC CORE OF MARINEOSIN A

2.1 LIMITATIONS OF PREVIOUS STRATEGIES

Previous syntheses performed by Lindsley and others, which target the spiroaminal and macrocyclic ring systems of marineosins A and B, have focused on the development of model systems. Additionally, biomimetic studies initiated by Fenical and Snider, have failed to generate the tetrahydropyran core and spiroiminal fragment of marineosins A and B. However, the cytotoxic activities and the unique structural aspects of marineosin A and B, continue to generate interest in these marine derived natural products. Therefore, a direct and efficient route towards the total synthesis of marineosins A and B is needed.

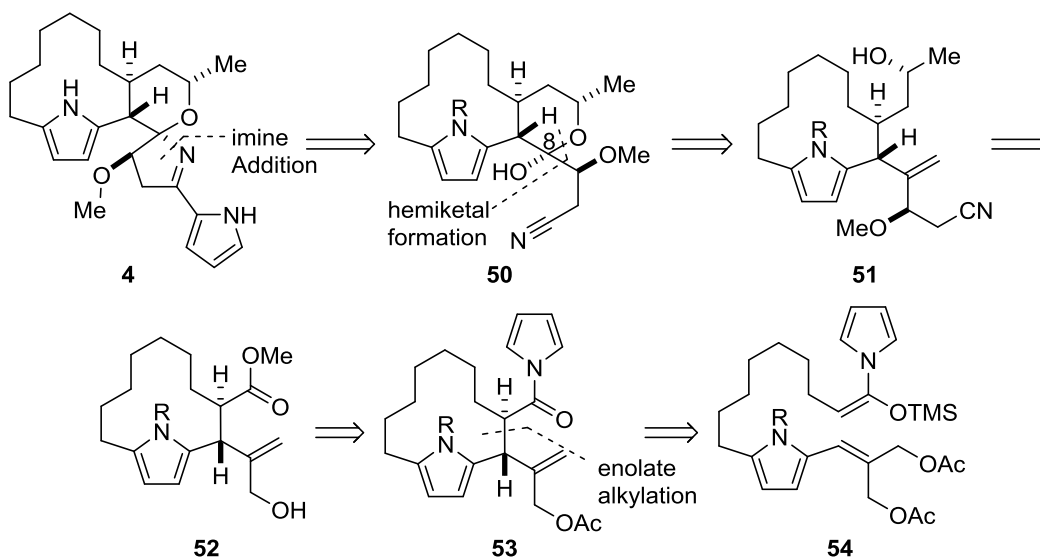
2.2 EFFORTS UTILIZING ENOLATE ALLYLIC ALKYLATION

2.2.1 Retrosynthetic Analysis

Our strategy features an intramolecular ruthenium-catalyzed enolate allylic alkylation of disubstituted allylic acetate **54**, resulting in the formation of product **53** containing the core of marineosin A (Scheme 10). The spiroiminal fragment of **4** was envisioned to be installed in two

subsequent steps. Addition of α -metalated pyrrole into the impending nitrile, followed by attack at C₈ by the resulting imine provides the first major disconnection. Ozonolysis of substrate **51**, results in hemiketal formation and construction of the pyran ring. We further planned a series global deprotection, oxidation, and asymmetric addition of cyanomethylzinc bromide to afford product **51**. With the major framework of the macrocycle to be constructed via an enolate allylic alkylation reaction of disubstituted allylic acetate **54**, we initially sought to generate model substrate **63** which lacked the C₁₄-C₁₉ fragment (Scheme 11).

Scheme 10. Proposed retrosynthetic analyses of marineosin A

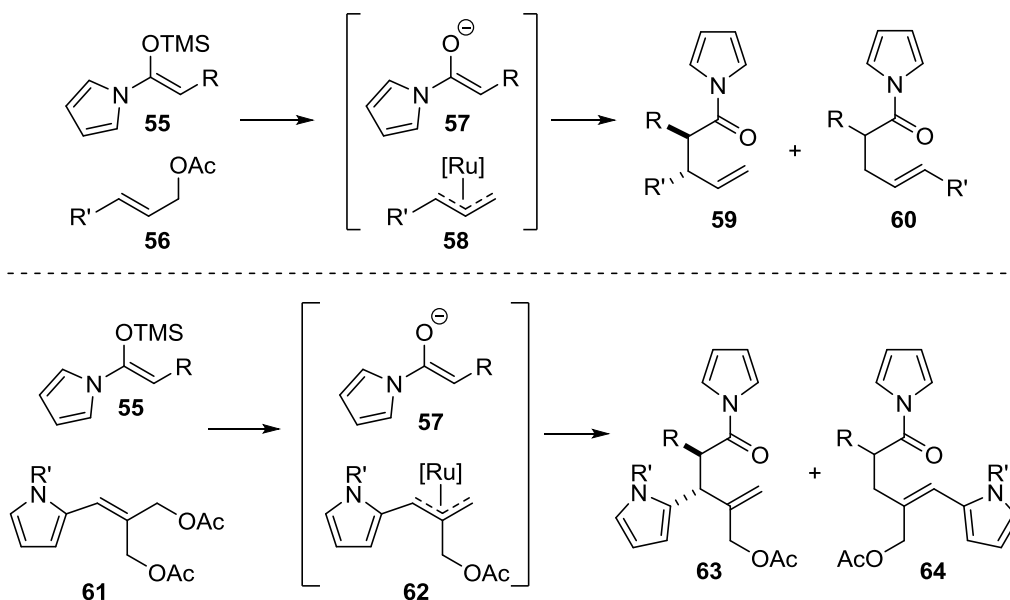


2.2.2 Ruthenium-Catalyzed Enolate Allylic Alkylation

An alternative route towards Claisen products of type **59** has previously been developed in our group, utilizing easily prepared pyrrole silyl enol ether **55**, and allylic acetate **56**.¹⁷ This ruthenium-catalyzed enolate allylic alkylation methodology provides similar C-C bond connections traditionally obtained from Claisen reactions, while maintaining high diastereo- and

enantioselectivity (Scheme 11). A mechanism for the transformation of **56** to **59** is believed to proceed via oxidative addition into the C-O σ -bond of allyl acetate **56**, followed by nucleophilic addition of silyl enol ether **57** to the resulting Ru-bound **58**. However, the extension of this methodology to disubstituted allylic acetates of type **61** as the pro-electrophile, and the application of this methodology to natural product synthesis is previously unexplored. An analogous mechanism leading to the formation of **63**, involves the oxidative addition of ruthenium into a single C-O σ -bond of allylic diacetate **61**. Nucleophilic addition of silyl enol ether **57** into the newly formed Ru-bound intermediate **62** is expected to result in the formation of **63** (Scheme 11).

Scheme 11. Ruthenium-catalyzed enolate alkylation of **56** and **61**

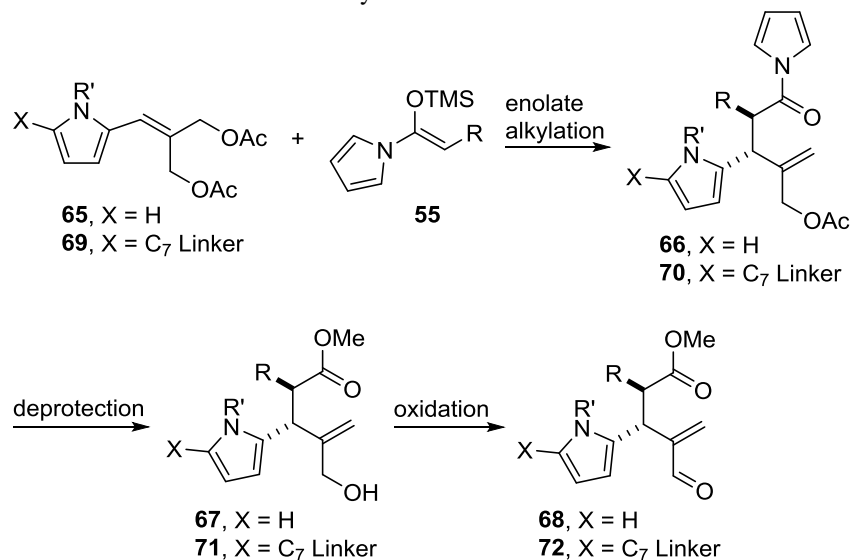


To investigate the applicability of the ruthenium-catalyzed enolate allylic alkylation methodology towards the synthesis of the core of marineosin A, we initially focused our efforts on the preparation of allylic diacetate **65**, which we planned to utilize in the reaction with pyrrole silyl enol ether **55** (Scheme 12). We chose to omit the C₁₄-C₁₉ linker, which would later

constitute the macrocyclic core during our initial studies, in order to probe the reactivity of the substrate. Completion of the synthesis of model substrate **68**, involves global deprotection of **66**, and subsequent oxidation of the resulting primary alcohol function of **67** (Scheme 12). Since the electronic properties of protecting groups are known to modulate pyrrole reactivity, we planned on implicating both benzyl and TIPS groups to test this effect. Additionally, both benzyl and TIPS groups are stable towards the planned deprotection and alcohol oxidation conditions (Scheme 12).

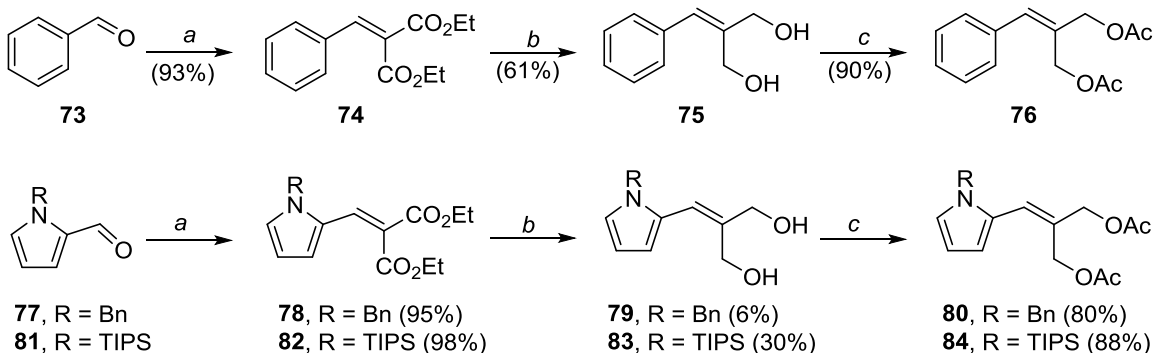
To begin our studies into the reactivity of allylic diacetates, we synthesized cinnamyl diacetate (**76**) as a precursor to the pyrrole derivative. Knoevenagel condensation of benzaldehyde (**73**) with diethylmalonate followed by DIBAL reduction and acylation afforded the pro-electrophile **76** in 51% yield over 3 steps (Scheme 13). Exposing cinnamyl diacetate (**76**) and pyrrole silyl enol ether **85** to 5 mol % of Ru(II) complex generated in situ through the reaction of $[\text{Cp}^*\text{Ru}(\text{CH}_3\text{CN})]\text{PF}_6$ with ligand **90**, in the presence of $\text{B}(\text{O}i\text{Pr})_3$ gave no reaction after 24 h.¹⁸ Additional reactions performed at 50 °C or using $[\text{CpRu}(\text{CH}_3\text{CN})_3]\text{PF}_6$ as an alternative catalyst gave no reaction after 48 h (eq 1).

Scheme 12. Forward synthetic route to model substrate **68**



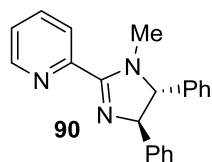
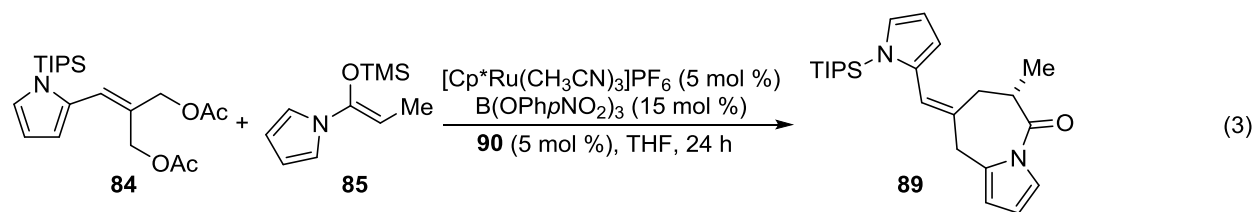
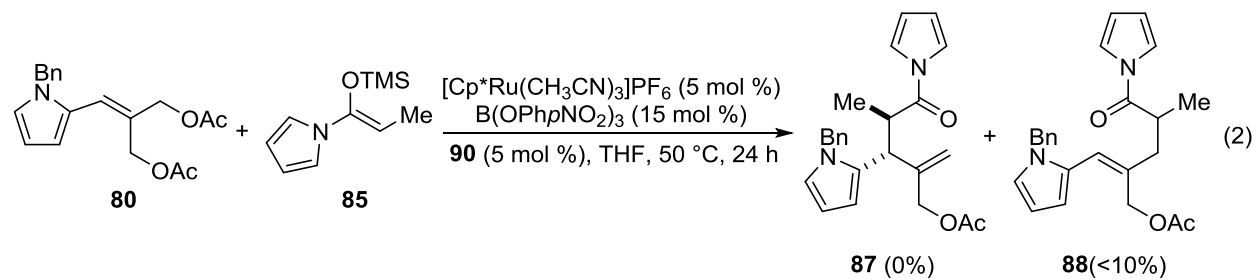
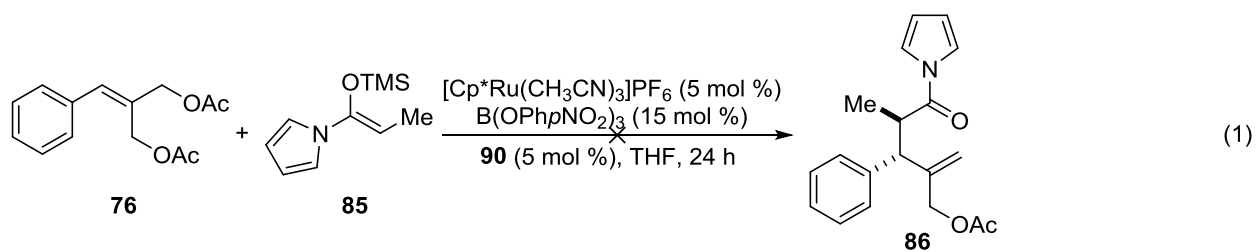
The inconclusive results obtained from our model system encouraged us to seek alternative substrates, to further investigate the application of this methodology. We next sought to directly synthesize diacetates **80** and **84**, which lack the C₁₄-C₁₉ linker (Scheme 13). Knoevenagel condensation of differentially protected pyrrole 2-carboxaldehydes **77** and **81** resulted in the formation of **78** and **82** in 95% and 98% yield. However, the reduction of **78** and **82** with DIBAL proceeded to 1, 4-reduction of the double bond as the dominant pathway. This may be attributed to the formation of a stabilized aluminum intermediate, which redirects hydride delivery. The competing 1, 2-reduction of **78** and **82** provided the desired products **79** and **83** in 6% and 30% yield, in 10 minutes at -78 °C. Acylation of the resulting diols delivered diacetates **80** and **84** in moderate yields of 80% and 88% (Scheme 13).

Scheme 13. Synthesis of diacetates **80** and **84**



a) diethyl malonate, piperidine, DMAP, 50 °C. b) DIBAL, CH₂Cl₂, -78 °C, 10 min. c) acetyl chloride, pyridine, THF, 0 °C. d) DMAP = 4-dimethylaminopyridine, DIBAL = diisobutylaluminium hydride.

To investigate the alkylation of *N*-protected pyrrole derivatives with silyl enol ethers, we next examined the reactions of diacetates **80** and **84**. Exposing *N*-benzylpyrrole allylic diacetate **80** and pyrrole silyl enol ether **85** to 5 mol % of Ru(II) complex generated in situ from [Cp**Ru*(CH₃CN)]PF₆ and ligand **90**, in the presence of B(OPh*p*NO₂)₃ resulted in <10% conversion to the linear product as determined by ¹H NMR (eq 2). Alternatively, exposing *N*-TIPS pyrrole allylic diacetate **84** to Ru(II)-catalytic conditions resulted in the complete conversion of **84** to bicyclic caprolactam **89** in 24 h (eq 3). An X-ray crystal structure of **89** is displayed in Figure 6.



Alternative reaction conditions:
rt, 50 °C and $[\text{CpRu}(\text{CH}_3\text{CN})_3]\text{PF}_6$

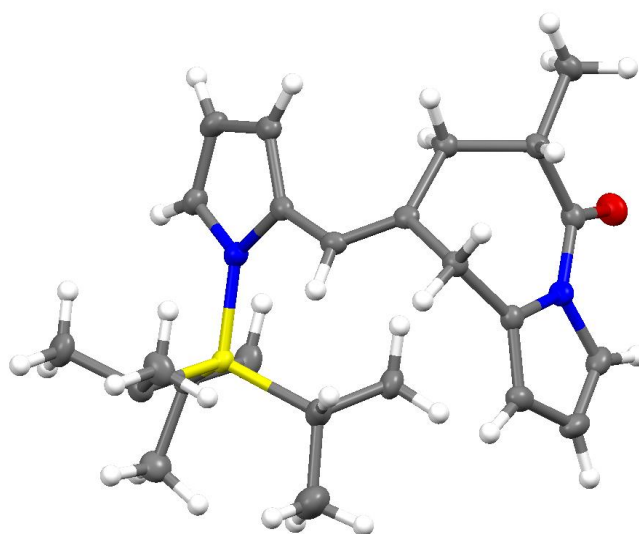
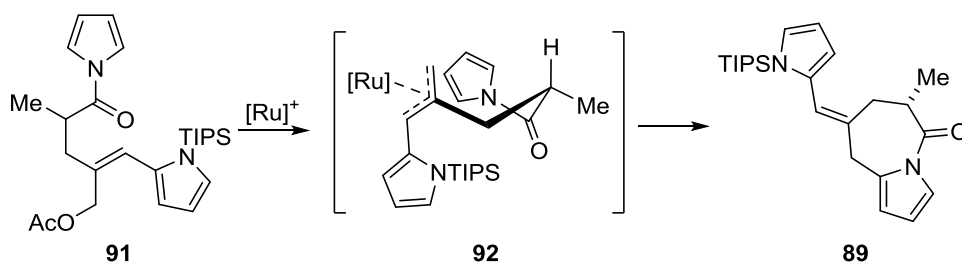


Figure 6. X-ray crystal structure of **89**

The mechanism of **89** formation is believed to involve oxidative addition of Ru(II) across the allylic acetate C-O σ -bond, resulting in the formation of a reactive allylic intermediate (Scheme 14). With simple substrates enolate addition typically favors the more highly substituted center, resulting in the bias formation of branched Claisen-type products. However, a reversal in enolate preference may be explained by a more sterically hindered allylic intermediate, leading to the exclusive formation of linear product **91**. Oxidative addition of Ru(II) across the second allylic acetate C-O σ -bond of **91**, results in the formation of allylic intermediate **92**. Intramolecular attack by pyrrole on the reactive intermediate (**92**) and subsequent rearomatization results in the formation of the observed product (**89**) (Scheme 14).

Scheme 14. Possible mechanism for the formation of **89**



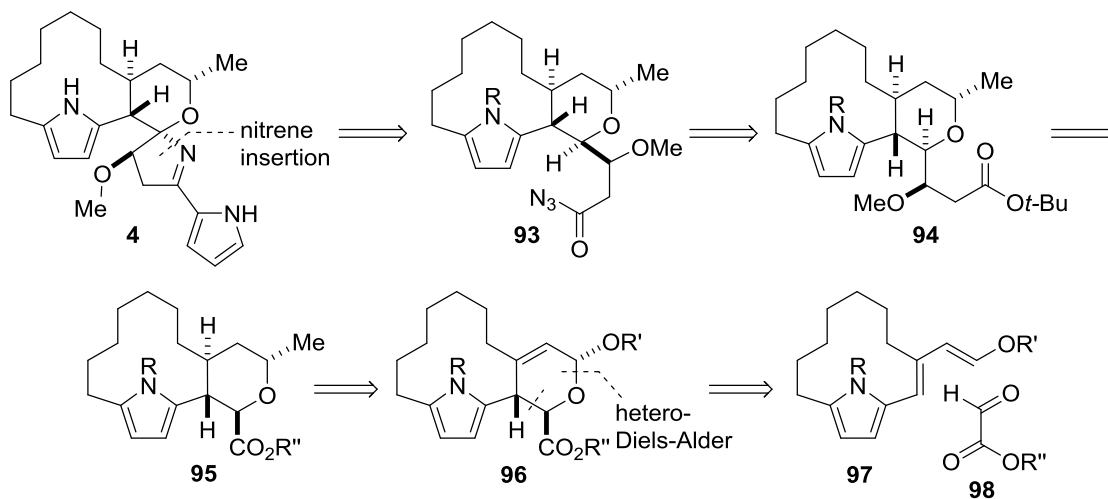
In conclusion, the extension of ruthenium-catalyzed enolate allylic alkylation methodology to disubstituted allylic acetates is a nonproductive route towards the synthesis of marineosin A (**4**). However, based on these studies a novel route to bicyclic caprolactam structures has been identified.

2.3 EFFORTS UTILIZING AZAFULVENE DIMER METATHESIS

2.3.1 Retrosynthetic Analysis

With the primary objective of developing an operative path towards the selective generation of marineosin A (**4**), we next developed an alternative retrosynthetic analysis implementing an *exo*-selective hetero Diels-Alder reaction. Our modified retrosynthetic analysis commences with the disconnection of the spiroiminal fragment via stereoselective C₈-H insertion of an acyl nitrene or nitrenoid intermediate, resulting from the breakdown of acyl azide **93**. A sequence of *t*-butyl ester hydrolysis, acid chloride conversion, followed by azide addition provides compound **93**. The *t*-butyl ester **94** was envisioned to be installed through metal hydride-mediated reduction of the C₈ α-alkoxy ester, followed by Mukaiyama aldol addition into the corresponding aldehyde. Hydrogenation of the C₂₁-C₂₂ double bond of **96**, and subsequent methyl transfer provides **95**. An *exo*-selective hetero Diels-Alder reaction with ethyl glyoxylate (**98**) generates tetrasubstituted pyran **96** (Scheme 15).

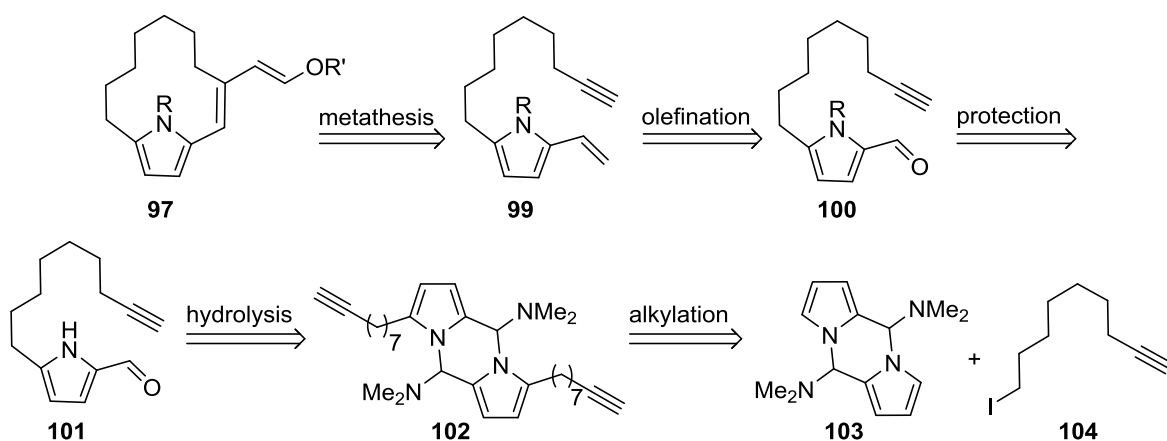
Scheme 15. Proposed retrosynthetic analyses of marineosin A



2.3.2 Azafulvene Dimer Derived Metathesis

To generate the key Diels-Alder precursor **97**, we chose to initiate our study with a domino ring-closing /cross-metathesis reaction of enyne **99** in the presence of vinyl acetate. Construction of **99** was expected to proceed through a short sequence of nitrogen protection, and subsequent olefination of pyrrole-2-carboxaldehyde **101**. Alkylation of azafulvene dimer **103** with iodoalkane **104**, and hydrolysis of the resulting intermediate (**102**) could provide **101** in a single step.¹⁹ Protecting the resulting aldehyde was especially important, since the basicity and nucleophilicity of nitrogen atoms deactivate the catalyst through coordination with the metal center. Notably, this process is advantageous due to the possible formation of a variety of 5-substituted pyrrole-2-carboxaldehydes (Scheme 16).

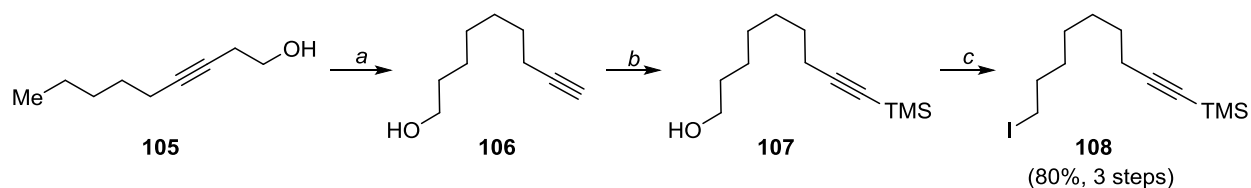
Scheme 16. Retrosynthetic analysis using azafulvene dimer



In order to investigate our planned ring-closing metathesis we first examined the synthesis of aldehyde precursor **101**. The three step synthesis of iodoalkyne **108** initiated with the triple bond isomerization of alkyne **105**, by a zipper reaction to afford terminal alkyne **106**. Trimethylsilyl protection of the terminal alkyne and successive halogenation afforded **108** in

80% yield over 3 steps (Scheme 17). To prevent the formation of the corresponding lithium acetylide during the course of the alkylation reaction, terminal alkyne protection was required. Employing **108** as the electrophile, alkylation of azafulvene dimer **103** with *n*-BuLi in THF at -78 °C resulted in the formation of **109** (32%). While attempts to install tosyl or *t*-Boc nitrogen protecting groups were unsuccessful on this substrate, benzyl protection proceeded to the desired substrate **111** in 60% yield. These results indicate steric hindrance, as well as, the electron withdrawing effect of the adjacent aldehyde may impact pyrrole protection. Olefination of the aldehyde function, followed by trimethylsilyl deprotection of the terminal alkyne proceeded to yield the metathesis substrate **114** in 74% yield over two steps (Scheme 18).

Scheme 17. Optimized synthesis of iodoalkyne **108**

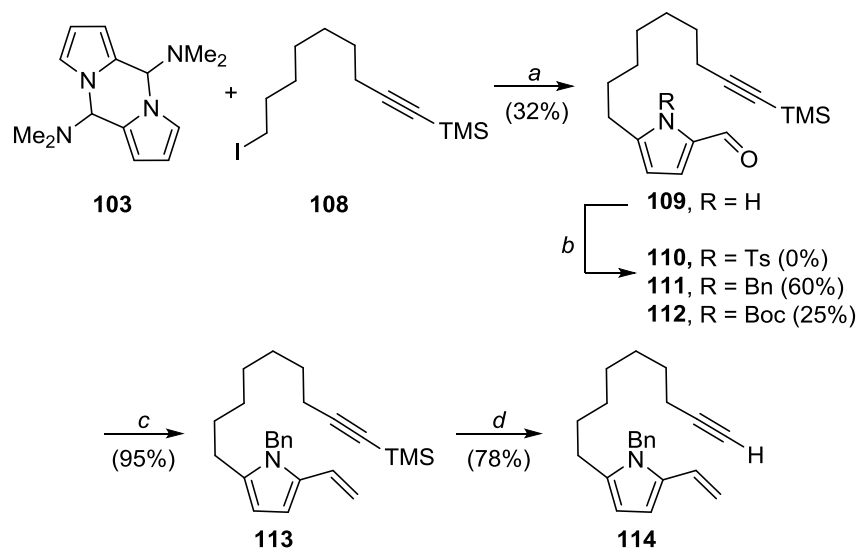


a) ethylene diamine, NaH, 60 °C. b) *n*-BuLi, TMSCl, -78 °C. c) PPh₃, ImH, I₂, rt. TMS = trimethylsilyl, ImH = imidazole.

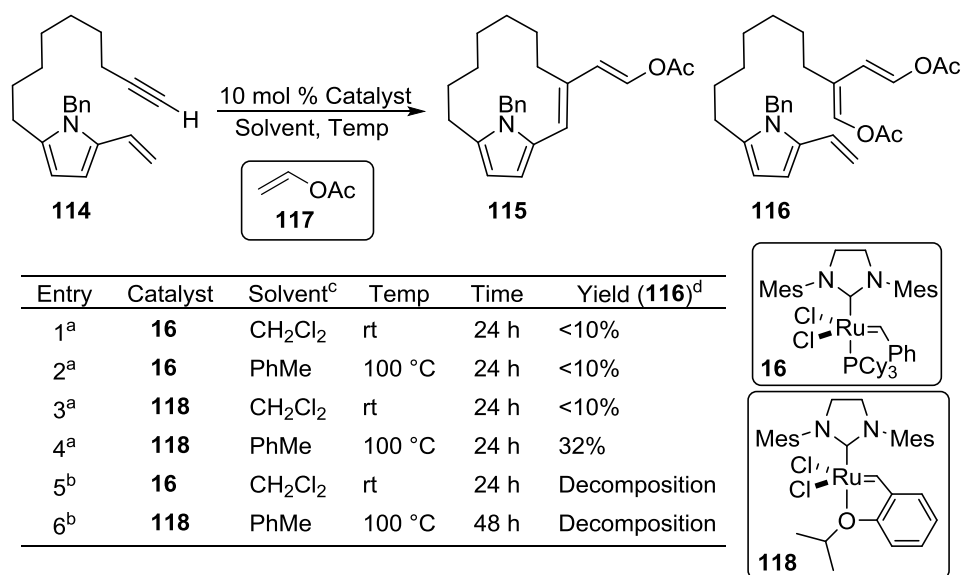
We next sought to investigate the tandem ring-closing/cross-metathesis reaction which would afford diene **115**. However, in the presence of 10 mol % Grubbs-II catalyst (**16**) and vinyl acetate (**117**) (0.01M CH₂Cl₂, rt) no anticipated ring-closed product was observed (Table 1, entry 1). Substituting Hoyveda-Grubbs-II catalyst (**118**) in place of Grubbs-II (**16**) resulted in the incomplete conversion of **114** to disubstituted derivative **116** (entry 3). Similar results were obtained at elevated temperatures (0.01M toluene, 100 °C), resulting in the formation of no ring-closed products (entries 2 and 4). However, derivative **116** was formed in 32% yield at elevated temperature utilizing Hoyveda-Grubbs-II catalyst (**118**), indicating that cross-metathesis of the

terminal alkyne with vinyl acetate (**117**) proceeded as the dominant pathway. Additionally, reactions performed in the presence of ethylene (1 atm) resulted in the complete decomposition of substrate **114**. This result was in accordance with previous reports in which metatheses of 2-vinyl aromatic heterocycles do not proceed at an appreciable rate.²⁰ In particular, 2-vinyl pyrroles may display diminished reactivity due to the possible formation of a charged resonance intermediate, impeding the formation of an electron rich carbon-ruthenium bond and enabling the competing alkyne metathesis.

Scheme 18. Synthesis of enyne substrate **114**



a) *n*-BuLi then NaHCO₃. b) NaH, TsCl; NaH BnBr; DMAP, Boc₂O. c) CH₃PPh₃Br, KHMDS. d) K₂CO₃, MeOH. Ts = tosyl, DMAP = 4-dimethylaminopyridine, Boc = *t*-butoxycarbonyl, KHMDS = Potassium hexamethyldisilazide.

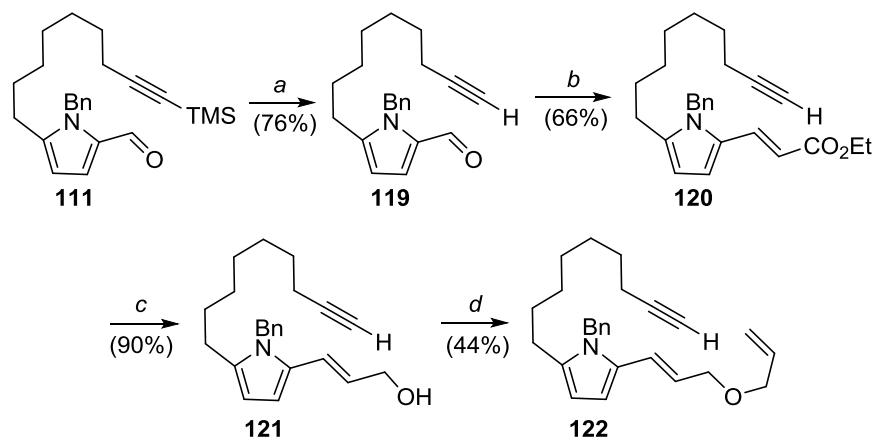
Table 1. Enyne metathesis approach to marineosin macrocycle

^a Reaction conditions: 4 equivalents of vinyl acetate (**117**). ^b Reaction conditions: ethylene (1 atm). ^c 0.01M solvent. ^d Determined by crude ¹H NMR spectra.

To promote intramolecular enyne metathesis, and favor the formation of the macrocyclic core, we next employed a relay ring-closing metathesis strategy for directing metal activation. This relay strategy, initially developed by Hoyer and coworkers, has previously been utilized to direct metal movement to poorly reactive alkenes.²¹ To generate relay substrate **122**, we initiated our synthesis with alkyne deprotection, followed by a Horner–Wadsworth–Emmons reaction to afford E-alkene **120** (Scheme 19). Diisobutylaluminum hydride-mediated reduction and *O*-allylation afforded the desired relay substrate **122**. As displayed in Table 2, ring-closing conditions utilizing 15 mol % Grubbs-II (**16**) at 60 °C over 24 h in 1,2-dichloroethane (DCE) produced none of the desired product **115** (entry 1). Similarly, the addition of 1-4 equivalents of vinyl acetate (**117**) yielded only starting material (entries 3 and 4). These results may be attributed to the formation of unstable 1,3-diene intermediates resulting in alkyne polymerization, in the absence of vinyl acetate (**117**). In an attempt to bypass 1,3-diene formation, 1,4-benzoquinone (BQ) was additionally investigated as an additive for the desired

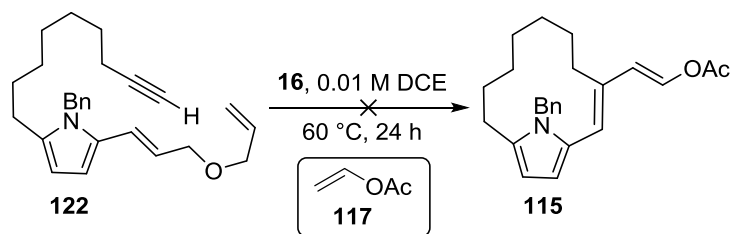
metathesis reaction based on the previous success of Diver and coworkers.²² Unfortunately, 7.5 mol % **16**, in the presence of 10 mol % BQ produced no desirable results (Table 2, entry 2).

Scheme 19. Synthesis of relay-ring closing substrate **122**



a) K_2CO_3 , MeOH. b) triethyl phosphonoacetate, KOH, THF. c) DIBAL-H, CH_2Cl_2 . d) allyl bromide, NaH, THF. DIBAL = diisobutylaluminium hydride.

Table 2. Relay-ring closing metathesis approach



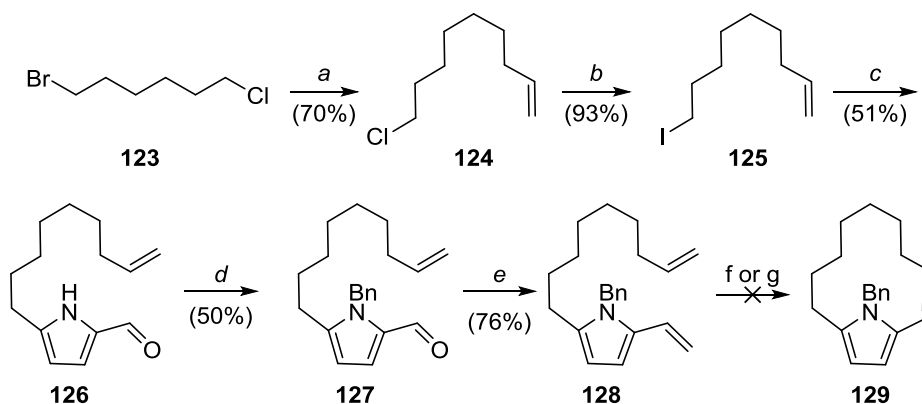
Entry	Additive	Alkene	Result
1 ^a	none	none	Decomposition
2 ^b	1,4-benzoquinone	none	Decomposition
3 ^a	none	117 ^c	Starting material
4 ^a	none	117 ^d	Starting material

^a Catalyst loading: 15 mol %. ^b Catalyst loading: 7.5 mol %. ^c 1 equivalent vinyl acetate (**117**). ^d 4 equivalents vinyl acetate (**117**).

Alternatively, we sought to synthesize **129**, which would constitute the macrocyclic core of diene **115**, with the goal of eliminating competing pathways associated with initiation at the alkyne. Based on the approach implemented by Donohoe for the completion of the furan core of cembranolide, we next investigated the utility of olefin metathesis for macrocycle formation

(Scheme 20).²³ Cross-coupling of 1-bromo-6-chlorohexane (**123**) with allylmagnesium bromide in the presence of CuCl afforded **124** in 70% yield. This species underwent chloride displacement under Finkelstein conditions to provide **125** in 93% yield (Scheme 20).²⁴ Accordingly, alkylation of azafulvene dimer **103** with **125**, followed by hydrolysis of the resulting alkylated species afforded aldehyde **126** in 51% yield. Nitrogen protection of the pyrrole **126**, followed by Wittig olefination of the aldehyde function provided the olefin metathesis substrate **128** in 38% yield over two steps. However, the attempted intramolecular olefin metathesis of **128** in the presence of either Grubbs-II (**16**) or Hoyveda-Grubbs (**118**) catalysts produced no detectable ring-closing derivative and recovery of the substrate (**128**). Furthermore, prolonged reaction times and elevated reaction temperatures were unable to effect the desired transformation. Presumably, entropic factors which limit the probability of end-to-end encounters in larger ring systems are responsible for the observed results. In addition, a higher activation barrier due to increased ring strain is evident in larger size rings.²⁵

Scheme 20. Ring-closing metathesis approach



a) allylmagnesium bromide, CuCl, Et₂O, -78 °C. b) NaI, acetone, 60 °C. c) **103**, *n*-BuLi than NaHCO₃. d) NaH, BnBr. e) CH₃PPh₃Br, KHMDS. f) 10 mol % **16** or **118**, ethylene (1 atm), 0.01M CH₂Cl₂, rt, 24 h. g) 10 mol % **16** or **118**, ethylene (1 atm), 0.01M toluene, 100 °C, 48 h. HMDS = hexamethyldisilazane.

2.4 CONCLUSIONS

We have presented two dissimilar approaches with the primary objective of developing an operative path towards the generation of marineosin A. The extension of an enolate allylic alkylation approach to disubstituted allylic acetates resulted in the formation of bicyclic caprolactam structure **89**. However, no operative route towards the synthesis of marineosin A was established. Primarily due to the diminished reactivity of *N*-protected pyrrole derivatives towards silyl enol ether **85**, in the presence of catalytic amounts of ruthenium (II). In addition, an azafulvene dimer metathesis strategy was investigated as a potential route towards the macrocyclic core of marineosin A. However, we were unable to affect the desired ring-closing metathesis, presumably due to the diminished reactivity of 2-vinyl pyrrole derivatives, as well as, entropic factors which limit the reactivity of larger ring systems.

3.0 INTRODUCTION

3.1 DIVERSITY-ORIENTED SYNTHESIS OF NATURAL PRODUCT-LIKE STRUCTURES

Diversity-oriented synthesis (DOS) involves the deliberate, simultaneous and efficient synthesis of multiple targets that are not only diverse in the appendages they display, but also in their molecular architectures.²⁶ In contrast to target-oriented synthesis and combinatorial chemistry (focused library synthesis), diversity-oriented syntheses are not aimed at one particular target (Figure 7). In these approaches retro-synthetic analysis is used to theoretically deconstruct complex target molecules into simple starting materials. In DOS, a “forward synthetic” strategy must be constructed to facilitate the transformation of simple starting materials into an array of complex and diverse products.²⁷

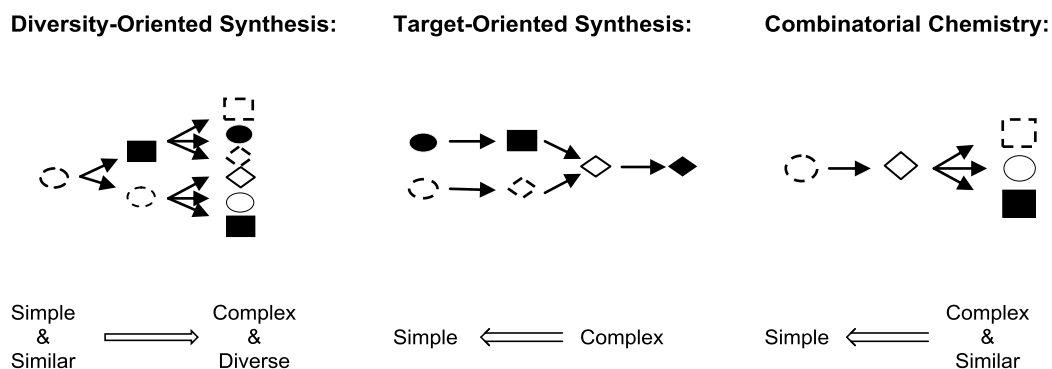


Figure 7. Sources of skeletally diverse small molecules

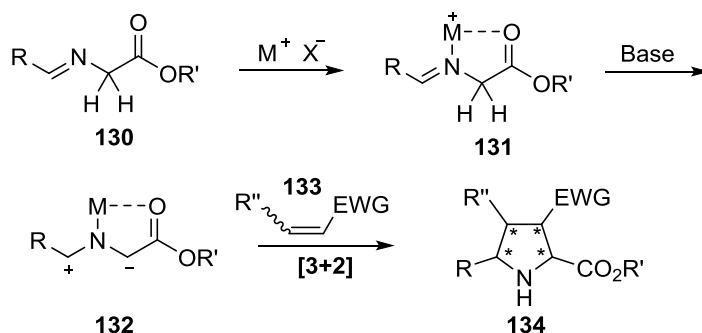
This process first described in the pioneering work of Schreiber, aims to synthesize collections of molecules that represent the variety of charges, polarities, bonding interactions and architectures that can potentially be recognized by nature's biomolecules.²⁶ Over the last few years, the potential for DOS has been exemplified by the synthesis of discrete skeletons with unique motifs. While several strategies have focused on structural motifs such as benzopyran, β -amino alcohol, allenolate and indole cores for the synthesis of alkaloid-like skeletons and ring systems, the diversity-oriented strategies of pyrrolidines remains relatively unexplored.^{28,29}

Pyrrolidines are an important class of heterocycles that have been found in numerous natural products and have served as useful molecular scaffolds in medicinal structures. For example, in cancer research small molecule MDM2 inhibitors based on the spirocyclic oxindole-pyrrolidine core of natural alkaloids such as spirotryprostatin A and alstonisine have showed good selectivity between cancer and normal cells with wild-type p53.³⁰ Neuroprotective agent kaitocephalin³¹, hepatitis C virus RNA polymerase small molecule inhibitors³², the synthetic influenza drug A-192558³³ and the antitumor antibiotic bioxalomycin β 1³⁴ all are examples in which the pyrrolidine ring is an important structural motif. Accordingly, the diversity-oriented synthesis of natural product-like libraries in which pyrrolidine scaffolds provide a core for the development of structurally complex, stereochemically rich and densely functionalized substructures are needed.

3.2 PREVIOUS APPLICATIONS OF 1, 3-CYCLOADDITION REACTIONS FOR REGIO- AND STEREO-SPECIFIC FORMATION OF PYRROLIDINES

The [3+2] cycloaddition reaction of azomethine ylides with electron poor dipolarophiles is a powerful and concise method for the synthesis of highly substituted five-membered ring heterocycles.³⁵ Specifically, the dipolar cycloaddition of an azomethine ylide and an electron-deficient olefin is a valuable transformation because it creates two carbon-carbon bonds and four potential stereocenters in a single step. The biological importance of pyrrolidines has encouraged the advancement of diastereo- and enantioselective [3+2] cycloadditions of azomethine ylides, and several routes to these 1, 3-dipoles have been developed.³⁶ Among the different versions of this reaction, the most practical approach has been the interaction of stabilized *N*-metalated azomethine ylides **132** with electron deficient alkenes **133** (Scheme 21).^{36a, 37}

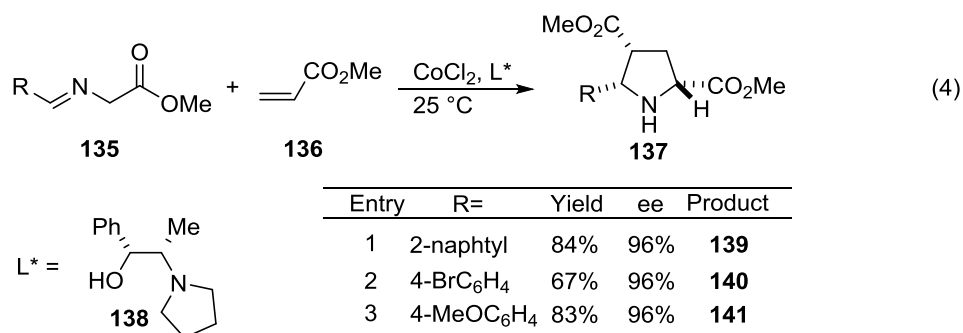
Scheme 21. [3+2] cycloaddition of *N*-metalated azomethine ylide with electron deficient alkenes



* New Potential Stereocenter

The enantioselective version of this transformation utilizing chiral based ligands was first investigated in 1991 by Grigg.³⁸ Using a stoichiometric amount of Co(II) and the chiral ephedrine ligand **138**, the reaction of azomethine ylide **135** with methyl acrylate (**136**) primarily resulted in a single enantiomer of pyrrolidine **137** (eq 4). While reaction time and enantiomeric

excess of the product remained unchanged in a variety of solvents, the use of cobalt chloride demonstrated a profound effect on both values. The choice of a molar equivalent of CoCl_2 and the chiral ephedrine ligand **138** gave the highest yields (45-84%) with an appreciable enantiomeric enrichment of 96%. However, a substantial amount of imine hydrolysis and dimerization was observed in these reactions.^{36a, 38}



The observed facial selectivity of these reactions is rationalized by using transition state **142** (Figure 8). Due to the *cis*-conformation of the methyl and phenyl groups on the ligand, addition occurs only at the less hindered face of the ylide.³⁸ Grigg has additionally reported utilizing AgOTf and a chiral bisphosphine ligand on identical substrates, however detailed reaction conditions such as catalyst loading and substrate scope were not reported.³⁹

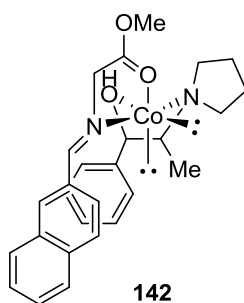
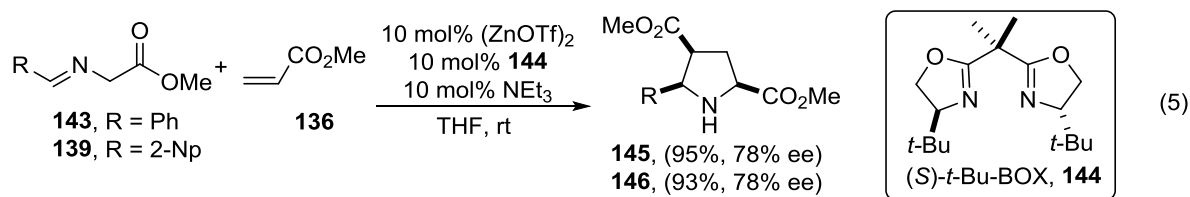
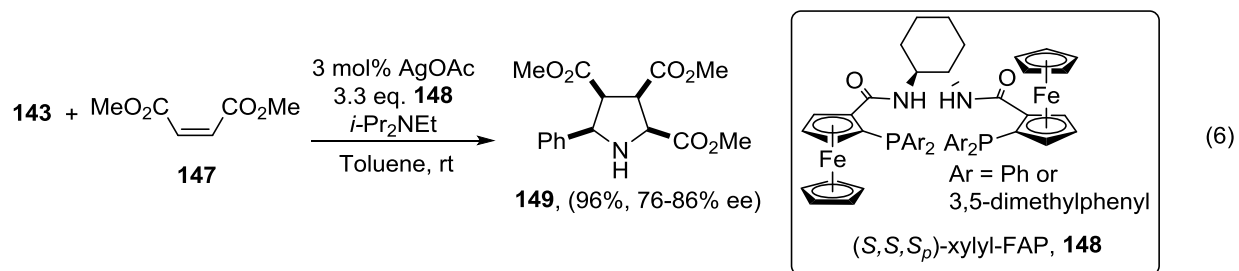


Figure 8. Proposed transition state of Co (II)/ephedrine ligand

Catalytic variants of Griggs' stoichiometric cycloadditions of *N*-metalated azomethine ylides have more recently been demonstrated by Jørgensen and Zhang.^{35, 40} In 2002, Jørgensen investigated the reactions of *N*-benzylidene- and *N*-(2-naphthylmethylidene) glycinates **143** and **139**, with methyl acrylate (**136**) in the presence of catalytic Cu(OTf)₂ and Zn(OTf)₂ and chiral bisoxazoline ligands. Optimized conditions for the formation of pyrrolidines **145** and **146** were obtained with catalytic Zn(OTf)₂ and chiral bisoxazoline ligand (*S*)-*t*-Bu-Box-ligand (**144**) (eq 5). Reactions with a series of imines of glycine methyl ester and various electron deficient alkenes catalyzed by Jørgensen's system have demonstrated a variety of yields (12% to > 95%) and enantiomeric enrichments (<5% to 94%) (Figure 9).³⁵



Work completed by Zhang further examined the cycloadditions of azomethine ylides utilizing catalytic Ag(I) in conjunction with various chiral phosphine ligands. However, initial investigations of this catalyst system with benzylidene glycinates **143** and dimethylmalonate (**147**), failed to promote substantial diastereo- or enantioselectivities and resulted in poor conversions.⁴⁰ Addition of the Trost modular ligand **148**,⁴¹ previously utilized in asymmetric allylic alkylations resulted in a significant improvement in reactivity and enantioselectivity (94% yield and 76% ee). An additional increase in selectivity was also observed upon replacement of the phenyl groups with 3,5-dimethylphenyl (86% ee) (eq 6).⁴⁰



Overall, reactions employing imines of glycine methyl ester with various olefins catalyzed by Zhang's AgOAc/xylyl-FAP system demonstrated higher yields (73-98%) and enantiomeric enrichment (70% to 97% ee) than previously reported by Jørgensen's system. Representative members resulting from the [3 + 2] cycloaddition of azomethine ylides with typically used olefins is shown in Figure 9. In all cases only the *endo* products were isolated. Alkyl imino esters were found to be significantly less reactive under the same conditions with lower yields and ee (82% yield over 48 h, 70-81% ee).⁴⁰

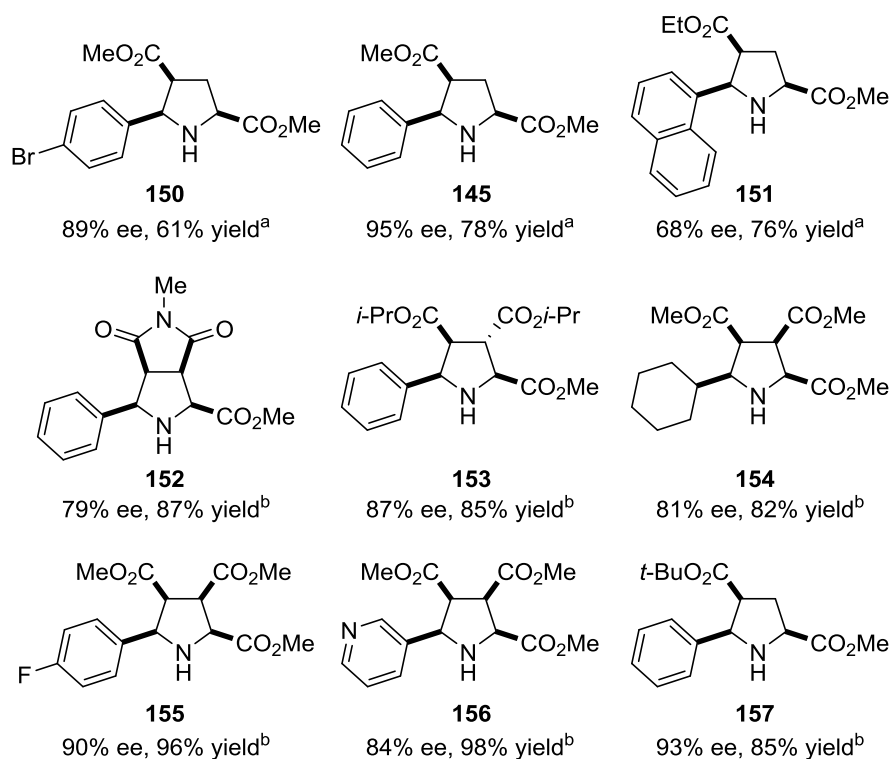
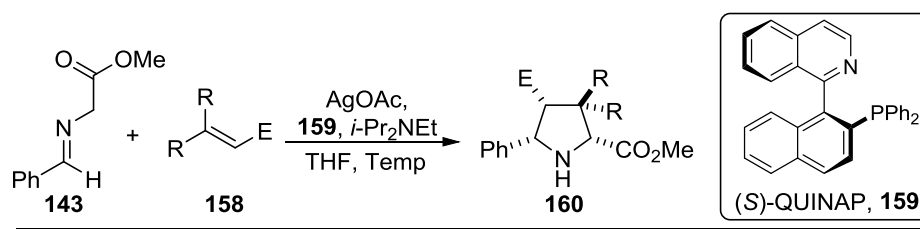


Figure 9. Application of Jørgensen's $\text{Zn}(\text{OTf})_2/t\text{-BuBOX}^{\text{a}}$ and Zhang's $\text{AgOAc}/\text{xylyl-FAP}^{\text{b}}$ systems to development of pyrrolidine libraries

3.3 SYNTHESIS OF FUSED PYRROLIDINE-HYBRID LIBRARIES

Based upon the previous chiral catalyst studies developed by both Zhang and Jørgensen, Schreiber has applied 1,3-dipolar cycloaddition reactions to the synthesis of fused pyrrolidine libraries. Focusing on silver (I) acetate reactions with chiral phosphine ligands previously engaged in Zhang's work, Schreiber has examined six additional commercially available chiral phosphines. The reaction which was initially explored with methyl *N*-benzylidene glycinate **143** and *t*-butyl acrylate is displayed in Table 3, entry 1. Unexpectedly, of the commercially available ligands examined the P, N ligand (*S*)-QUINAP (**159**) displayed the best levels of both diastereo- and enantioselectivity.⁴²

Table 3. Exploration of dipolarophile reactivity with Schreiber's catalyst


Entry	Dipolarophile	Temp	Time	Yield	Endo:Exo ^e	% ee
1 ^a	<i>tert</i> -butyl acrylate	-45 °C	20 h	84%	>20:1	91%
2 ^a	dimethyl maleate	-60 °C	48 h	88%	>20:1	60%
3 ^b	<i>tert</i> -butyl crotonate	-20 °C	85 h	97%	>20:1	84%
4 ^b	<i>tert</i> -butyl cinnamate	-20 °C	85 h	62% ^c	2:1	81%, 50% ^d

^a Catalyst loading: 3 mol%. ^b Catalyst loading: 10 mol%. ^c Combined yield endo/exo products. ^d Enantioselectivity exo product. ^e Determined by crude ¹H NMR spectra.

To further expand the scope of the reaction, the nature of the aromatic group was also explored. Exchanging the aromatic substituent on α -imino ester **143**, with 4-methoxyphenyl, 4-cyanophenyl, 2-tolyl, and 2-naphthyl groups under the same conditions similarly demonstrated high levels of diastereoselectivity (>20:1) and enantioselectivity (94-96% ee) regardless of the electronic properties of the rings. However, the sterically hindered 2-tolyl gave lower enantioselectivity (95% yield, 89% ee). Analysis of the reactivity of the Schreiber's catalyst system with different electron-deficient olefins is shown in Table 3. The proposed transition state **161** is thought to derive selectivity by sterically hindering one face of the 1, 3-dipole limiting the approach of the incoming dienophile (Figure 10).⁴²

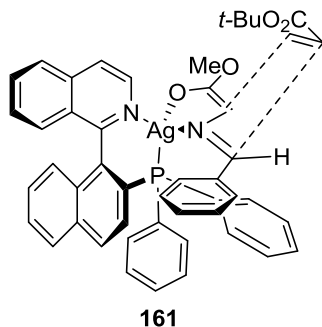
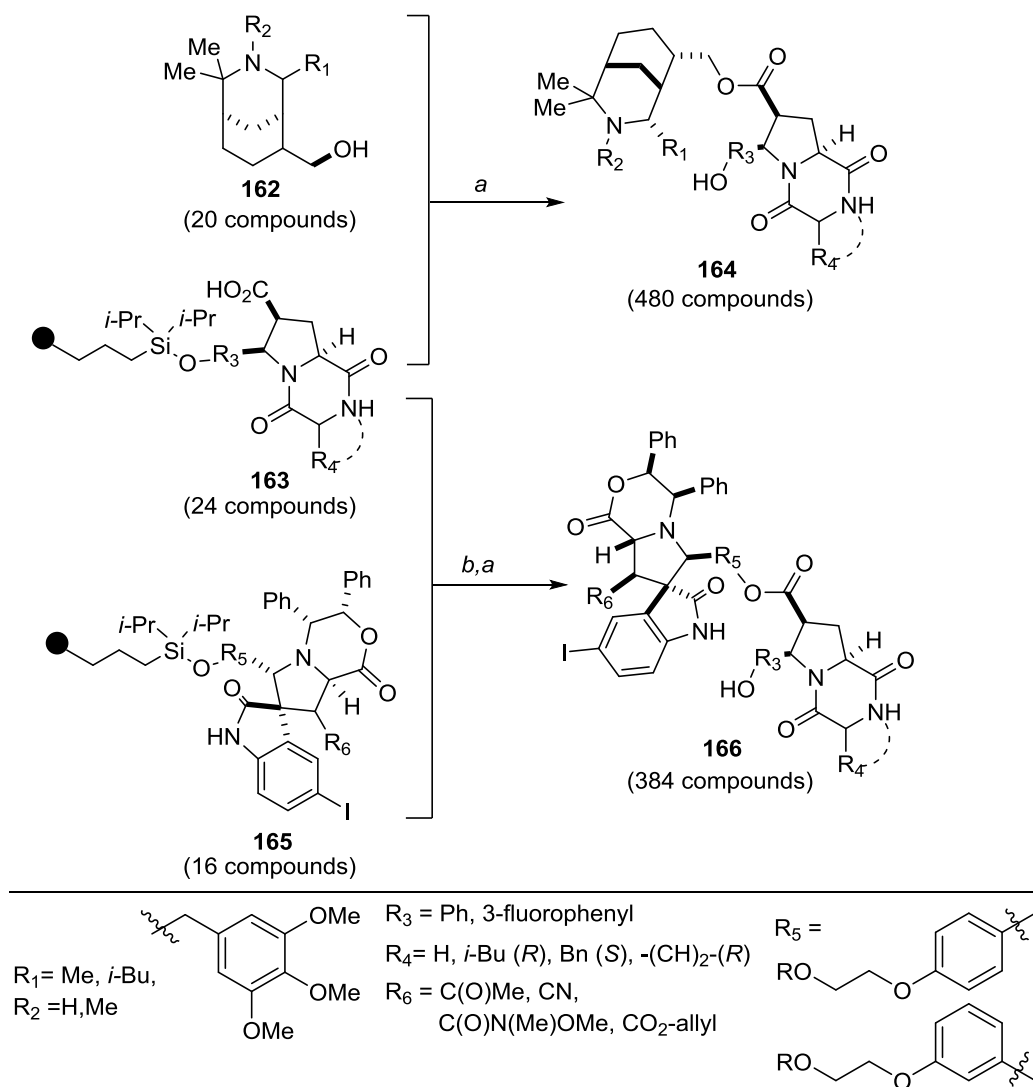


Figure 10. Proposed transition state of Ag(I)/QUINAP catalyst

Schreiber's work is the first example of a catalytic asymmetric cycloaddition of azomethine ylides to be featured in the parallel synthesis of a fused pyrrolidine scaffolds. The diversity-oriented synthesis which builds upon these scaffolds has resulted in the formation of bridged-piperidine/fused-pyrrolidine and spirocycle-oxindole/fused-pyrrolidine hybrid libraries.⁴³ A key feature of Schreiber's new catalyst system for diversity-oriented synthesis of pyrrolidine hybrid-libraries is the extension of this reaction to 500-600 μm polystyrene "macrobeads". As displayed in Scheme 22, pyrrolidine scaffolds could be initially loaded onto alkylsilyl-derivatized macrobeads. Coupling with various protected amino acids (glycine, leucine, phenylalanine, and proline) provided after deprotection the 24 member sublibrary (**163**). The resulting pyrrolidine scaffolds were then released and coupled to bridged piperidine (**162**) structures and spirocyclic-oxindole (**165**) structures or inversely coupled then released to yield the final small molecule hybrids. In each case, final sublibrary coupling involved PyBOP/DMAP-promoted esterification and HF-pyridine mediated release of the surrogate bead.^{43,44,45}

Scheme 22. Synthesis of fused-pyrrolidine hybrid libraries



a) 1. PyBOP, DMAP, CH_2Cl_2 , 23 °C, 16h; 2. HF-py, THF, 23 °C, 2h, then TMSOEt. b) **165**, HF-py, THF, 23 °C, 2h, then TMSOEt. DMAP = 4-dimethylaminopyridine, py = pyridine, PyBOP = benzotriazol-1-yl-oxytrypyrrolidinophosphonium hexafluorophosphate, TMS = trimethylsilyl.

4.0 DEVELOPMENT OF PYRROLIDINE SCAFFOLDS FOR DIVERSITY-ORIENTED SYNTHESIS BY CLAISEN REARRANGEMENT OF ALLYL VINYL ETHERS

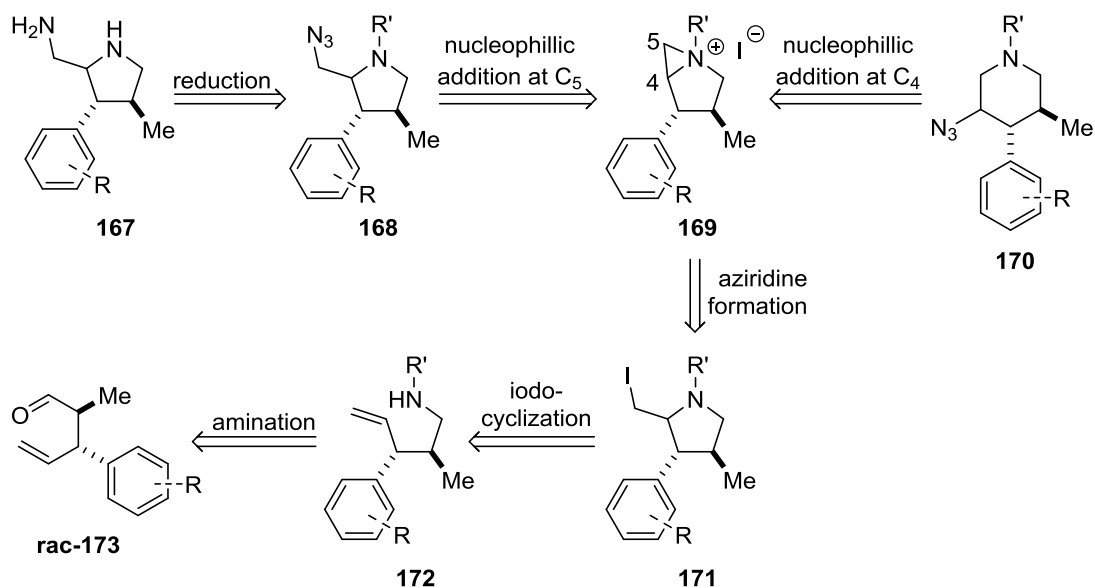
4.1 LIMITATIONS OF PREVIOUS STRATEGIES

Diversity-oriented synthesis is an emerging field that seeks to enrich chemical space by the development of divergent pathways towards new pharmaceutically active compounds. Previous methodologies developed by Grigg, Zhang, and Schreiber have resulted in the formation of hybrid-pyrrolidine libraries. However, the electronic requirements inherent within dipolar cycloaddition reactions have restricted the substrate scope available via this strategy. Moreover, the compounds derived from this approach have yet to display any biological activities. Therefore, novel pyrrolidine scaffolds which build structural complexity from simple and similar compounds are needed to synthesize diverse libraries of natural product- and drug-like molecules.

4.2 RETROSYNTHETIC ANALYSIS OF FUNCTIONALIZED PYRROLIDINE SCAFFOLDS

In the past few years, our laboratory has demonstrated the value of Ir(I)-based catalyst systems for the chemo- and stereoselective isomerization of bis(allyl) ether substrates.⁴⁶ Additionally, the enantio- and diastereoselective Ru(II)-catalyzed Claisen rearrangement of unactivated allyl vinyl ethers has also been demonstrated.⁴⁷ To validate the potential applicability of these methodologies to the diversity-oriented synthesis of drug-like compounds, we sought to develop a route to functionalized pyrrolidine scaffolds. Our retrosynthetic analysis commences with the reductive deprotection of β -azido amine **168**, resulting in the formation of diamine **167**.⁴⁸ Nucleophilic ring opening by azide at C₅ or C₄ of **169** results in the formation of both desired kinetic (**168**) and thermodynamic (**170**) products.^{49,50} The predominant process of nucleophilic displacement of iodine, is next expected to proceed through a S_Ni mechanism to generate aziridinium ion **169**. Preferential 5-*exo*-cyclization of **172** generates the anticipated β -iodo amine **171**. Lastly, reductive amination of γ,δ -unsaturated aldehyde **173** will afford **172** (Scheme 23).

Scheme 23. Retrosynthetic analysis of racemic pyrrolidine scaffolds



4.3 SYNTHESIS OF A GENERAL PYRROLIDINE SCAFFOLD FOR DIVERSIFICATION

4.3.1 Formation of Claisen Products from Simple Allyl Vinyl Ethers

Since its discovery in 1912 by Ludwig Claisen, the [3, 3] sigmatropic rearrangement of allyl vinyl ethers (**174**) to produce γ,δ -unsaturated carbonyl compounds (**176**) has been highly utilized in synthetic transformations.⁵¹ The rearrangement which proceeds through a chair-like transition state (**175**) to provide racemic *syn*-diastereomer **177**, results in the generation of a new carbon-carbon bond and two adjacent stereocenters (Figure 11).⁵²

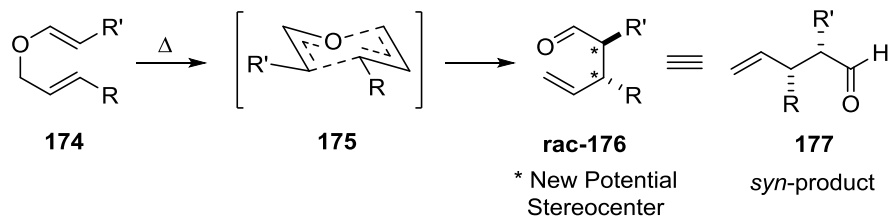
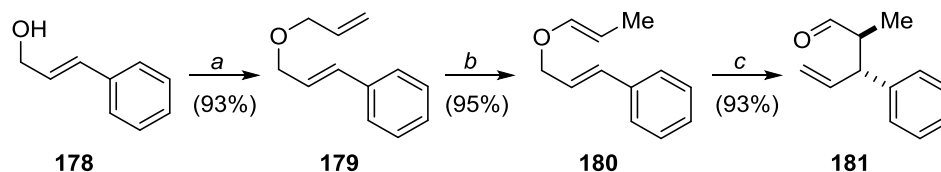


Figure 11. Thermal Claisen rearrangement of general allyl vinyl ether (**174**)

Based upon the success of Ir(I)-based catalyst systems developed in our laboratory, we initially synthesized aldehyde **181** as a model compound en route to pyrrolidine scaffolds (Scheme 24). Williamson ether synthesis of cinnamyl alcohol (**178**) with allyl bromide, followed by iridium catalyzed isomerization of the terminal double bond afforded allyl vinyl ether **180** in 88% yield over two steps.⁴⁶ Claisen rearrangement under thermal conditions of **180** afforded γ,δ -unsaturated aldehyde **181** in 93% yield (Scheme 24).

Scheme 24. Synthesis of γ,δ -unsaturated aldehyde



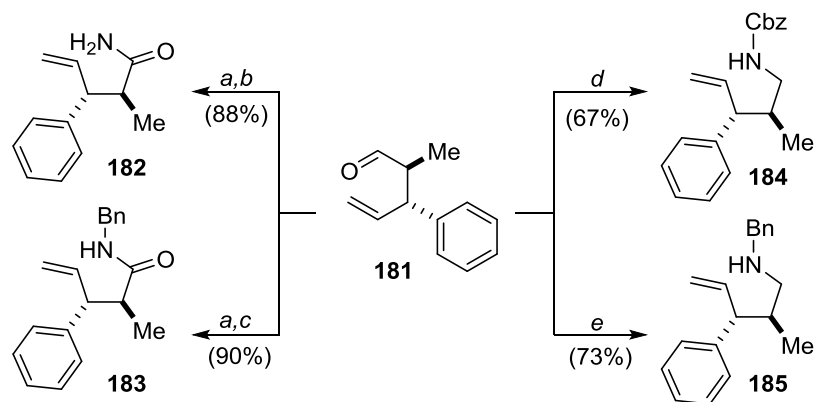
a) allyl bromide, NaH, THF. b) [Ir(COE)₂Cl]₂, PCy₃, NaBPh₄, CH₂Cl₂/acetone. c) 80 °C, toluene. COE = cyclooctene

4.3.2 Formation of Pyrrolidines from Claisen Products

To validate our synthesis design, we initiated our investigation with the generation of amides **182** and **183**, along with, amines **184** and **185** (Scheme 25). Pinnick oxidation followed by treatment of the resulting γ, δ -carboxylic acid derivative with ammonium hydroxide and benzylamine, afforded primary and secondary amides **182** and **183** in 88% and 90% yield, respectively.⁵³ The secondary amine **184** was synthesized in 67% yield via reductive amination with triethylsilane and benzylcarbamate. Similarly, treatment of **181** with sodium triacetoxyborohydride, and

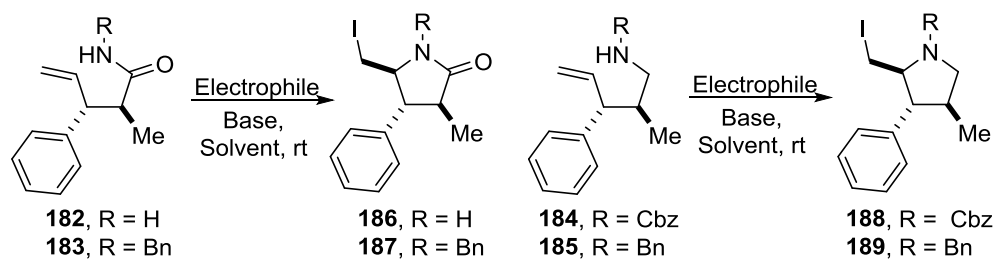
benzylamine afforded secondary amine **185** 73% yield (Scheme 25).⁵⁴ Having successfully established routes to the syntheses of **182** to **185**, we next sought to probe the reactivity of these compounds towards various electrophilic sources of iodine to complete the desired cyclization.

Scheme 25. Synthesis of γ,δ -unsaturated amides and amines



a) NaClO_2 , NaH_2PO_4 , 2-methyl-2-butene, *t*-BuOH, H_2O then oxalyl chloride. b) NH_4OH (aq). c) benzylamine, CH_2Cl_2 . d) benzyl carbamate, TES, TFA, MeCN. e) benzylamine, $\text{NaHB}(\text{OAc})_3$, AcOH, CH_2Cl_2 . TES = triethylsilane, TFA = trifluoroacetic acid.

Proceeding with our planned synthesis we subjected amines **182-185** to various electrophilic sources of iodine, to affect the desired cyclization reaction. The use of 3 equivalents of elemental iodine, in combination with NaHCO_3 and K_2CO_3 provided β -iodo amines **186-189** in 34-51% (Table 4, entries 1-5). Alternatively, utilizing 1.1 equivalents of NIS, amines **185** and **184**, selectively afforded 5-*exo*-products **189** and **188** in 70% and 64% yield respectively (entries 6 and 7). However, *N*-benzyl amine **185** displayed a shorter reaction time, with complete conversion in 20 minutes. In contrast *N*-carboxylbenzyl amine **184** reached completion only after 2 h. The diminished yields and elongated reaction time of **184** may be explained by increased steric volume or diminished nucleophilicity of the nitrogen atom.

Table 4. Cyclization conditions with various electrophilic iodine sources

Entry	Substrate	Electrophile ^c	Base ^d	Solvent	Product (Yield) ^e
1	182	I ₂	NaHCO ₃	MeCN	186 (35%)
2	183	I ₂	NaHCO ₃	MeCN	187 (41%)
3	184	I ₂	NaHCO ₃	MeCN	188 (48%)
4	185	I ₂	NaHCO ₃	MeCN	189 (51%)
5	185	I ₂	K ₂ CO ₃	CH ₂ Cl ₂	189 (34%)
6 ^a	184	NIS	none	THF	188 (64%)
7 ^a	185	NIS	none	THF	189 (70%)
8 ^b	184	NIS	none	THF	188 (67%)
9 ^b	185	NIS	none	THF	189 (75%)

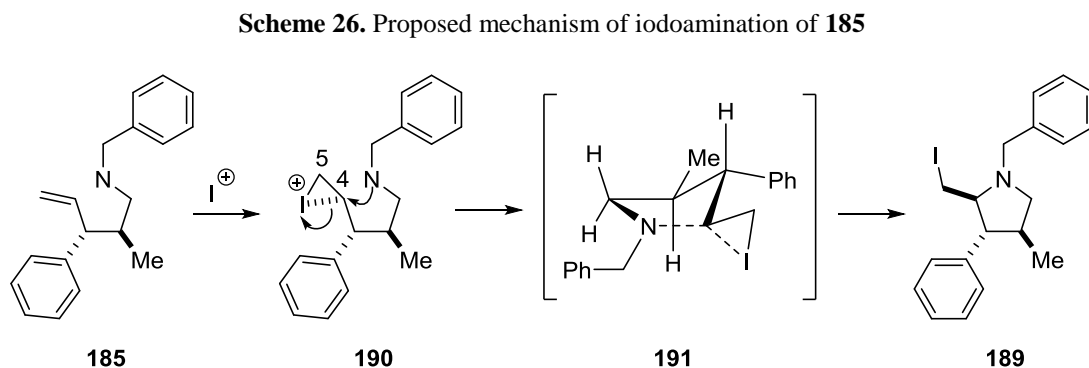
^a Reaction performed in the dark. ^b Reaction performed in the presence of ambient light. ^c 3 equivalents of I₂; 1.1 equivalents of NIS were utilized. ^d 3 equivalents of base.

^e Isolated yields. NIS = *N*-iodosuccinimide.

To decipher any effect of light on the cyclization reaction, identical reactions employing 1.1 equivalents of NIS and *N*-benzyl amine **184** or *N*-carboxybenzyl amine **185** were monitored under ambient light. As demonstrated in Table 4, minimal improvements in isolated yields were observed for both substrates **184** and **185**. These results led us to conclude, that the presence of light was not a decisive factor in the successful cyclization of **184** or **185**. However, having obtained complete conversion of **185** to **189** within 20 min, along with higher isolated yields in comparison to the conversion of **184** to **188**, we decided to employ *N*-benzyl amine **185** for further methodology development.

A plausible mechanism for the formation of pyrrolidine **189**, involves the reversible formation of iodonium ion **190** upon reaction of **185** with an electrophilic source of iodine (Scheme 26). Intramolecular ring-opening by nitrogen at C₄ of **190**, provides 5-*exo*-cyclization product **189**. Furthermore, transition state **191** which allows the iodonium ion, phenyl, and

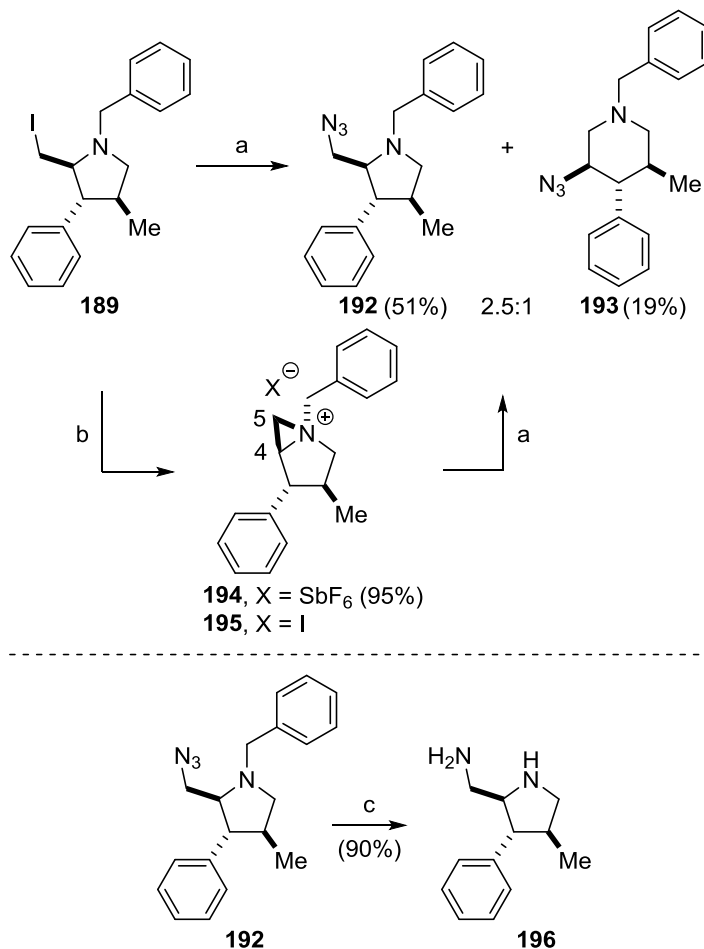
methyl groups to occupy pseudoequatorial positions around the developing pyrrolidine ring provides the most stable conformation of **189**.



At this stage, we sought to convert β -iodo amine **189** to the desired β -azido amine **192** which, through reductive deprotection, would be converted to the desired diamine scaffold. To accomplish this, we planned to generate both pyrrolidine (**192**) and piperidine (**193**) products via an aziridinium intermediate **195** (Scheme 27). The existence of **195** would be expected to arise, from the intramolecular substitution of primary iodide by the pyrrolidine nitrogen of **189**. Subsequent ring-opening by the azide nucleophile at either C₄ or C₅, would result in the formation of **192** and **193**. Reacting **189** with sodium azide (1.5 equivalents, DMF, 50 °C) led to the formation of pyrrolidine **192** as the major product (**192:193** = 2.5:1). This ratio remained consistent in the presence of bulky azide sources, such as tetrabutylammonium azide.⁵⁵ Indicating azide anions liberated from various sources, displayed a similar preference for nucleophilic attack at the least hindered carbon of the aziridine ring.⁵⁶ We further sought to investigate the effect of a larger counter ion on the regioselectivity of the ring-opening reaction. This was to be accomplished by iodide abstraction and exchange for the non-nucleophilic hexafluoroantimonate ion. Treating β -iodoamine **189** with 1.2 equivalents of AgSbF₆ resulted in

the formation of the crystalline product **194** (95% yield), which was further reacted with sodium azide (1.5 equivalents, DMF, 50 °C) (Figure 12). Analysis of the products by ¹H NMR indicated the formation of **192** and **193** in a 2.5:1 ratio. Thus, the azide anion preferentially attacks at the sterically least hindered center, independent of iodide or hexafluoroantimonate counter ion.

Scheme 27. Synthesis β-azido amine **192** and diamine **196**



a) NaN₃, DMF. b) AgSbF₆, THF, rt. c) 10 mol % Pd(OH)₂/C, NH₄HCO₂, EtOH, 80 °C.

With the completion of a route to model β-azido amine **192**, we next sought to generate the desired diamine scaffold utilizing a global reduction strategy. To accomplish this, we first investigated several strategies utilizing palladium on carbon (5% and 10%) to generate diamine

196, resulting from concomitant azide reduction and benzyl deprotection (Scheme 27). In a majority of instances, reduction of the azide function without deprotection occurred or complete decomposition of the product was observed. However, using Pearlman's catalyst ($\text{Pd}(\text{OH})_2/\text{C}$) in conjunction with ammonium formate, we obtained diamine **196**. Treating **192** with 10 mol % $\text{Pd}(\text{OH})_2/\text{C}$ in the presence of 12.5 equivalents of NH_4HCO_2 at 80 °C provided **196** in 90% yield.⁵⁷ These results indicate that $\text{Pd}(\text{OH})_2/\text{C}$ serves as a superior catalyst when both *N*-debenzylation and azide reduction are desired.

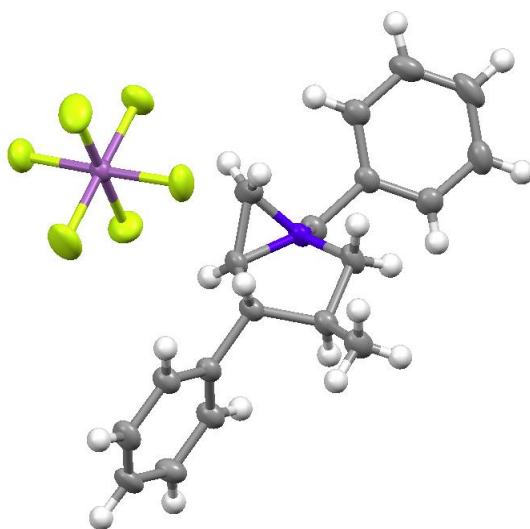


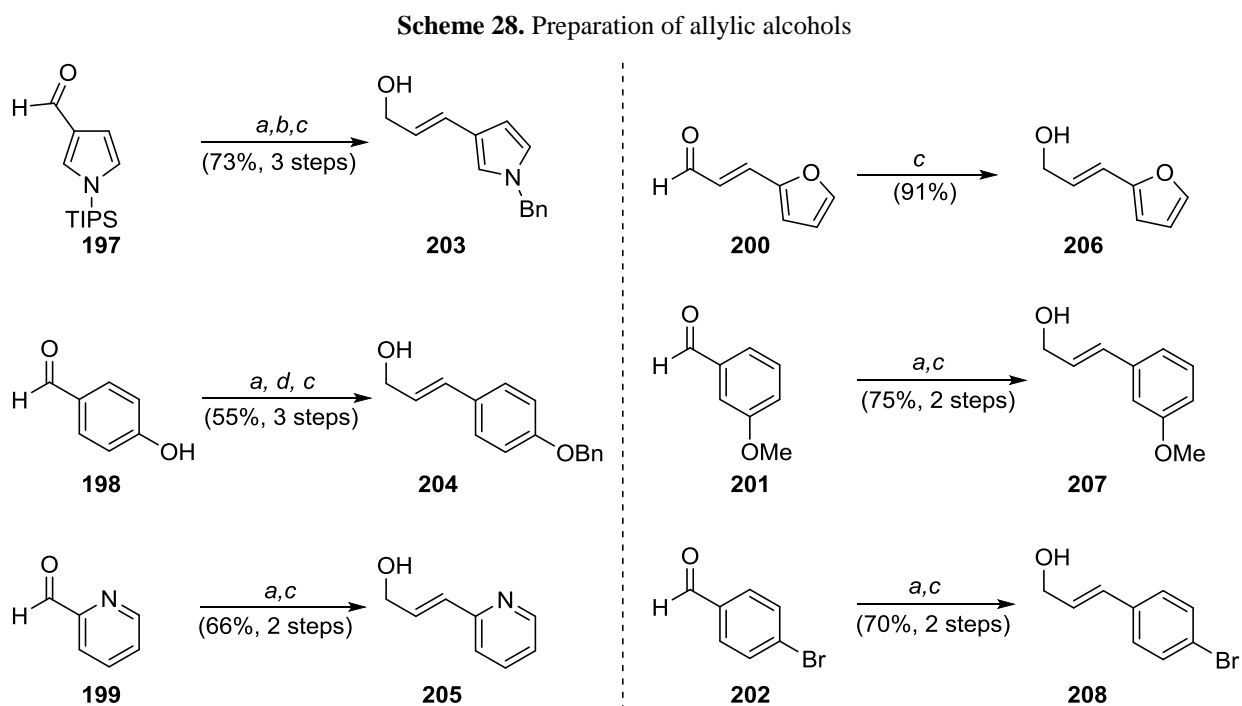
Figure 12. X-ray crystal structure of aziridinium **194**

4.4 DIVERSITY BY INCORPORATION OF C_3 SUBSTITUTION

Having established a synthetic route towards pyrrolidine **196**, we next focused on the generation of various pyrrolidine scaffolds for DOS. To demonstrate the versatility of this approach and integrate heterocycles with multifunctional sites, we initially identified **203-208** as potential

substrates. The work presented within this section, describes the alternative C₃ substitutions made in place of the phenyl group (Scheme 28).

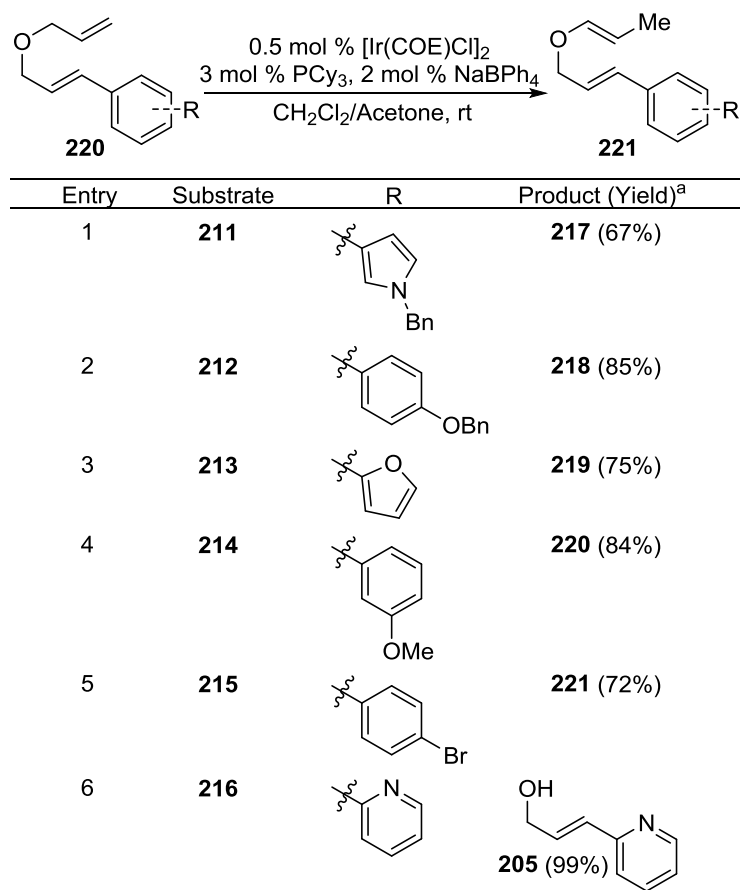
The preparation of allylic alcohols **203-208** from simple compounds is displayed in Scheme 28. 1-(Triisopropylsilyl)pyrrole-3-carbaldehyde (**197**) was prepared according to literature procedure.⁵⁸ Knoevenagel condensation of aldehyde **197** with monoethylmalonate, followed by benzyl protection and DIBAL-H reduction afforded allyl alcohol **203** in 73% yield over 3 steps. Unexpectedly, simultaneous TIPS deprotection was found to occur during condensation. A similar sequence of condensation, protection and reduction generated **204** in 55% yield over 3 steps. Simple reduction of trans-3-(2-furyl)acrolein (**200**) afforded desired alcohol **206** in 91% yield. Allyl alcohols **205**, **207**, and **208** were synthesized through a two-step protocol of condensation and reduction from aldehydes **199**, **201**, and **202** in acceptable yields (66-75% yield).



a) monoethylmalonate, DMAP, piperidine, DMF, rt. b) BnBr, NaH, DMF, 0 °C to rt. c) DIBAL, CH₂Cl₂, -78 °C. d) BnBr, K₂CO₃, DMF, 0 °C to rt. DMAP = 4-Dimethylaminopyridine.

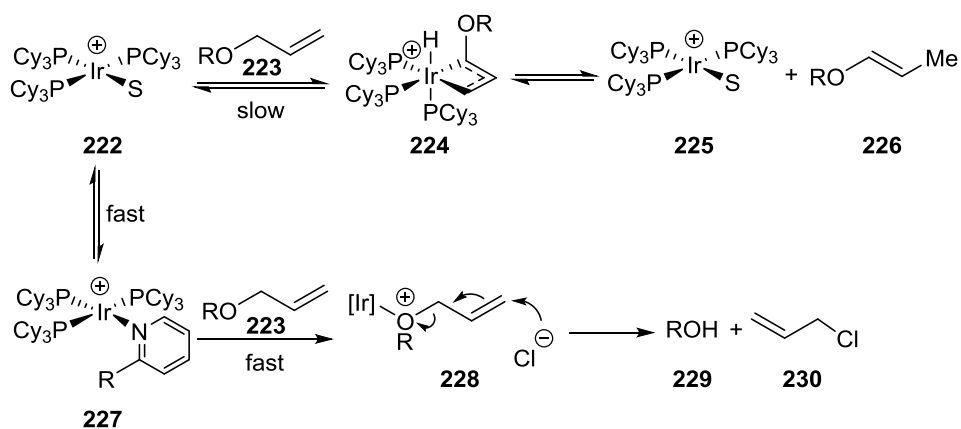
Following the procedure previously developed for the incorporation of cinnamyl aldehyde (**178**) into the pyrrolidine scaffold (**196**), we next sought to generate the corresponding aldehydes from allylic alcohols **203-208**. The reaction of allylic alcohols **203-208** with 1.2 equivalents of allyl bromide and 1.3 equivalents of NaH in THF, provided bis(allyl) ethers **211-216** in 89-99% yield (Table 5). Subsequent iridium catalyzed isomerization of ethers **211-215** (0.5 mol % [Ir(COE)Cl]₂, 3 mol % PCy₃, 2 mol % NaBPh₄, CH₂Cl₂/Acetone) provided **217-221** in 67-85% yield, with the exception of pyridine di(allyl) ether **216**. Interestingly, iridium-catalyzed deallylation of **216** proceeded to completion in less than a minute, and provided allylic alcohol **205** in 99% yield. Facile *O*-deallylation of bis(allyl) ether **216** can be attributed to the rapid formation of cationic tetrasubstituted complex **227**. Coordination of the pyridine ring to the metal center, deactivates the triphosphene catalyst (**222**) towards isomerization enabling the competing S_N2'-type reaction. Nucleophilic attack of chlorine, present in the reaction mixture results in the formation of allylic alcohol **229** and allyl chloride (**230**) (Scheme 29).

Table 5. Iridium catalyzed isomerization of bis(allyl) ethers **211-216**

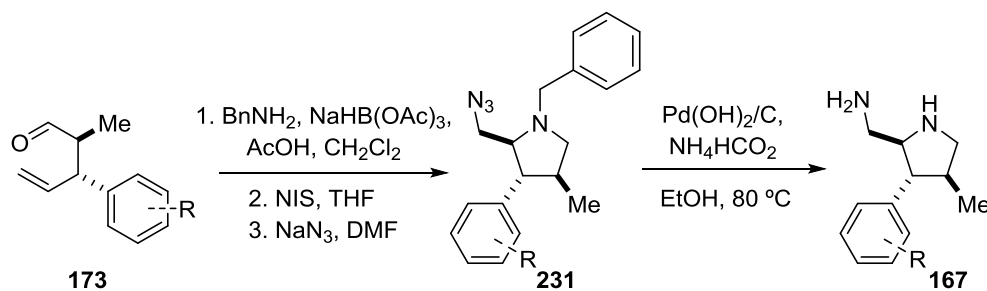


^a Isolated yields. COE = cyclooctene.

Scheme 29. Iridium-catalyzed deallylation



We next examined the conversion of allyl vinyl ethers **217-221** into the corresponding diamines, according to our previously determined protocol. Claisen rearrangement of **217-221** afforded γ,δ -unsaturated aldehydes **232-236** under thermal conditions. Reductive amination of the pending aldehydes followed by iodocyclization, and azide substitution ultimately afforded β -azido pyrrolidines **238-241** (Table 6).^{46, 55,57,59,60} We were unable to isolate β -azido pyrrolidine **237** following treatment with 2 equivalents of benzylamine (NaHB(OAc)₃, AcOH, CH₂Cl₂). This may be explained by the reactive nature of the pyrrole ring, which underwent frequent decomposition. Reductive deprotection of β -azido pyrrolidines **239** and **240** utilizing Pearlman's catalyst provided **244** and **245** in 91% and 93% yield, respectively. However, global reductive deprotection of 4-hydroxybenzyl derivative **238** could not accurately be reproduced utilizing our standard reductive deprotection conditions (10 mol % Pd(OH)₂/C, 12.5 equivalents NH₄HCO₂, EtOH, 80 °C). Pearlman's catalyst was additionally found to effect the dehalogenation of aryl halide **241** with concomitant reduction to afford diamine **196**. In all cases, decreased catalyst loading produced similar results, with 100% conversion of **241** to model diamine **196**. It was therefore concluded, that palladium hydroxide on carbon in the presence of ammonium formate effectively catalyzes dehalogenation of aryl bromides at an appreciable rate.

Table 6. Synthesis of C₃ substituted diamines

Entry	Substrate	R	231 Product (Yield) ^a	167 Product (Yield) ^a
1	232		237 Decomposition	242 ^b
2	233		238 (16%)	243 Decomposition
3	234		239 (16%)	244 (91%)
4	235		240 (15%)	245 (93%)
5	236		241 (14%)	196 Dehalogenation

^a Isolated yields. ^b Not determined. Bn = benzyl, NIS = *N*-iodosuccinimide.

4.5 ASYMMETRIC SYNTHESIS OF β-iodo PYRROLIDINE SCAFFOLD

The enantio- and diastereoselective Ru (II)-catalyzed Claisen rearrangement of unactivated allyl vinyl ethers has recently been investigated in our laboratory (Figure 13).⁴⁷ Having developed a racemic synthesis of diamines **196**, **244**, and **245** we sought to develop an asymmetric route to β-iodo amine **253** and decipher the configuration at the newly formed stereocenter (Scheme 30).

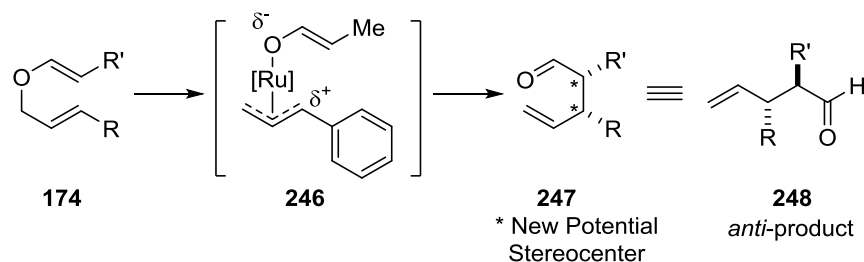
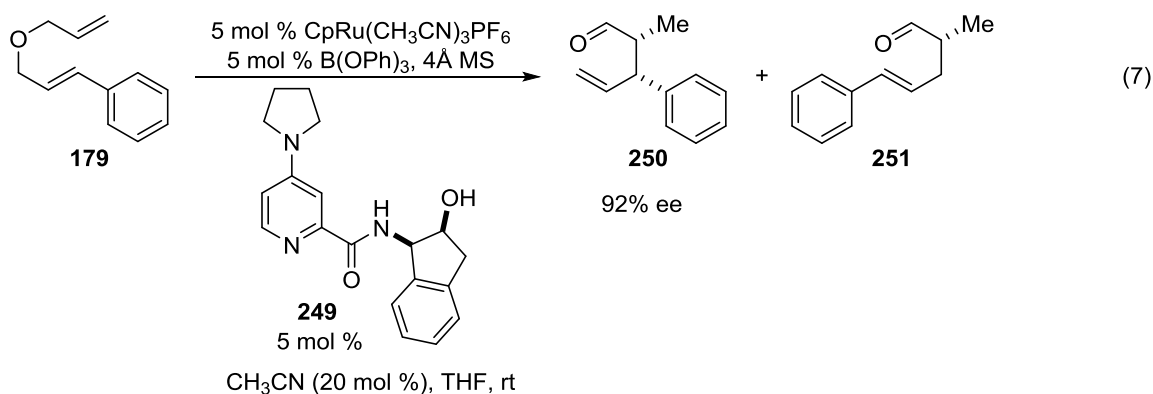


Figure 13. Asymmetric Ru (II)-catalyzed [3,3]-sigmatropic rearrangement of general allyl vinyl ether (**174**)

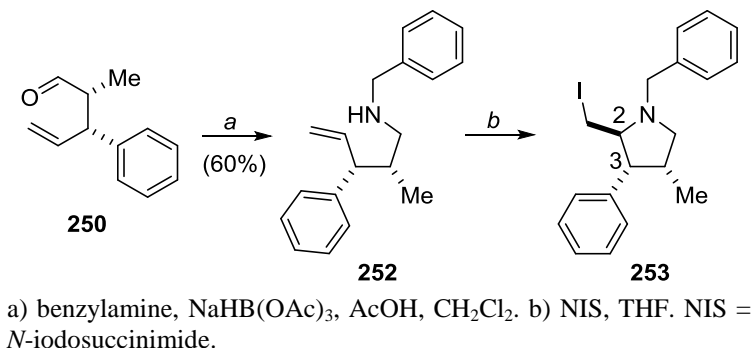
The mechanism of the transformation of allyl vinyl ether **174** to *anti*-product **247** involves the formation of π -allyl intermediate (**246**), which undergoes enantioselective attack by a ruthenium-bound enolate (Figure 13). Oxidative addition into the C-O σ -bond of allyl vinyl ether **174** is facilitated by the presence of Lewis acids, through oxygen coordination. In agreement with previous reports, the ruthenium-catalyzed rearrangement of allylic vinyl ether **179**, employing 5 mol % CpRu(CH₃CN)₃PF₆ and 5 mol % B(OPh)₃ as the Lewis acid provided *anti*-[3,3] product **250** and [1,3]-product **251** (**250**:**251** = 5:1, **250**_{*anti*}:**250**_{*syn*} = 10:1, 92% ee) in 91% yield (eq 7).



Reductive amination of (*2R*, *3R*)-2-methyl-3-phenylpent-4-enal (**250**) with benzylamine in the presence of sodium triacetoxyborohydride, followed by iodocyclization with *N*-

iodosuccinimide provided (2*S*,3*R*,4*R*)- β -iodo amine **253** (Scheme 30). NOESY analysis revealed no correlation between H₂ and H₃, suggesting an arrangement which diminishes steric interactions between the iodo and phenyl substituents. The relative stereochemistry of C₂ and C₃ is also in agreement with previous X-ray data (Figure 12).

Scheme 30. Synthesis of β -iodo amine **253**



4.6 CONCLUSIONS

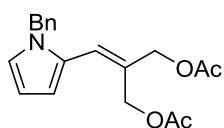
We have presented a novel route to the synthesis of diverse pyrrolidine scaffolds for diversity-oriented synthesis. This route involves the incorporation of a previously developed Ir(I)-based catalyst systems for selective isomerization of bis(allyl) ether substrates, as well as, reductive amination, iodocyclization, azide formation, and reductive deprotection protocols developed herein.⁴⁶ Additionally, an asymmetric approach to the synthesis of (2*S*,3*R*,4*R*)- β -iodo amine **253** has been presented using selective Ru(II)-catalyzed Claisen rearrangement methodology.⁴⁷ Pyrrolidine scaffolds present an avenue of interest, since to our knowledge no other diversity-oriented syntheses have previously been developed. Furthermore, our scaffolds are capable of further diversification through the incorporation of various electrophilic reagents.

5.0 EXPERIMENTAL

General Information: All reactions were performed in dry glassware under an atmosphere of oxygen-free nitrogen using standard inert atmosphere techniques for the manipulation of both solvents and reagents. Anhydrous solvents were obtained by passage through successive alumina- and Q5-packed columns on a solvent purification system. Acetone was distilled from Drierite[®] and stored under nitrogen over 4 Å MS. Sodium hydride (60% dispersion in mineral oil) and sodium triacetoxyborohydride were purchased from Sigma-Aldrich, and used directly. Palladium hydroxide (10% on carbon) and ammonium formate were purchased from Alfa-Aesar. Allyl bromide was purchased from Sigma-Aldrich and purified by distillation over CaH₂. Cinnamyl alcohol, [Ir (COE) Cl] ₂, and PCy₃ were purchased from Strem, and were stored and weighed out in a nitrogen-filled glove box. NMR spectra were recorded on a Bruker Avance-400 (400 MHz) spectrometer with chemical shifts reported relative to residual CHCl₃ (7.26 ppm) for ¹H and CDCl₃ (77.00 ppm) for ¹³C NMR spectra. Infrared spectra were recorded on a Nicolet Avatar 360 FT-IR spectrometer. High resolution mass spectra were obtained on a VG-7070 or Fisons Autospec high-resolution magnetic sector mass spectrometer. Analytical thin layer chromatography (TLC) was performed on EM Reagent 0.25 mm silica gel 60-F plates. Flash chromatography was performed over EM silica gel 60 (230-240 mesh). The *anti* Claisen adduct **250** utilized in the asymmetric synthesis was prepared according to literature procedure.⁴⁷ The enantiomer ratio was determined by chiral stationary phase GLC (Varian Chirasil-Dex CB

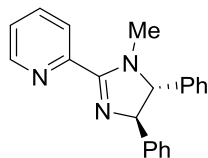
WCOT Fused Silica CP 7502 Column, 25m x 0.25 mm) and was assigned by comparison to previous reports.⁴⁷

5.1 EFFORTS TOWARDS THE SYNTHESIS OF MARINEOSIN A



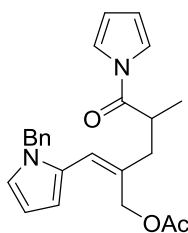
2-((1-Benzyl-1H-pyrrol-2-yl)methylene)propane-1,3-diol diacetate (**80**):

Acetyl chloride (3.0 equiv, 0.3 mL, 4.14 mmol) was added over 15 minutes to a solution of pyridine (4.0 equiv, 0.45 mL, 5.52 mmol) and 2-((1-benzyl-1H-pyrrol-2-yl)methylene)propane-1,3-diol (**79**) (335 mg, 1.38 mmol) in THF (3.0 mL) at 0°C . The reaction was then warmed to ambient temperature and stirred for 12 h. The resulting solution was quenched with 10 mL of water and the aqueous and organic portions were separated. The aqueous portion was extracted with Et₂O (3 x 10 mL) and the combined organic layers were washed with aqueous CuSO₄, water, and brine. The organic portion was dried over anhydrous Na₂SO₄, concentrated and purified by flash chromatography (40% ethyl acetate in hexanes) to afford 361 mg of the title compound (80%) as a light yellow oil. ¹H NMR (400 MHz, CDCl₃): δ 7.32-7.27 (m, 3H), 7.01-6.99 (m, 2H), 6.77 (app s, 1H), 6.47 (app s, 1H), 6.31 (app s, 1H), 6.22 (app s, 1H), 5.10 (s, 2H), 4.87 (s, 2H), 4.64 (s, 2H), 2.08 (s, 3H), 2.01 (s, 3H); ¹³C NMR (100 MHz, CDCl₃): δ 170.9, 170.7, 137.7, 128.8, 127.6, 126.4, 123.8, 122.9, 111.9, 108.8, 66.8, 61.52, 50.8, 20.9.²

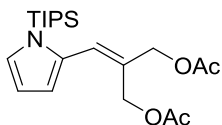


2-((4R,5R)-1-Methyl-4,5-diphenyl-4,5-dihydro-1H-imidazol-2-yl)pyridine

(90): ^1H NMR (400 MHz, CDCl_3): δ 8.71 (ddd, $J = 1.0, 2.0, 5.0$ Hz, 1H), 8.10 (td, $J = 1.0, 7.5$ Hz, 1H), 7.81 (dt, $J = 2.0, 8.0$ Hz, 1H), 7.32 (m, 11H), 4.99 (d, $J = 10.5, 1\text{H}$), 4.36 (d, $J = 10.5, 1\text{H}$), 2.99 (s, 3H). This compound was prepared according to literature procedure and matches the characterization data provided in the following the publication: Davenport, A. J.; Davies, D. L.; Fawcett, J.; Russell, D. R., *J. Chem. Soc. Perk. T I* **2001**, (13), 1500-1503.



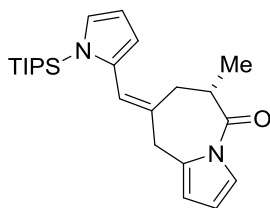
(Z)-2-((1-Benzyl-1H-pyrrol-2-yl)methylene)-4-methyl-5-oxo-5-(1H-pyrrol-1-yl)pentyl acetate (88): [$\text{Cp}^*\text{Ru}(\text{CH}_3\text{CN})_3$] PF_6 (5 mol %, 15.4 mg, 0.03 mmol) and ligand **90** (5 mol %, 9.6 mg, 0.03 mmol) were added to THF (1.22 mL) inside a nitrogen-filled glovebox, and the mixture was periodically agitated over 15 minutes. The resulting solution was then transferred to a mixture containing allylic diacetate **80** (200 mg, 0.61 mmol), (Z)-1-(1-((trimethylsilyl)oxy)prop-1-en-1-yl)-1H-pyrrole (**85**) (1.05 equiv, 125 mg, 0.64 mmol), and $\text{B}(\text{OPhNO}_2)_3$ (15 mol %, 38.9 mg, 0.09 mmol). The solution was removed from the glovebox and stirred at ambient temperature for 24 h. After 24 h the reaction mixture was concentrated under a stream of N_2 , diluted with pentanes and filtered through a pad of Florisil[®]. The product was purified by flash chromatography (30% ethyl acetate in hexanes) to afford 21 mg of the title compound (9%) as a light yellow oil. ^1H NMR (400 MHz, CDCl_3): δ 8.17 (d, $J = 9.0$ Hz, 1H), 7.31-7.28 (m, 3H), 6.98 (d, $J = 7.0$ Hz, 2H), 6.91 (d, $J = 9.0$ Hz, 1H), 6.71 (t, $J = 1.5$ Hz, 1H), 6.29-6.27 (m, 3H), 6.19-6.16 (m, 2H), 5.00 (s, 2H), 4.90 (d, $J = 12.5$ Hz, 1H), 4.79 (d, $J = 12.5$ Hz, 1H), 3.32 (m, 1H), 2.77 (m, 1H), 2.29 (m, 1H), 2.09 (s, 3H), 1.18 (d, $J = 6.5$ Hz, 3.0H); ^{13}C NMR (100 MHz, CDCl_3): δ 173.8, 171.1, 137.8, 131.3, 128.8, 128.0, 127.5, 126.4, 126.2, 123.0, 122.3, 119.0, 115.6, 113.3, 110.9, 108.3, 63.1, 50.7, 39.9, 37.1, 20.9, 17.5. ²



2-((1-(Triisopropylsilyl)-1H-pyrrol-2-yl)methylene)propane-1,3-diy

diacetate (84): Acetyl chloride (3.0 equiv, 0.63 mL, 8.73 mmol) was added

over 15 minutes to a solution of pyridine (4.0 equiv, 0.95 mL, 11.6 mmol) and 2-((1-(triisopropylsilyl)-1H-pyrrol-2-yl)methylene)propane-1,3-diol (**83**) (900 mg, 2.91 mmol) in THF (15 mL) at 0°C. The reaction was then warmed to ambient temperature and stirred for 12 h. The resulting solution was quenched with 30 mL of water and the aqueous and organic portions were separated. The aqueous portion was extracted with Et₂O (3 x 15 mL) and the combined organic layers were washed with aqueous CuSO₄, water, and brine. The organic portion was dried over anhydrous Na₂SO₄, concentrated and purified by flash chromatography (30% ethyl acetate in hexanes) to afford 1.01 g of the title compound (88%) as a light yellow oil. ¹H NMR (400 MHz, CDCl₃): δ 6.89 (d, *J* = 1.0 Hz, 1H), 6.74 (s, 1H), 6.33 (d, *J* = 2.0 Hz, 1H), 6.27 (t, *J* = 2.0 Hz, 1H), 4.87 (s, 2H), 4.72 (s, 2H), 2.09 (s, 3H), 2.08 (s, 3H), 1.53-1.45 (m, 3H), 1.08 (d, *J* = 5.5 Hz, 18H).¹



(*S,E*)-6-Methyl-8-((1-(triisopropylsilyl)-1H-pyrrol-2-yl)methylene)-

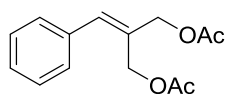
6,7,8,9-tetrahydro-5H-pyrrolo[1,2-a]azepin-5-one (89):

[Cp**Ru*(CH₃CN)₃]PF₆ (5 mol %, 6.40 mg, 0.01 mmol) and ligand **90** (5 mol

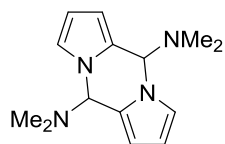
%, 4.0 mg, 0.01 mmol) were added to THF (0.5 mL) inside a nitrogen-filled

glovebox, and the mixture was periodically agitated over 15 minutes. The resulting solution was then transferred to a mixture containing allylic diacetate **84** (100 mg, 0.25 mmol), (*Z*)-1-(1-((trimethylsilyloxy)prop-1-en-1-yl)-1H-pyrrole (**85**) (1.05 equiv, 52 mg, 0.27 mmol), and B(OPhNO₂)₃ (15 mol %, 16.2 mg, 0.04 mmol). The solution was removed from the glovebox and stirred at ambient temperature for 24 h. After 24 h the reaction mixture was concentrated under a stream of N₂, diluted with pentanes and filtered through a pad of Florisil[®]. The resulting product was

purified by flash chromatography (15% ethyl acetate in hexanes) to afford the title compound as a white solid. Recrystallization of **89** from Et₂O/Hexanes yielded crystals suitable for X-ray diffraction analysis (Appendix A); ¹H NMR (400 MHz, CDCl₃): δ 7.43 (app s, 1H), 6.79 (app s, 1H), 6.32-6.03 (m, 5H), 3.78 (d, *J* = 15 Hz, 1H), 3.58 (d, *J* = 15 Hz, 1H), 3.20 (m, 1H), 2.76 (m, 2H), 1.42 (m, 3H), 1.36 (d, *J* = 6.5 Hz, 3H), 1.03 (d, *J* = 7.5 Hz, 18H); ¹³C NMR (100 MHz, CDCl₃): δ 173.2, 133.7, 132.2, 131.8, 125.8, 119.9, 119.3, 113.1, 111.2, 110.7, 109.9, 37.8, 36.8, 36.2, 18.1, 17.9, 12.9. ²



2-Benzylidene-1,3-diacetate (76): Acetyl chloride (3.0 equiv, 0.21 mL, 2.91 mmol) was added over 15 minutes to a solution of pyridine (4.0 equiv, 0.32 mL, 3.88 mmol) and 2-benzylidene-1,3-diol (**75**) (159 mg, 0.97 mmol) in THF (5 mL) at 0°C. The reaction was then warmed to ambient temperature and stirred for 12 h. The resulting solution was quenched with 10 mL of water and the aqueous and organic portions were separated. The aqueous portion was extracted with Et₂O (3 x 10 mL) and the combined organic layers were washed with aqueous CuSO₄, water, and brine. The organic portion was dried over anhydrous Na₂SO₄, concentrated and purified by flash chromatography (20% ethyl acetate in hexanes) to afford 216 mg of the title compound (90%) as a light yellow oil. ¹H NMR (400 MHz, CDCl₃): δ 7.37-7.23 (m, 5H), 6.84 (s, 1H), 4.78 (s, 2H), 4.74 (s, 2H), 2.11 (s, 3H), 2.08 (s, 3H). ¹

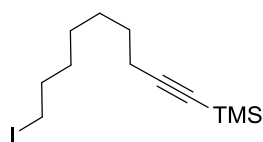


***N5, N5, N10, N10*-Tetramethyl-5*H*,10*H*-dipyrrolo[1,2-*a*:1',2'-*d*]pyrazine-**

5,10-diamine (103): ^1H NMR (400 MHz, CDCl_3): δ 6.96 (dd, $J = 2.5, 1.0$

Hz, 2H), 6.26 (dd, $J = 4.5, 4.0$ Hz, 2H), 6.17 (m, 2H), 5.87 (s, 2H), 2.22 (s,

12H). This compound was prepared according to literature procedure and matches the characterization data provided in the following the publication: Muchowski, J. M.; Hess, P. *Tetrahedron Lett.* **1988**, 29 (7), 777-780.

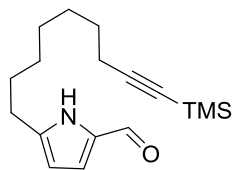


(9-Iodonon-1-yn-1-yl)trimethylsilane (108): *n*-Butyllithium (2.0 equiv,

56 mL, 78.5 mmol) was added drop wise to a solution of non-8-yn-1-ol

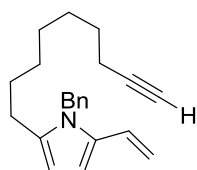
(106) (5.5 g, 39.2 mmol) in THF (131 mL) at -78 $^\circ\text{C}$, and the resulting

mixture was stirred for 1 h. After this time, chlorotrimethylsilane (2.5 equiv, 12.5 mL, 98 mmol) was added and the reaction was stirred an additional 30 min at -78 $^\circ\text{C}$. The resulting solution was then warmed to 0 $^\circ\text{C}$ and slowly quenched with 45 ml of water. The aqueous portion was extracted with Et_2O (3 x 50 mL) and the combined organic layers were washed with water, 2 M HCl, saturated aqueous NaHCO_3 , and brine. The organic portion was dried over anhydrous Na_2SO_4 and concentrated. The resulting residue was dissolved in CH_2Cl_2 (197 mL), and triphenylphosphine (1.2 equiv, 12.4 g, 47.1 mmol) and imidazole (2.0 equiv, 5.33 g, 78.4 mmol) were added at ambient temperature. Then mixture was then cooled to 0 $^\circ\text{C}$ prior to the addition of I_2 (1.2 equiv, 11.95 g, 47.1 mmol) and stirred for 1 h. After 1 h, the reaction was quenched with saturated aqueous $\text{Na}_2\text{S}_2\text{O}_3$ until the solution changed from red to clear. The aqueous portion was extracted with CH_2Cl_2 (3 x 50 mL), concentrated, diluted with hexanes and filtered through a pad of Celite[®]. ^1H NMR (400 MHz, CDCl_3): δ 3.19 (t, $J = 4.5$ Hz, 2H), 2.21 (t, $J = 9.5$ Hz, 2H), 1.80 (m, 2H), 1.41-1.26 (m, 8H), 0.1 (s, 9H).¹



5-(9-(Trimethylsilyl)non-8-yn-1-yl)-1H-pyrrole-2-carbaldehyde (109): *n*-

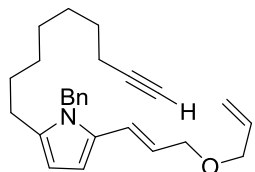
Butyllithium (3.0 equiv, 18.1 mL, 21.7 mmol) was added to a solution of azafulvene dimer **103** (1.77 g, 7.23 mmol) in THF (145 mL) at -15 °C, and stirred for 1.5 h. The resulting deep purple solution was cooled to -60 °C and a solution of iodoalkyne **108** (2.2 equiv, 5.13 g, 15.9 mmol) in THF (5 mL) was added. The pale yellow solution was warmed to ambient temperature and stirred 12 h, during which the solution became orange in color. After this time, 75 mL of saturated aqueous NaHCO₃ was added and the reaction solution was further diluted with THF (50 mL) and heated to 80 °C. The reaction was refluxed for 3 h at 80 °C, cooled to ambient temperature and poured into a solution of aqueous NaHCO₃ (50 mL). The aqueous portion was extracted with Et₂O (3 x 50 mL), and the combined organic layers were washed with water and brine. The organic portion was dried over anhydrous Na₂SO₄, concentrated and purified by flash chromatography (30% ethyl acetate in hexanes) to afford 1.32 g of the title compound (32%) as a yellow oil. ¹H NMR (400 MHz, CDCl₃): δ 9.37 (s, 1H), 9.31 (broad s, 1H), 6.89 (t, *J* = 3.0 Hz, 1H), 6.08 (t, *J* = 3.0 Hz, 1H), 2.66 (t, *J* = 7.5 Hz, 2H), 2.22 (t, *J* = 7.0 Hz, 2H), 1.52 (m, 2H), 1.40 (m, 8H), 0.1 (s, 9H). ¹



1-Benzyl-2-(non-8-yn-1-yl)-5-vinyl-1H-pyrrole (114): Potassium carbonate

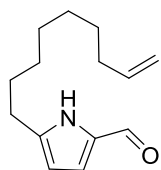
(2.0 equiv, 554 mg, 4.0 mmol) was added to a solution of 1-benzyl-2-(9-(trimethylsilyl)non-8-yn-1-yl)-5-vinyl-1H-pyrrole (**113**) (757 mg, 2.0 mmol) in MeOH/THF (10 mL/4 mL) at ambient temperature and stirred 2 h. The resulting solution was diluted with Et₂O (20 mL), filtered through a pad of Celite® then purified by flash chromatography (10% ethyl acetate in hexanes) to afford 480 mg the title compound (78%) as a light yellow oil. ¹H NMR (400 MHz, CDCl₃): δ 7.33-7.22 (m, 3H), 6.91 (d, *J* = 7.5 Hz), 6.42 (m, 2

H), 5.96 (d, $J = 3.0$ Hz, 1H), 5.42 (d, $J = 17$ Hz, 1H), 5.11 (s, 2H), 4.88 (d, $J = 11$ Hz), 2.45 (t, $J = 7.5$ Hz, 2H), 2.15 (t, $J = 7.0$ Hz, 2H), 1.92 (t, $J = 3.0$ Hz, 1H), 1.56-1.46 (m, 2H), 1.34-1.28 (m, 8H).¹



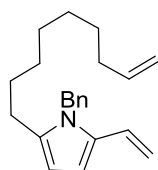
(E)-2-(3-(Allyloxy)prop-1-en-1-yl)-1-benzyl-5-(non-8-yn-1-yl)-1H-pyrrole (122): (*E*)-3-(1-Benzyl-5-(non-8-yn-1-yl)-1H-pyrrol-2-yl)prop-2-en-1-ol (**121**) (100 mg, 0.30 mmol) was slowly added to a suspension of

NaH (1.3 equiv, 16.0 mg, 0.39 mmol) in THF (20 mL) at 0 °C. The resulting mixture was warmed to ambient temperature and stirred for 1.5 h. After this time, allyl bromide (1.2 equiv, 30.0 μ L, 0.36 mmol) was added and the reaction was stirred 3 h before being quenched with 25 mL of water. The aqueous portion was extracted with Et₂O (3 x 40 mL) and the combined organic layers were washed with water, and brine. The organic portion was dried over anhydrous Na₂SO₄, concentrated and purified by flash chromatography (20% ethyl acetate in hexanes) to afford 50 mg of the title compound (44%) as a light yellow oil. ¹H NMR (400 MHz, CDCl₃): δ 7.31-7.22 (m, 3H), 6.91-6.89 (m, 2H), 6.38 (d, $J = 3.5$ Hz, 1H), 6.35 (d, $J = 15$ Hz, 1H), 6.03-5.81 (m, 3 H), 5.14-5.10 (m, 4H), 4.09 (d, $J = 5.5$ Hz, 2H), 3.89 (d, $J = 5.5$ Hz, 2H), 2.44 (t, $J = 7.5$ Hz, 2 H), 2.14 (dt, $J = 2.5, 4.0$ Hz, 2H), 1.92 (t, $J = 3.0$ Hz, 1H), 1.56-1.46 (m, 2H), 1.36-1.26 (m, 8H).¹



5-(Non-8-en-1-yl)-1H-pyrrole-2-carbaldehyde (127): ¹H NMR (400 MHz, CDCl₃): δ 9.58, (broad s, 1H) 9.53 (s, 1H), 6.89 (appt s, 1H), 6.08 (appt s, 1H), 5.84-5.75 (m, 1H), 5.01-4.92 (m, 2H), 2.66 (t, $J = 7.5$ Hz, 2H), 2.05-2.00 (m, 2H),

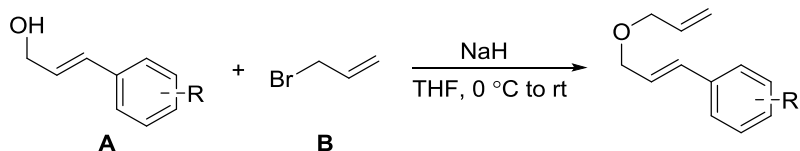
1.67-1.63 (m, 3H), 1.39-1.26 (m, 10H). This compound was prepared according to the following the publication: Muchowski, J. M.; Hess, P. *Tetrahedron Lett.* **1988**, 29 (7), 777-780.



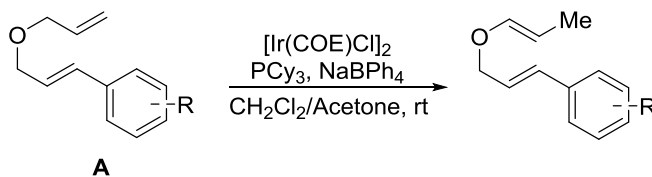
1-Benzyl-2-(non-8-en-1-yl)-5-vinyl-1H-pyrrole (128): Potassium

hexamethyldisilazide (1.3 equiv, 6.14 mL, 3.07 mmol) was added to a solution of methyltriphenylphosphonium bromide (1.5 equiv, 1.26 g, 3.54 mmol) in THF (35 mL) at ambient temperature, and was stirred vigorously for 30 min. After 30 min, a solution of aldehyde **127** (730 mg, 2.36 mmol) in THF (24 mL) was added and the reaction was stirred an additional 1 h. The resulting solution was poured into 130 mL of Et₂O: water (1:1) and the aqueous and organic layers were separated. The aqueous portion was extracted with Et₂O (3 x 50 mL) and the combined organic layers were washed with water, and brine. The organic portion was dried over anhydrous Na₂SO₄, concentrated and purified by flash chromatography (20% ethyl acetate in hexanes) to afford 551 mg of the title compound (76%) as a light yellow oil. ¹H NMR (400 MHz, CDCl₃): δ 7.32-7.18 (m, 3H), 6.92-6.90 (m, 2H), 6.44-6.39 (m, 2H), 5.96 (d, *J* = 3.5 Hz, 1H), 5.79 (m, 1H), 5.42 (dd, *J* = 1.5, 150.5 Hz, 1H), 5.11 (s, 2H), 5.00-4.89 (m, 3H), 2.45 (t, *J* = 7.5 Hz, 2H), 2.00 (m, 2H), 1.53 (m, 2H), 1.35-1.25 (m, 8H). ¹

5.2 DEVELOPMENT OF PYRROLIDINE SCAFFOLDS FOR DIVERSITY- ORIENTED SYNTHESIS

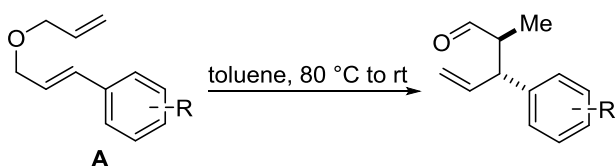


General Procedure for the Formation of Di(Allyl) Ethers (General Procedure A): Sodium Hydride (1.3 equiv, 60% suspension in mineral oil) was added to a solution of alcohol **A** (1.0 equiv) in THF (0.8 M) at 0 °C, and the solution stirred 30 minutes. Allyl bromide **B** (1.2 equiv) was added and the resulting suspension was warmed to ambient temperature and stirred an additional 3 hrs. The reaction mixture was slowly quenched with a saturated solution of NH₄Cl and extracted with Et₂O. Combined organic extracts were dried over anhydrous Na₂SO₄ and concentrated. The crude product was further purified by flash chromatography.



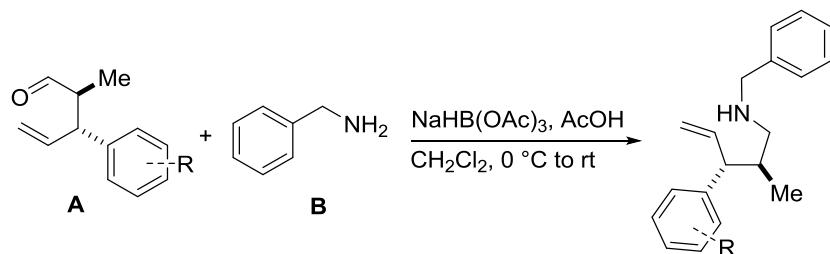
General Procedure for the Formation Allyl Vinyl Ethers (General Procedure B): [Ir(COE)Cl]₂ (0.5 mol %), PCy₃ (3 mol %) and NaBPh₄ (2 mol %) were combined in a nitrogen-filled glovebox. Immediately after removal from the glovebox, a solution of CH₂Cl₂/acetone (0.6 M, 30:1) was added and the resulting red-orange solution was stirred 5 min at ambient temperature. Di(Allyl) ether **A** (1 equiv) was added to the catalyst solution in a minimal amount of CH₂Cl₂ and the reaction was monitored by TLC (1-30 min.). The reaction mixture was

concentrated under a steam of N₂, diluted with pentanes and the resulting heterogeneous mixture was filtered through a pad of Florisil[®]. The resulting solution was then concentrated and purified by flash chromatography.



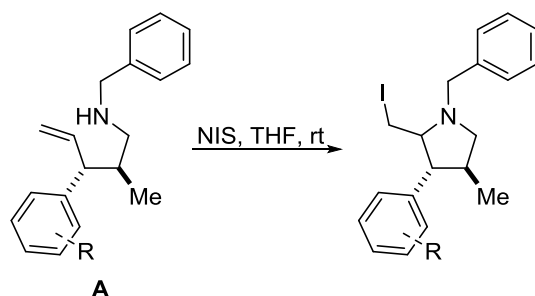
General Procedure for the Formation of γ, δ -Unsaturated Aldehydes (General Procedure C):

C): Allyl vinyl ether **A** (1.0 equiv) was added to toluene (0.5 M) and the reaction was heated to 80 °C and stirred for 12 hrs. The resulting solution was then concentrated and purified by flash chromatography.



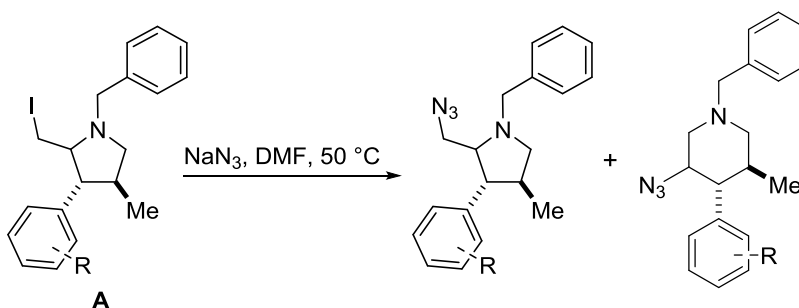
General Procedure for the Formation of γ, δ -Unsaturated Amines (General Procedure D):

Aldehyde **A** (1.0 equiv), NaHB(OAc)₃ (2.0 equiv), benzylamine (2.0 equiv), and acetic acid (1.0 equiv) were added to CH₂Cl₂ (0.1M) at 0 °C. After 15 minutes the reaction was warmed to rt and stirred an additional 12 hrs. The resulting solution was quenched with sodium carbonate (0.1M) and extracted with CH₂Cl₂. Combined organic extracts were dried over anhydrous Na₂SO₄ and concentrated. The crude product was further purified by flash chromatography.



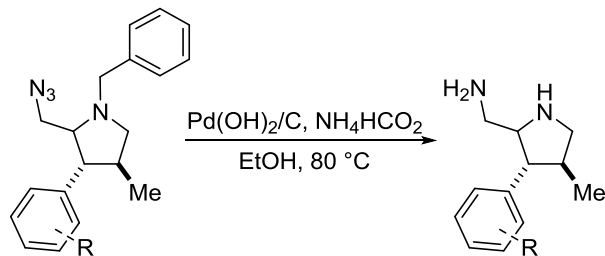
General Procedure for the Formation of β -Iodo Pyrrolidines (General Procedure E):

Pentenamine **A** (1.0 equiv) and NIS (1.1 equiv) were added to THF (0.3 M) at ambient temperature and the reaction was stirred for 1 hr. The resulting mixture was then concentrated and immediately purified by flash chromatography.



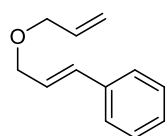
General Procedure for the Formation of β -Azido Pyrrolidines and 3-AzidoPiperdines

(General Procedure F): Pyrrolidine **A** (1.0 equiv) and NaN_3 (1.5 equiv) were added to DMF (0.12 M) and the reaction was heated to 50 °C and stirred for 1h. The resulting solution was diluted with water (0.1M) and extracted with CH_2Cl_2 . Combined organic layers were dried over anhydrous Na_2SO_4 and concentrated. The crude product was then purified by flash chromatography.

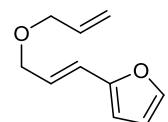


General Procedure for the Formation of β -Amino Pyrrolidines (General Procedure G):

Pyrrolidine A (1 equiv) was added drop wise to a slurry of $\text{Pd}(\text{OH})_2/\text{C}$ (10 mol %) and NH_4HCO_2 (12.5 equiv) in EtOH (0.5 M) at rt. After 30 minutes, the reaction was warmed to 80 °C and refluxed for an additional 4 hrs. The mixture was then cooled and filtered through a pad of Celite[®] eluting with MeOH. The resulting viscous oil was purified by reverse phase MPLC.

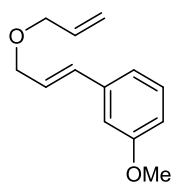


(E)-3-(Allyloxy)prop-1-en-1-ylbenzene (179): General procedure A was followed employing 2.87 mL of cinnamyl alcohol (22.3 mmol), 1.16 g of NaH (29 mmol), and 2.33 mL of allyl bromide (26.7 mmol) in 30 mL of THF. The resulting product was purified by flash chromatography (10% diethyl ether in hexanes) to afford 3.90 g of the title compound (93%) as a colorless oil. This compound matches the characterization data provided in the following the publication: Kerrigan, N. J.; Bungard, C. J.; Nelson, S. G. *Tetrahedron* **2008** (64) 6863-6869.



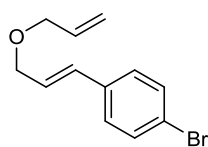
(E)-2-(3-(Allyloxy)prop-1-en-1-yl)furan (213): General procedure A was followed employing 1.2 g of (*E*)-3-(furan-2-yl)prop-2-en-1-ol (10 mmol), 521mg of NaH (13 mmol), and 1.0 mL of allyl bromide (12 mmol) in 12.5 mL of THF. The resulting product was purified by flash chromatography (10% diethyl ether in hexanes) to afford 1.6 g of the title compound (99%) as a colorless oil. This compound matches the characterization data

provided in the following the publication: Geherty, M. Catalytic Asymmetric Claisen Rearrangements. The Development of Ru(II)-Catalyzed Formal [3,3] Sigmatropic Rearrangements and Related Enolate Allylation Reactions. Ph.D. Thesis, University of Pittsburgh, December 2012.



(E)-1-(3-(Allyloxy)prop-1-en-1-yl)-3-methoxybenzene (214): General

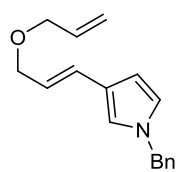
procedure A was followed employing 1.73 g of (*E*)-3-(3-methoxyphenyl)prop-2-en-1-ol (11 mmol), 557 mg of NaH (14.3 mmol), and 1.14 mL of allyl bromide (13.2 mmol) in 13 mL of THF. The resulting product was purified by flash chromatography (10% diethyl ether in hexanes) to afford 2.2 g of the title compound (99%) as a colorless oil. This compound matches the characterization data provided in the following the publication: Geherty, M. Catalytic Asymmetric Claisen Rearrangements. The Development of Ru(II)-Catalyzed Formal [3,3] Sigmatropic Rearrangements and Related Enolate Allylation Reactions. Ph.D. Thesis, University of Pittsburgh, December 2012.



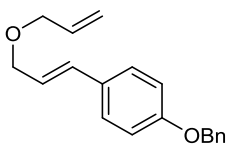
(E)-1-(3-(Allyloxy)prop-1-en-1-yl)-4-bromobenzene (215): General

procedure A was followed employing 2.10 g of (*E*)-3-(4-bromophenyl)prop-2-en-1-ol (10 mmol), 521 mg of NaH (13.1 mmol), and 1.0 mL of allyl bromide (12 mmol) in 12 mL of THF. The resulting product was purified by flash chromatography (50 % diethyl ether in hexanes) to afford 2.33 g of the title compound (92%) as a colorless oil. This compound matches the characterization data provided in the following the publication: Geherty, M. Catalytic Asymmetric Claisen Rearrangements. The Development of Ru(II)-Catalyzed Formal [3,3] Sigmatropic Rearrangements and Related Enolate Allylation

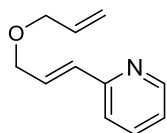
Reactions. Ph.D. Thesis, University of Pittsburgh, December 2012.



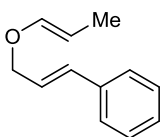
(E)-3-(3-(Allyloxy)prop-1-en-1-yl)-1-benzyl-1H-pyrrole (211): General procedure A was followed employing 165 mg of (*E*)-3-(1-benzyl-1H-pyrrol-3-yl)prop-2-en-1-ol (0.77 mmol), 40.1 mg of NaH (1.0 mmol), and 80 μ L of allyl bromide (0.92 mmol) in 4 mL of THF. The resulting product was purified by flash chromatography (50 % diethyl ether in hexanes) to afford 180 mg of the title compound (92%) as a light yellow oil. ^1H NMR (400 MHz, CDCl_3): δ 7.42-7.27 (m, 3H), 7.13 (d, $J = 7.0$ Hz, 2H), 6.64 (t, $J = 8.0$ Hz, 1H), 6.63 (m, 1H), 6.50 (s, 1H), 6.33 (m, 1H), 6.01-5.92 (m, 2H), 5.33 (d, $J = 1.5$ Hz, 1H), 5.29 (d, $J = 1.5$ Hz, 1H), 5.18 (s, 2H), 4.10 (d, $J = 7.0$ Hz, 2H), 4.02 (d, $J = 6.0$ Hz, 2H).



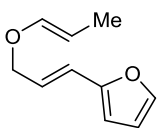
(E)-1-(3-(Allyloxy)prop-1-en-1-yl)-4-(benzyloxy)benzene (212): General procedure A was followed employing 1.0 g of (*E*)-3-(4-bromophenyl)prop-2-en-1-ol (4.16 mmol), 217 mg of NaH (5.40 mmol), and 0.432 mL of allyl bromide (5 mmol) in 13 mL of THF. The resulting product was purified by flash chromatography (8 % ethyl acetate in hexanes) to afford 1.6 g of the title compound (100%) as a colorless oil. ^1H NMR (400 MHz, CDCl_3): δ 7.42-7.31 (m, 5H), 6.92 (d, $J = 9.0$ Hz, 2H), 6.54 (d, $J = 15.5$ Hz, 1H), 6.16 (dt, $J = 6.5, 6.0$ Hz, 1H), 5.95 (m, 1H), 5.30 (dd, $J = 1.0, 1.6$ Hz, 1H), 5.21 (d, $J = 10.5$ Hz, 1H), 5.06 (s, 2H), 4.13 (d, $J = 6.0$ Hz, 2H), 4.02 (d, $J = 6.0$ Hz, 2H).



(E)-2-(3-(Allyloxy)prop-1-en-1-yl)pyridine (216): General procedure A was followed employing 540 mg of (*E*)-3-(pyridin-2-yl) prop-2-en-1-ol (4 mmol), 208 mg of NaH (5.2 mmol), and 0.415 mL of allyl bromide (4.8 mmol) in 5 ml of THF. The resulting product was purified by flash chromatography (10% ethyl acetate in hexanes) to afford 624mg of the title compound (89%) as a colorless oil. ¹H NMR (400 MHz, CDCl₃): δ 8.55 (d, *J* = 4.5 Hz, 1H), 7.62 (dt, *J* = 1.5, 6.0 Hz, 1H), 7.29 (d, *J* = 7.5 Hz, 1H), 7.12 (dt, *J* = 1.5, 6.0 Hz, 1H), 6.79 (m, 2H), 5.97 (m, 1H), 5.32 (dd, *J* = 1.5, 15.5 Hz, 1H), 5.21 (dd, *J* = 1.0, 9.0 Hz, 1H), 4.22 (d, *J* = 4.5, 2H), 4.06 (d, *J* = 5.5 Hz, 2H).

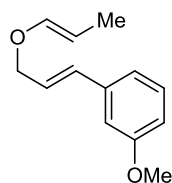


((E)-3-(((E)-Prop-1-en-1-yl)oxy)prop-1-en-1-yl)benzene (180): General procedure B was followed employing 2.0 g of di(allyl) ether **179** (11.5 mmol), 52 mg of [Ir(COE)Cl]₂ (0.057 mmol), 96 mg of PCy₃ (0.345 mmol), and 79 mg of NaBPh₄ (0.23 mmol) in 18.4 mL of CH₂Cl₂/ 0.6 mL Acetone. The resulting product was purified by flash chromatography (gradient elution 5% diethyl ether in hexanes) to afford 1.5 g of the title compound (75%) as a colorless oil. This compounds characterization materials match the data provided in the following publication: Kerrigan, N. J.; Bungard, C. J.; Nelson, S. G. *Tetrahedron* **2008** (64) 6863-6869.



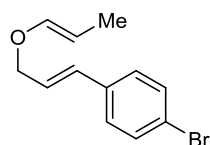
2-(((E)-3-(((E)-Prop-1-en-1-yl)oxy)prop-1-en-1-yl)furan (219): General procedure B was followed employing 1.6 g of di(allyl) ether **213** (10 mmol), 44.8 mg of [Ir(COE)Cl]₂ (0.05 mmol), 84 mg of PCy₃ (0.3 mmol), and 68.4 mg of NaBPh₄ (0.2 mmol) in 16.4 mL of CH₂Cl₂/ 0.6 mL Acetone. The resulting product was purified by flash chromatography (5% diethyl ether in hexanes) to afford 1.1 g of the title compound (75%)

as a colorless oil. This compounds characterization materials match the data provided in the following publication: Geherty, M. E.; Dura, R. D.; Nelson, S. G. *J. Am. Chem. Soc.* **2010**, 132, 11875-11877.



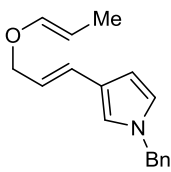
1-Methoxy-3-((E)-3-(((E)-prop-1-en-1-yl)oxy)prop-1-en-1-yl)benzene (220):

General procedure B was followed employing 2.32 g of di(allyl) ether **214** (11 mmol), 49.28 mg of $[\text{Ir}(\text{COE})\text{Cl}]_2$ (0.055 mmol), 92.4 mg of PCy_3 (0.33 mmol), and 75.24 mg of NaBPh_4 (0.22 mmol) in 17.4 mL of CH_2Cl_2 / 0.6 mL Acetone. The resulting product was purified by flash chromatography (10% diethyl ether in hexanes) to afford 1.95 g of the title compound (84%) as a colorless oil. This compounds characterization materials match the data provided in the following publication: Geherty, M. E.; Dura, R. D.; Nelson, S. G. *J. Am. Chem. Soc.* **2010**, 132, 11875-11877.



1-Bromo-4-((E)-3-(((E)-prop-1-en-1-yl)oxy)prop-1-en-1-yl)benzene (221):

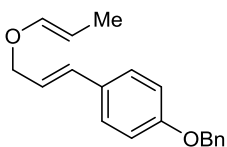
General procedure B was followed employing 2.51 g of di(allyl) ether **215** (10 mmol), 44 mg of $[\text{Ir}(\text{COE})\text{Cl}]_2$ (0.05 mmol), 84 mg of PCy_3 (0.3 mmol), and 68.1 mg of NaBPh_4 (0.2 mmol) in 16.5 mL of CH_2Cl_2 / 0.5 mL Acetone. The resulting product was purified by flash chromatography (10% ethyl acetate in hexanes) to afford 1.80 g of the title compound (72%) as a colorless oil. This compounds characterization materials match the data provided in the following publication: Geherty, M. Catalytic Asymmetric Claisen Rearrangements. The Development of Ru(II)-Catalyzed Formal [3,3] Sigmatropic Rearrangements and Related Enolate Allylation Reactions. Ph.D. Thesis, University of Pittsburgh, December **2012**.



1-Benzyl-3-((E)-3-(((E)-prop-1-en-1-yl)oxy)prop-1-en-1-yl)-1H-pyrrole

(217): General procedure B was followed employing 180 mg of di(allyl) ether **211** (0.71 mmol), 3.18 mg of $[\text{Ir}(\text{COE})\text{Cl}]_2$ (3.5 mmol), 96 mg of

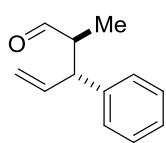
PCy_3 (0.21 mmol), and 79 mg of NaBPh_4 (0.014 mmol) in 1.1 mL of CH_2Cl_2 / 0.2 mL Acetone. The resulting product was utilized directly without purification to afford 121 g of the title compound (67%) as a light yellow oil. ^1H NMR (400 MHz, CDCl_3): δ 7.35-7.30 (m, 3H), 7.11 (d, $J = 8.5$ Hz, 2H), 6.92 (t, $J = 1.5$ Hz, 1H), 6.17 (t, $J = 2.0$ Hz, 1H), 6.49 (d, $J = 15.5$ Hz, 1H), 6.32 (t, $J = 1.5$ Hz, 1H), 6.24 (dd, $J = 1.5, 11.0$ Hz, 1H), 5.96 (dt, $J = 6.5, 15.5$ Hz, 1H), 5.00 (s, 2H), 4.84 (m, 1H), 4.25 (dd, $J = 1, 5.5$ Hz, 2H), 1.55 (d, $J = 5.5$ Hz, 3H).



1-(Benzyloxy)-4-((E)-3-(((E)-prop-1-en-1-yl)oxy)prop-1-en-1-yl)benzene

(218): General procedure B was followed employing 1.0 g of di(allyl)

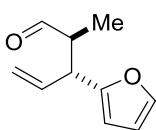
ether **212** (3.56 mmol), 16 mg of $[\text{Ir}(\text{COE})\text{Cl}]_2$ (0.017 mmol), 30 mg of PCy_3 (0.11 mmol), and 24.5 mg of NaBPh_4 (0.071 mmol) in 5.8 mL of CH_2Cl_2 / 0.2 mL Acetone. The resulting product was utilized directly without further purification to afford 0.85 g of the title compound (85%) as a white solid. ^1H NMR (400 MHz, CDCl_3): δ 7.38-7.31 (m, 7H), 6.92 (d, $J = 8.5$ Hz, 2H), 6.57 (d, $J = 16.0$ Hz, 1H), 6.27 (d, $J = 16.0$ Hz, 1H), 6.16 (dt, $J = 6.5, 15.5$ Hz, 1H), 5.07 (s, 2H), 4.86 (m, 1H), 4.31 (d, $J = 6.5$ Hz, 2H), 1.56 (d, $J = 5.0$ Hz, 3H).



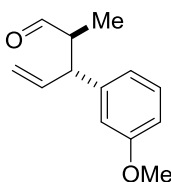
rac-(2R,3S)-2-Methyl-3-phenylpent-4-enal (181): General procedure C was followed employing 2.8 g of allyl vinyl ether **180** (16 mmol) in 32 mL of toluene.

The resulting product was utilized directly without further purification to afford 2.8 g of the title compound (99%). This compounds characterization materials match the data

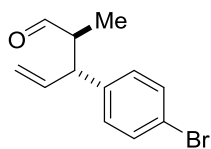
provided in the following publication: Kerrigan, N. J.; Bungard, C. J.; Nelson, S. G. *Tetrahedron* **2008**, *64* (29), 6863-6869.



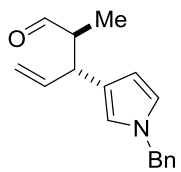
***rac*-(2*R*,3*S*)-3-(Furan-2-yl)-2-methylpent-4-enal (234)**: General procedure C was followed employing 519 mg of allyl vinyl ether **219** (3.16 mmol) in 7 mL of toluene. The resulting product was utilized directly without further purification to afford 490 mg of the title compound (94%). This compounds characterization materials match the data provided in the following publication: Geherty, M. E.; Dura, R. D.; Nelson, S. G. *J. Am. Chem. Soc.* **2010**, *132*, 11875-11877.



***rac*-(2*R*,3*S*)-3-(3-Methoxyphenyl)-2-methylpent-4-enal (235)**: General procedure C was followed employing 1.95 g of allyl vinyl ether **220** (10 mmol) in 20 mL of toluene. The resulting product was utilized directly without further purification to afford 1.89 g of the title compound (97%). This compounds characterization materials match the data provided in the following publication: Geherty, M. E.; Dura, R. D.; Nelson, S. G. *J. Am. Chem. Soc.* **2010**, *132*, 11875-11877.



***rac*-(2*R*,3*S*)-3-(4-Bromophenyl)-2-methylpent-4-enal (236)**: General procedure C was followed employing 1.26 g of allyl vinyl ether **221** (5 mmol) in 10 mL of toluene. The resulting product was utilized directly without further purification to afford 1.16 g of the title compound (92%). This compounds characterization materials match the data provided in the following publication: Geherty, M. E.; Dura, R. D.; Nelson, S. G. *J. Am. Chem. Soc.* **2010**, *132*, 11875-11877.



***rac*-(2*R*,3*S*)-3-(1-Benzyl-1H-pyrrol-3-yl)-2-methylpent-4-enal (232):** General

procedure C was followed employing 40 mg of allyl vinyl ether **217** (0.15 mmol)

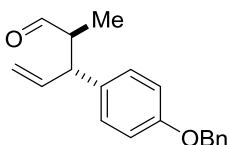
in 5 mL of toluene. The resulting product was utilized directly without further

purification to afford 35 mg of the title compound (87%). ¹H NMR (300 MHz, CDCl₃): δ 9.71

(d, *J* = 2.5 Hz, 1H), 7.38-7.28 (m, 3H), 7.10 (d, *J* = 6.0 Hz, 2H), 6.54 (t, *J* = 2.5 Hz, 1H), 6.50 (t,

J = 2.0 Hz, 1H), 6.4 (d, *J* = 3.0 Hz, 1H), 5.99 (m, 1H), 5.13 (m, 2H), 5.02 (s, 2H), 3.61 (t, *J* =

7.5 Hz, 1H), 2.70 (dt, *J* = 2.5, 4.5 Hz, 1H), 0.89 (d, *J* = 7.5 Hz, 3H).



***rac*-(2*R*,3*S*)-3-(4-(Benzyloxy)phenyl)-2-methylpent-4-enal (233):** General

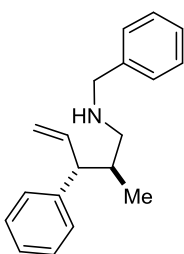
procedure C was followed employing 633 g of allyl vinyl ether **218** (2.25

mmol) in 5 mL of toluene. The resulting product was utilized directly

without further purification to afford 517 mg of the title compound (82%). ¹H NMR (400 MHz,

CDCl₃): δ 9.70 (d, 3.0 Hz, 1H), 7.47-6.95 (m, 9H), 6.02 (m, 1H), 5.11 (m, 2H), 5.05 (s, 2H),

3.51 (t, *J* = 9.0 Hz, 1H), 2.76 (dt, *J* = 3.5, 7.0 Hz, 1H), 0.94 (d, *J* = 7.0 Hz, 3H).



***rac*-(2*R*,3*S*)-*N*-Benzyl-2-methyl-3-phenylpent-4-en-1-amine (185):** General

procedure D was followed employing 100 mg **181** (0.57 mmol), 242 mg of

NaHB(OAc)₃ (1.15 mmol), 0.125 mL of benzylamine (1.15 mmol), and 33 μL

of acetic acid (0.57 mmol) in 6 mL of CH₂Cl₂. The crude product was purified

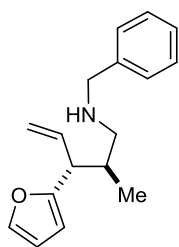
by flash chromatography (50% diethyl ether in hexanes) to afford 99 mg of the title compound

(65%) as a light yellow oil. ¹H NMR (400 MHz, CDCl₃): δ 7.33-7.15 (m, 10H), 6.06 (m, 1H),

5.01 (m, 2H), 3.77 (d, *J* = 9.0 Hz, 2H), 3.14 (t, *J* = 9.0 Hz, 1H), 2.76 (dd, *J* = 5.0, 7.0 Hz, 1H),

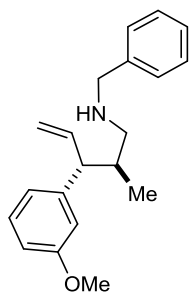
2.45 (m, 1H), 2.06 (m, 1H), 0.79 (d, *J* = 6.5 Hz, 3H); ¹³C NMR (100 MHz, CDCl₃): δ 143.3,

141.0, 128.4, 128.1, 127.5, 126.3, 115.0, 54.9, 54.2, 53.6, 37.9, 16.4; IR (thin film): 3061, 3026, 2961, 2875, 2816, 1492, 1452, 1117, 1072, 1028, 994, 913, 736 cm^{-1} ; HRMS (ESI) m/z calcd for $\text{C}_{19}\text{H}_{24}\text{N}$ ($\text{M} + \text{H}$)⁺: 266.1909; found 266.1906.



***rac*-(2*R*,3*S*)-*N*-Benzyl-3-(furan-2-yl)-2-methylpent-4-en-1-amine (234b):**

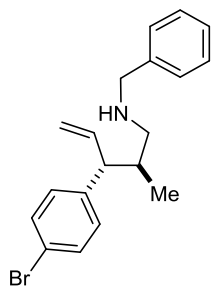
General procedure D was followed employing 490 mg of **234** (2.98 mmol), 1.26 mg of $\text{NaHB}(\text{OAc})_3$ (5.96 mmol), 0.652 mL of benzylamine (5.96 mmol), and 0.172 mL of acetic acid (2.98 mmol) in 30 mL of CH_2Cl_2 . The crude product was purified by flash chromatography (60% diethyl ether in hexanes) to afford 600 mg of the title compound (79%) as a colorless oil. ^1H NMR (400 MHz, CDCl_3): δ 7.25-7.19 (m, 6H), 6.21 (t, $J = 2.0$ Hz, 1H), 5.89 (d, $J = 3$ Hz, 1H), 5.88 (m, 1H), 5.04-5.00 (m, 2H), 3.68 (d, $J = 3.5$ Hz, 2H), 3.40 (t, $J = 7.5$ Hz), 2.58 (dd, $J = 5.0, 6.5$ Hz, 1H), 2.36 (m, 1H), 2.03 (m, 1H), 0.81 (d, $J = 6.5$ Hz, 3H); ^{13}C NMR (100 MHz, CDCl_3): δ 155.9, 140.8, 137.4, 128.1, 127.8, 126.6, 116.0, 109.8, 105.7, 53.9, 52.9, 47.1, 37.02, 15.7; IR (thin film): 3063, 3030, 2973, 1640, 1557, 1500, 1454, 1402, 1279, 1148, 1010, 922, 734 cm^{-1} ; HRMS (ESI) m/z calcd for $\text{C}_{17}\text{H}_{22}\text{NO}$ ($\text{M} + \text{H}$)⁺: 256.1701; found 256.1711.



***rac*-(2*R*,3*S*)-*N*-Benzyl-3-(3-methoxyphenyl)-2-methylpent-4-en-1-amine**

(235b): General procedure D was followed employing 2.10 g of **235** (10 mmol), 4.2 g of $\text{NaHB}(\text{OAc})_3$ (20 mmol), 2.25 mL of benzylamine (20 mmol), and 0.590 mL of acetic acid (10 mmol) in 100 mL of CH_2Cl_2 . The crude product was purified by flash chromatography (60% diethyl ether in hexanes) to afford 2.01 g of the title compound (65%) as a light yellow oil. ^1H NMR (400 MHz, CDCl_3): δ 7.33-

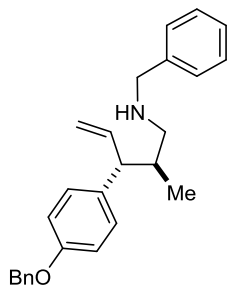
7.20 (m, 7H), 6.74 (m, 2H), 6.00 (m, 1H), 5.02 (m, 2H), 3.78 (m, 5H), 3.10 (t, $J = 8.0$ Hz, 1H), 2.77 (dd, $J = 4.5, 7.0$ Hz, 1H), 2.46 (m, 1H), 2.03 (m, 1H), 0.81 (d, $J = 6.5$ Hz, 3H); ^{13}C NMR (100 MHz, CDCl_3): δ 159.6, 145.1, 140.9, 129.3, 128.3, 128.0, 126.8, 120.4, 115.0, 114.0, 111.1, 55.0, 54.2, 53.6, 37.8, 16.4; IR (thin film): 3062, 3026, 2999, 2957, 2904, 2832, 1600, 1584, 1489, 1453, 1316, 1262, 1161, 1117, 1047, 994, 913, 780, 735 cm^{-1} ; HRMS (ESI) m/z calcd for $\text{C}_{20}\text{H}_{25}\text{NO}$ ($\text{M} + \text{H}$) $^+$: 295.1936; found 295.1918.



***rac*-(2*R*,3*S*)-*N*-Benzyl-3-(4-bromophenyl)-2-methylpent-4-en-1-amine**

(236b): General procedure D was followed employing 1.0 g of **236** (3.95 mmol), 1.67 g of $\text{NaHB}(\text{OAc})_3$ (8.0 mmol), 0.870 mL of benzylamine (8.0 mmol), and 0.225 mL of acetic acid (4.0 mmol) in 40 mL of CH_2Cl_2 . The crude product was purified by flash chromatography (60% ethyl acetate in

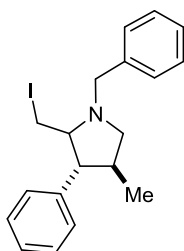
hexanes) to afford 842 mg of the title compound (62%) as a colorless oil. ^1H NMR (400 MHz, CDCl_3): δ 7.34-6.95 (m, 9H), 5.89 (m, 1H), 4.97 (m, 2H), 3.68 (d, $J = 3.5$ Hz, 2H), 3.09 (t, $J = 8.0$ Hz, 1H), 2.64 (dd, $J = 4.5, 7.0$ Hz, 1H), 2.39 (m, 1H), 1.92 (m, 1H), 0.71 (d, $J = 6.5$ Hz, 3H); ^{13}C NMR (100 MHz, CDCl_3): δ 142.3, 140.4, 131.4, 129.9, 128.3, 128.2, 127.9, 119.8, 115.5, 54.2, 53.9, 53.4, 37.8, 16.2; IR (thin film): 3063, 3026, 2961, 2874, 2816, 1637, 1487, 1453, 1402, 1117, 1073, 1028, 1010, 915, 819, 736, 698 cm^{-1} ; HRMS (ESI) m/z calcd for $\text{C}_{19}\text{H}_{23}\text{NBr}$ ($\text{M} + \text{H}$) $^+$: 344.1014; found 344.1021.



***rac*-(2*R*,3*S*)-*N*-Benzyl-3-(4-(benzyloxy)phenyl)-2-methylpent-4-en-1-amine (233b):** General procedure D was followed employing 517 mg of **233**

(1.84 mmol), 778 g of NaHB(OAc)₃ (3.68 mmol), 0.403 mL of benzylamine (3.68 mmol), and 0.105 mL of acetic acid (1.84 mmol) in 19 mL of CH₂Cl₂.

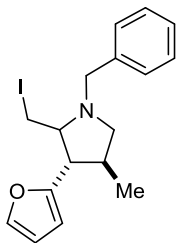
The crude product was purified by flash chromatography (60% diethyl ether in hexanes) to afford 496 mg of the title compound (72%) as a colorless oil. ¹H NMR (300 MHz, CDCl₃): δ 7.45-6.91 (m, 14H), 5.56 (m, 1H), 5.04 (m, 4H), 3.81 (m, 2H), 3.13 (t, *J* = 8.5 Hz, 1H), 2.76 (m, 1H), 2.46 (m, 1H), 2.04 (m, 1H), 0.82 (d, *J* = 6.5 Hz, 3H).



***rac*-(3*S*,4*R*)-1-Benzyl-2-(iodomethyl)-4-methyl-3-phenylpyrrolidine (189):**

General procedure E was followed employing 2.0 g of pentamine **185** (7.53 mmol), and 1.86 g of NIS (8.28 mmol) in 25 mL of THF. The resulting mixture was concentrated and immediately purified by flash chromatography (10%

diethyl ether in hexanes) to afford 2.21 g of the title compound (75%) as a light yellow oil. ¹H NMR (400 MHz, CDCl₃): δ 7.27-7.05 (m, 10H), 4.29 (dt, 4.0, 7.0 Hz, 1H), 3.51 (d, *J* = 5 Hz, 2H), 3.43 (dd, *J* = 3.0, 8.0 Hz, 1H), 2.93 (dd, *J* = 1.5, 6.5 Hz, 1H), 2.56 (t, *J* = 11 Hz, 1H), 2.31 (t, *J* = 11 Hz, 1H), 1.94 (m, 1H), 1.86 (t, *J* = 11 Hz, 1H), 0.55 (d, 6.5 Hz, 3H); ¹³C NMR (100 MHz, CDCl₃): δ 143.4, 137.6, 128.9, 128.3, 127.2, 126.9, 64.6, 62.0, 60.9, 60.5, 38.8, 35.9, 18.1; IR (thin film): 3521, 2930, 2862, 1669, 1501, 1439, 1388, 1256, 1094, 1064 cm⁻¹; HRMS (ESI) *m/z* calcd for C₁₉H₂₃NI (M + H)⁺: 392.0875; found 392.0877.

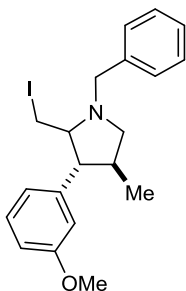


***rac*-(3*R*,4*R*)-1-Benzyl-3-(furan-2-yl)-2-(iodomethyl)-4-methylpyrrolidine**

(234c): General procedure E was followed employing 600 mg of pentamine **234b** (2.45 mmol), and 579 mg of NIS (2.58 mmol) in 7.5 mL of THF. The resulting mixture was concentrated and immediately purified by flash

chromatography (10% diethyl ether in hexanes) to afford 521 mg of the title compound (58%)

as a colorless oil. ^1H NMR (400 MHz, CDCl_3): δ 7.28-7.18 (m, 6H), 6.25 (m, 1H), 6.05 (d, J = 3.0 Hz, 1H), 4.37 (dt, J = 4.5, 10 Hz, 1H), 3.50 (d, J = 3.5 Hz, 2H), 3.40 (ddd, J = 2.0, 2.5, 5.5 Hz, 1H), 2.90 (ddd, J = 2.0, 2.0, 6.0 Hz, 1H), 2.60 (q, J = 11 Hz, 2H), 2.03 (m, 1H), 1.81 (t, J = 11.5 Hz, 1H), 0.65 (d, J = 6.5 Hz, 3H); ^{13}C NMR (100 MHz, CDCl_3): δ 155.7, 141.1, 137.7, 128.9, 128.3, 127.2, 109.9, 107.1, 64.2, 61.8, 60.6, 54.0, 37.2, 32.2, 18.0; IR (thin film): 3027, 2954, 2926, 2872, 2801, 2758, 1495, 1454, 1126, 1009, 732 cm^{-1} ; HRMS (ESI) m/z calcd for $\text{C}_{17}\text{H}_{21}\text{NOI}$ ($\text{M} + \text{H}$) $^+$: 382.0668; found 382.0704.

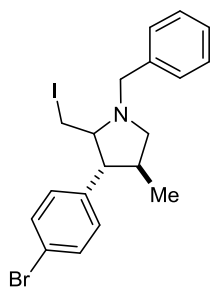


***rac*-(3*S*, 4*R*) - 1 - Benzyl - 2 - (iodomethyl) - 3 - (3 - methoxyphenyl) -**

4-methylpyrrolidine (235c): General procedure E was followed employing 500 mg of pentamine **235b** (1.69 mmol), and 417 mg of NIS (1.86 mmol) in 5.6 mL of THF. The resulting mixture was concentrated and immediately purified by flash chromatography (10% diethyl ether in hexanes) to afford 361

mg of the title compound (50%) as a light yellow oil. ^1H NMR (400 MHz, CDCl_3): δ 7.25-7.14 (m, 6H), 6.73-6.62 (m, 3H), 4.27 (dt, J = 4.0, 7.0 Hz, 1H), 3.71 (s, 3H), 3.50 (d, J = 13 Hz, 2H), 3.44 (ddd, J = 2.0, 2.0, 4.0 Hz, 1H), 2.92 (ddd, J = 2.0, 2.0, 6.0 Hz, 1H), 2.55 (t, J = 11 Hz, 1H), 2.30 (t, J = 11 Hz, 1H), 1.96 (m, 1H), 1.92 (t, J = 11 Hz, 1H), 0.56 (d, J = 6.5 Hz, 3H); ^{13}C NMR (100 MHz, CDCl_3): δ 159.8, 159.6, 145.1, 137.7, 129.1, 128.4, 127.3, 112.0,

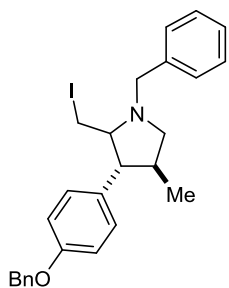
64.7, 62.0, 61.0, 60.6, 55.2, 38.8, 35.8, 18.2; IR (thin film): 3027, 2952, 2831, 2801, 2759, 1601, 1585, 1491, 1454, 1435, 1365, 1317, 1264, 1155, 1046, 909, 876, 779, 734 cm^{-1} ; HRMS (ESI) m/z calcd for $\text{C}_{20}\text{H}_{25}\text{NOI}$ ($\text{M} + \text{H}$)⁺: 422.0981; found 422.0952.



***rac* - (3*S*, 4*R*) -1 - Benzyl - 3 - (4 - bromophenyl) - 2 - (iodomethyl) -4-**

methylpyrrolidine (236c): General procedure E was followed employing 700 mg of pentamine **236b** (2 mmol), and 505 mg of NIS (2.2 mmol) in 7 mL of THF. The resulting mixture was concentrated and immediately purified by

flash chromatography (10% diethyl ether in hexanes) to afford 517 mg of the title compound (55%) as a light yellow oil. ¹H NMR (400 MHz, CDCl_3): δ 7.39-6.95 (m, 6H), 4.21 (dt, $J = 4.0$, 7.0 Hz, 1H), 3.5 (d, $J = 13$ Hz, 2H), 3.42 (ddd, $J = 3.0$, 9.0 Hz, 1H), 2.93 (appt d, $J = 10$ Hz, 1H), 2.55 (t, $J = 11$ Hz, 1H), 2.30 (t, $J = 11$ Hz, 1H), 1.93 (m, 1H), 1.90 (t, $J = 11$ Hz, 1H), 0.52 (d, $J = 6.5$ Hz, 3H); ¹³C NMR (100 MHz, CDCl_3): δ 142.4, 137.6, 131.4, 128.9, 128.3, 127.2, 120.6, 64.4, 61.8, 60.8, 60.0, 38.7, 35.2, 17.9; IR (thin film): 3026, 2953, 2802, 1491, 1454, 1407, 1365, 1339, 1264, 1126, 1100, 1069, 1028, 1010, 877.6, 815, 738, 700 cm^{-1} ; HRMS (ESI) m/z calcd for $\text{C}_{19}\text{H}_{23}\text{NBrI}$ ($\text{M} + \text{H}$)⁺: 471.0059; found 471.0052.

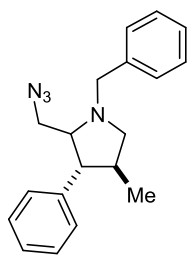


***rac*-(3*S*,4*R*)-1-Benzyl-3-(4-(benzyloxy)phenyl)-2-(iodomethyl)-4-**

methylpyrrolidine (233c): General procedure E was followed employing 496 mg of pentamine **233b** (1.33 mmol), and 329 mg of NIS (1.46 mmol) in 4.5 mL of THF. The resulting mixture was concentrated and immediately

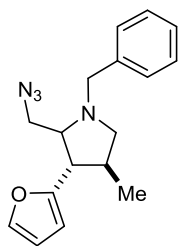
purified by flash chromatography (10% diethyl ether in hexanes) to afford 325 mg of the title compound (48%) as a colorless oil. ¹H NMR (300 MHz, CDCl_3): δ 7.48-6.97 (m, 14H), 5.15

(s, 2H), 4.39 (dt, $J = 4.0, 7.0$ Hz, 1H), 3.65 (d, $J = 13.5$ Hz, 2H), 3.57 (m, 2H), 3.57 (m, 1H), 3.04 (app d, $J = 10$ Hz, 1H), 2.69 (t, $J = 11.5$ Hz, 1H), 2.40 (t, $J = 10.5$ Hz, 1H), 2.09 (m, 1H), 2.05 (m, 1H), 0.68 (t, $J = 6.5$ Hz, 3H).



***rac*-(3*S*, 4*R*)-2-(Azidomethyl)-1-benzyl-4-methyl-3-phenylpyrrolidine**

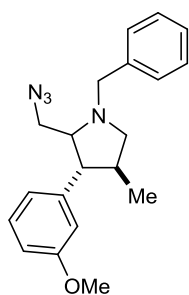
(192): General procedure F was followed employing 360 mg of pyrrolidine **189** (0.920 mmol), and 90 mg of NaN₃ (1.38 mmol) in 8 mL of DMF. The resulting product was purified by flash chromatography (10% ethyl acetate in hexanes) to afford 143 mg of the title compound **203** (51%) and 53 mg of compound **204** (19%). ¹H NMR (400 MHz, CDCl₃): δ 7.27-7.14 (m, 10H), 3.53 (m, 1H), 3.50 (d, $J = 4.5$ Hz, 2H), 3.11 (ddd, $J = 4.0, 4.5, 6.5$ Hz, 1H), 2.85 (ddd, $J = 1.5, 2.0, 9.5$ Hz, 1H), 2.00 (m, 3H), 1.71 (t, $J = 11$ Hz, 1H), 0.58 (d, $J = 6$ Hz, 3H); ¹³C NMR (100 MHz, CDCl₃): δ 140.7, 137.7, 129.0, 128.6, 128.3, 128.1, 127.2, 127.1, 63.4, 62.6, 60.8, 58.0, 56.1, 36.0, 16.8; IR (thin film): 3061, 3028, 2952, 2905, 2804, 2762, 2097, 1494, 1453, 1367, 1346, 1264, 1109, 1071, 1052, 754 cm⁻¹; HRMS (ESI) m/z calculated for C₁₉H₂₃N₄ (M + H)⁺: 307.1923; found 307.1921.



***rac*-(3*R*, 4*R*)-2-(Azidomethyl)-1-benzyl-3-(furan-2-yl)-4-methylpyrrolidine**

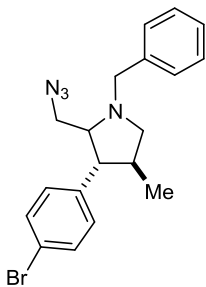
(239): General procedure F was followed employing 521 mg of pyrrolidine **234c** (1.36 mmol), and 133 mg of NaN₃ (2.05 mmol) in 11.5 mL of DMF. The resulting product was purified by flash chromatography (10% ethyl acetate in hexanes) to afford 138 mg of the title compound **239** (34%) and 136 mg of compound **239b** (33%). ¹H NMR (400 MHz, CDCl₃): δ 7.31-7.17 (m, 6H), 6.27 (dd, $J = 2.0, 1.0$ Hz, 1H),

6.12 (d, $J = 3.0$ Hz, 1H), 3.66 (dt, $J = 6.5, 4.5$ Hz, 1H), 3.51 (d, $J = 5.0$ Hz, 2H), 3.08 (ddd, $J = 1.0, 2.5, 5.0$ Hz, 1H), 2.83 (ddd, $J = 1.0, 2.5, 5.0$ Hz, 1H), 2.14 (t, $J = 11$ Hz, 1H), 1.97 (m, 1H), 1.86 (t, $J = 11$ Hz, 1H), 1.66 (t, $J = 11$ Hz, 1H), 0.67 (d, $J = 6.5$ Hz, 3H); ^{13}C NMR (100 MHz, CDCl_3): δ 153.8, 141.5, 137.7, 129.0, 128.3, 127.2, 110.2, 107.8, 62.5, 61.8, 60.6, 57.6, 49.3, 34.4, 16.9; IR (thin film): 3062, 3028, 2955, 2927, 2807, 2763, 2097, 1600, 1506, 1454, 1368, 1348, 1265, 1148, 1109, 1069, 1052, 1028, 1010, 966, 918, 869, 803, 733, 699, 674, 598 cm^{-1} ; HRMS (ESI) m/z calculated for $\text{C}_{17}\text{H}_{21}\text{N}_4\text{O}$ ($\text{M} + \text{H}$) $^+$: 297.1715; found 297.1710.



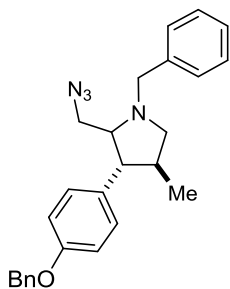
rac - (3S, 4R) - 2 - (Azidomethyl) -1 - benzyl -3 - (3 -methoxyphenyl)-4-methylpyrrolidine (240): General procedure F was followed employing 361 mg of pyrrolidine **235c** (0.857 mmol), and 83.5 mg of NaN_3 (1.28 mmol) in 7 mL of DMF. The resulting product was purified by flash chromatography (10% ethyl acetate in hexanes) to afford 132 mg of the title compound **240**

(46%) and 74 mg of compound **240b** (26%). ^1H NMR (400 MHz, CDCl_3): δ 7.35-7.28 (m, 6H), 6.84-6.78 (m, 3H), 3.81 (s, 3H), 3.63 (m, 1H), 3.59 (d, $J = 5$ Hz, 2H), 3.19 (ddd, $J = 1.5, 3.0, 4.5$ Hz, 1H), 2.98 (ddd, $J = 1.5, 2.0, 6$ Hz, 1H), 2.04 (m, 3H), 1.80 (t, $J = 11$ Hz, 1H), 0.69 (d, $J = 6.5$ Hz, 3H); ^{13}C NMR (100 MHz, CDCl_3): δ 159.8, 142.4, 137.7, 129.6, 129.0, 128.4, 128.3, 127.3, 112.2, 63.4, 62.7, 60.9, 57.9, 56.2, 55.1, 36.0, 16.8; IR (thin film): 3027, 2953, 2804, 2763, 2096, 1601, 1585, 1491, 1454, 1436, 1368, 1264, 1155, 1109, 1049, 779, 744 cm^{-1} ; HRMS (ESI) m/z calculated for $\text{C}_{20}\text{H}_{25}\text{N}_4\text{O}$ ($\text{M} + \text{H}$) $^+$: 337.2028; found 337.2036.



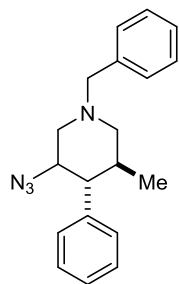
***rac*-(3*S*,4*R*)-2-(Azidomethyl)-1-benzyl-3-(4-bromophenyl)-4-methylpyrrolidine (241):** General procedure F was followed employing

500 mg of pyrrolidine **236c** (1.1 mmol), and 104 mg of NaN₃ (1.6 mmol) in 9 mL of DMF. The resulting product was purified by flash chromatography (10% ethyl acetate in hexanes) to afford 178 mg of the title compound **241** (42%) and 116 mg of compound **241b** (27%). ¹H NMR (400 MHz, CDCl₃): δ 7.46 (d, *J* = 9.5 Hz, 2H), 7.35-7.23 (m, 5H), 7.10 (d, *J* = 8.0 Hz, 2H), 3.59 (d, *J* = 3 Hz, 2H), 3.56-3.52 (m, 2H), 3.19 (ddd, *J* = 1.5, 3.0, 5.0 Hz, 1H), 2.91 (ddd, *J* = 1.0, 2.5, 6.5 Hz, 1H), 2.02 (q, *J* = 11 Hz, 2H), 1.98 (m, 1H), 1.78 (t, *J* = 11 Hz, 1H), 0.61 (d, *J* = 6.5 Hz, 3H); ¹³C NMR (100 MHz, CDCl₃): δ 139.9, 137.7, 131.8, 129.0, 128.4, 127.3, 120.9, 63.3, 62.6, 60.8, 57.8, 55.6, 34.0, 16.8; IR (thin film): 3331, 3085, 3062, 3027, 2954, 2904, 2806, 2763, 2097, 1602, 1591, 1491, 1463, 1454, 1407, 1368, 1346, 1307, 1265, 1185, 1131, 1110, 1071, 1053, 1028, 1010, 965, 909, 871, 815, 734, 700, 648, 617, 541 cm⁻¹; HRMS (ESI) *m/z* calculated for C₁₉H₂₂N₄Br (M + H)⁺: 385.1028; found 385.1020.

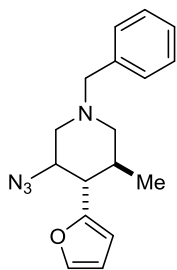


***rac*-(3*S*,4*R*)-2-(Azidomethyl)-1-benzyl-3-(4-(benzyloxy)phenyl)-4-methylpyrrolidine (238):** General procedure F was followed employing 325

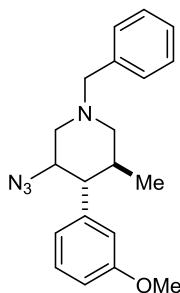
mg of pyrrolidine **233c** (0.653 mmol), and 63.7 mg of NaN₃ (0.980 mmol) in 5.5 mL of DMF. The resulting product was purified by flash chromatography (10% ethyl acetate in hexanes) to afford 123 mg of the title compound **238** (46%) and 94 mg of compound **238b** (34%). ¹H NMR (300 MHz, CDCl₃): δ 7.45-6.94 (m, 14H), 5.08 (s, 2H), 3.59 (m, 3H), 3.22 (m, 1H), 2.93 (m, 1H), 2.05 (m, 3H), 1.84 (t, *J* = 11 Hz, 1H), 0.67 (d, *J* = 6.0 Hz, 3H).



***rac*-(4*S*,5*R*)-3-Azido-1-benzyl-5-methyl-4-phenylpiperidine (193):** ^1H NMR (400 MHz, CDCl_3): δ 7.40-7.22 (m, 10H), 4.14 (d, $J = 13.5$ Hz, 1H), 3.58 (d, $J = 13.5$ Hz, 1H), 3.48 (dd, $J = 3.0, 9.5$ Hz, 1H), 2.97 (m, 2H), 2.79 (m, 3H), 2.31 (m, 1H), 0.96 (d, $J = 6$ Hz, 3H); ^{13}C NMR (100 MHz, CDCl_3): δ 141.3, 139.5, 128.7, 128.6, 128.4, 128.2, 127.0, 126.9, 72.6, 60.6, 59.4, 56.4, 51.0, 39.5, 18.0; IR (thin film): 3084, 3062, 3028, 3003, 2957, 2923, 2869, 2796, 2729, 2097, 1724, 1703, 1601, 1584, 1494, 1452, 1373, 1357, 1335, 1286, 1203, 1137, 1071, 1029, 991, 959, 915, 827, 755, 700, 649 cm^{-1} ; HRMS (ESI) m/z calculated for $\text{C}_{19}\text{H}_{23}\text{N}_4$ ($\text{M} + \text{H}$) $^+$: 307.1923; found 307.1916.

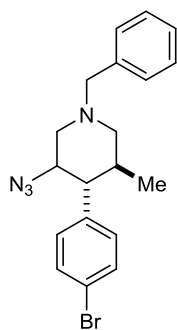


***rac*-(4*R*,5*R*)-3-Azido-1-benzyl-4-(furan-2-yl)-5-methylpiperidine (239b):** ^1H NMR (400 MHz, CDCl_3): δ 7.29-7.15 (m, 6H), 6.22 (dd, $J = 1.5, 2.0$ Hz, 1H), 6.00 (d, $J = 3.0$ Hz, 1H), 4.00 (d, $J = 13$ Hz, 1H), 3.42 (dd, $J = 5.0, 10.0$ Hz, 1H), 3.38 (d, $J = 13$ Hz, 1H), 3.03 (dd, $J = 3.5, 10$ Hz, 1H), 2.91 (m, 1H), 2.88 (t, $J = 9.0$ Hz, 1H), 2.63 (d, $J = 9.0$ Hz, 2H), 2.28 (m, 1H), 0.98 (d, $J = 4$ Hz, 3H); ^{13}C NMR (100 MHz, CDCl_3): 155.0, 141.5, 139.2, 128.4, 128.2, 127.0, 110.0, 105.7, 69.5, 60.0, 59.1, 51.3, 49.0, 36.4, 18.4; IR (thin film): 3028, 2959, 2925, 2870, 2798, 2098, 1596, 1506, 1496, 1452, 1376, 1333, 1290, 1239, 1147, 1070, 1011, 911, 803, 734 cm^{-1} ; HRMS (ESI) m/z calcd for $\text{C}_{17}\text{H}_{21}\text{N}_4\text{O}$ ($\text{M} + \text{H}$) $^+$: 297.1715; found 297.1711.



***rac*-(4*S*,5*R*)-3-Azido-1-benzyl-4-(3-methoxyphenyl)-5-methylpiperidine (240b):** ^1H NMR (400 MHz, CDCl_3): δ 7.32-7.14 (m, 6H), 6.75-6.69 (m, 3H), 4.03 (d, $J = 11, 5.0$ Hz, 1H), 3.73 (s, 3H), 3.44 (d, $J = 11.5$ Hz, 1H), 3.37 (dd, $J = 3.0, 10.0$ Hz, 1H), 2.93 (dd, $J = 3.0, 10.0$ Hz, 1H), 2.86 (td, $J = 3.0, 13$

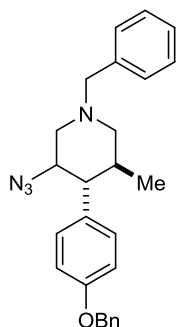
Hz, 1H), 2.69 (m, 3H), 2.21 (m, 1H), 0.88 (d, $J = 7.0$ Hz, 3H); ^{13}C NMR (100 MHz, CDCl_3): δ 159.7, 142.9, 139.4, 129.6, 128.5, 128.2, 126.9, 120.4, 114.0, 111.6, 72.3, 60.4, 59.2, 56.2, 55.1, 51.0, 39.3, 18.0; IR (thin film): 3027, 2956, 2923, 2868, 2834, 2794, 2097, 1601, 1584, 1491, 1453, 1373, 1285, 1266, 1159, 1047, 777, 738 cm^{-1} ; HRMS (ESI) m/z calcd for $\text{C}_{20}\text{H}_{25}\text{N}_4\text{O}$ ($\text{M} + \text{H}$) $^+$: 337.2028; found 337.2013.



***rac*-(4*S*,5*R*)-3-Azido-1-benzyl-4-(4-bromophenyl)-5-methylpiperidine**

(241b): ^1H NMR (400 MHz, CDCl_3): δ 7.44 (d, $J = 8.5$ Hz, 2H), 7.38-7.34 (m, 5H), 7.10 (d, $J = 8.5$ Hz, 2H), 4.11 (d, $J = 13$ Hz, 1H), 3.52 (d, $J = 3.0$ Hz, 1H), 3.45 (dd, $J = 3.0, 10.0$ Hz, 1H), 3.00 (dd, 3.0, 10.0 Hz, 1H), 2.90 (m, 1H), 2.78 (dd, $J = 2.5, 6.0$ Hz, 2H), 2.76 (t, $J = 10$ Hz, 1H), 2.24 (m, 1H), 0.98 (d, $J = 7.0$

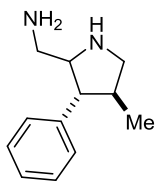
Hz, 3H); ^{13}C NMR (100 MHz, CDCl_3): δ 140.2, 139.2, 131.7, 129.8, 128.5, 128.3, 126.9, 120.5, 72.3, 60.3, 59.1, 55.7, 50.8, 39.4, 17.7; IR (thin film): 3027, 2957, 2924, 2797, 2097, 1489, 1452, 1410, 1283, 1136, 1073, 1010, 910, 816, 737, 699; HRMS (ESI) m/z calcd for $\text{C}_{19}\text{H}_{22}\text{N}_4\text{Br}$ ($\text{M} + \text{H}$) $^+$: 385.1028; found 385.1036.



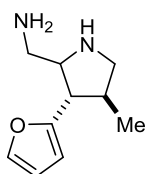
***rac*-(4*S*,5*R*)-3-Azido-1-benzyl-4-(4-(benzyloxy)phenyl)-5-methylpiperidine**

(238b): ^1H NMR (400 MHz, CDCl_3): 7.33-6.81 (m, 14H), 4.92 (s, 2H), 3.98 (d, $J = 13$ Hz, 1H), 3.39 (d, $J = 13.5$ Hz, 1H), 3.30 (dd, $J = 3.0, 10$ Hz, 1H), 2.85 (dd, $J = 3.0, 10.0$ Hz, 1H), 2.77 (m, 1H), 2.63 (d, $J = 7.5$ Hz, 2H), 2.60 (t, $J = 10.0$ Hz, 1H), 2.12 (m, 1H), 0.81 (d, $J = 7.0$ Hz, 3H); ^{13}C NMR (100 MHz,

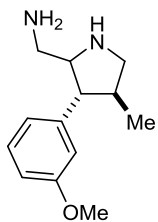
CDCl_3): δ 157.7, 139.5, 137.1, 133.4, 129.2, 129.1, 128.6, 128.6, 128.4, 128.3, 128.0, 127.6, 127.5, 127.0, 115.0, 72.5, 70.0, 60.4, 59.3, 55.5, 51.0, 39.3, 17.8.



***rac*-((3*S*,4*R*)-4-Methyl-3-phenylpyrrolidin-2-yl)methanamine (196):** General procedure G was followed employing 1.03 g of pyrrolidine **192** (3.38 mmol), 473 mg of Pd(OH)₂/C (0.338 mmol), and 2.66 g of NH₄HCO₂ (42.3 mmol) in 35 mL of EtOH. The resulting oil was utilized directly without any further purification to yield 578 mg of the title compound (90%). ¹H NMR (400 MHz, CDCl₃): δ 7.32-7.18 (m, 5H), 3.23 (dd, *J* = 1.0, 3.5 Hz, 1H), 3.08 (dd, *J* = 1.0, 3.5 Hz, 1H), 2.92 (dt, *J* = 4.5, 10 Hz, 1H), 2.44 (t, *J* = 10.5 Hz, 1H), 2.36 (t, *J* = 10.5 Hz, 1H), 1.89 (t, *J* = 11.0 Hz, 1H), 1.79 (m, 1H), 1.49, (broad s, 3H), 0.59 (d, *J* = 6 Hz, 3H); ¹³C NMR (100 MHz, CDCl₃): δ 141.7, 128.6, 126.7, 60.2, 54.5, 54.4, 54.3, 37.4, 17.0; IR (thin film): 3027, 2954, 2922, 2867, 2795, 2360, 2339, 1493, 1453, 753 cm⁻¹; HRMS (ESI) *m/z* calculated for C₁₂H₁₈N₂ (M)⁺ : 190.146999; found 190.146829.



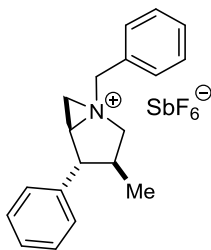
***rac*-((3*R*,4*R*)-3-(Furan-2-yl)-4-methylpyrrolidin-2-yl)methanamine (244):** General procedure G was followed employing 136 mg of pyrrolidine **239** (0.459 mmol), 64 mg of Pd(OH)₂/C (0.045 mmol), and 361 mg of NH₄HCO₂ (5.73 mmol) in 5 mL of EtOH. The resulting oil was utilized directly without any further purification to yield 75 mg of the title compound (91%). ¹H NMR (400 MHz, MeOD): δ 7.47 (appt s, 1H), 6.39 (dd, *J* = 2.0, 3.0 Hz, 1H), 6.23(d, *J* = 3.0 Hz, 1H), 3.19 (dd, *J* = 5.0, 8.5 Hz, 1H), 3.04 (dd, *J* = 5.0, 8.5 Hz, 1H), 2.94 (dt, *J* = 4.0, 6.0 Hz, 1H), 2.36 (t, *J* = 11 Hz, 1H), 2.27 (t, *J* = 11.0 Hz, 1H), 2.18 (t, *J* = 10.5 Hz, 1H), 1.94 (m, 1H), 0.71 (d, *J* = 7.0 Hz, 3H); ¹³C NMR (100 MHz, MeOD): δ 154.4, 141.6, 109.7, 107.4, 52.7, 52.0, 51.9, 51.4, 35.0, 15.8; IR (thin film): 3849, 3741, 3583, 3365, 2298, 1588, 1468 cm⁻¹; HRMS (ESI) *m/z* calculated for C₁₀H₁₇N₂O (M)⁺ : 181.13354; found 181.13308.



rac- ((3S, 4R)-3-(3-Methoxyphenyl)-4-methylpyrrolidin-2-yl) methanamine

(245): General procedure G was followed employing 132 mg of pyrrolidine **240** (0.392 mmol), 55 mg of Pd(OH)₂/C (0.039 mmol), and 308 mg of NH₄HCO₂ (4.90 mmol) in 4 mL of EtOH. The resulting oil was utilized directly without any

further purification to yield 79 mg of the title compound (93%). ¹H NMR (400 MHz, CDCl₃): δ ¹H NMR (400 MHz, MeOD): δ 7.29-7.23 (m, 1H), 6.84-6.81 (m, 3H), 3.72 (s, 3H), 3.58 (m, 1H), 3.33 (dd, *J* = 3.5, 9.0 Hz, 1H), 2.98 (t, *J* = 11.5 Hz, 1H), 2.72 (t, *J* = 12.5 Hz, 1H), 2.42 (t, *J* = 11.0 Hz, 1H), 2.14 (m, 2H), 0.65 (d, *J* = 6.0 Hz, 3H); ¹³C NMR (100 MHz, MeOD): δ 138.8, 130.2, 129.2, 128.1, 127.3, 113.3, 54.4, 53.1, 50.2, 49.7, 46.4, 33.9, 15.0; IR (thin film): 3904.1, 3871.7, 3854.1, 3854.1, 3840.3, 3821.8, 3806.8, 3751.4, 3735.7, 3712.2, 3690.3, 3676.4, 3649.5, 3629.7, 3399.7, 1647.7, 1387.7, 1324.9, 1064.7 cm⁻¹; HRMS (ESI) *m/z* calculated for C₁₃H₂₁N₂O (M)⁺ : 221.16484; found 221.16457.

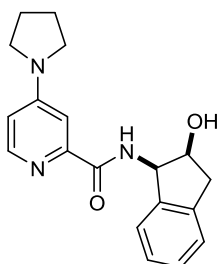


rac- (3S,4R)-1-Benzyl-3-methyl-4-phenyl-1-azoniabicyclo[3.1.0]hexane

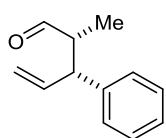
hexafluoroantimonate (V) (194): To a rt solution of pyrrolidine **189** (130 mg, 0.332 mmol) in CH₂Cl₂ (11 mL) was added Silver hexafluoroantimonate (V) (1.2 equiv, 114 mg, 0.398 mmol) in the dark. The resulting mixture

was stirred 2 h at rt, then filtered through a pad of Celite[®]. The resulting solid was recrystallized with CH₂Cl₂/Hexanes to afford 157 mg of the title compound (95%) as a colorless solid. Recrystallization of **194** from Et₂O/Hexanes yielded crystals suitable for X-ray diffraction analysis (Appendix B). mp 38-42 °C; ¹H NMR (400 MHz, CDCl₃): δ 7.57-7.02 (m, 10H), 4.80 (d, *J* = 13.5 Hz, 1H), 4.32 (d, *J* = 13.5 Hz, 1H), 4.09 (m, 1H), 3.77 (m, 1H), 3.62 (m, 1H), 3.36 (m, 2H), 3.08 (dd, *J* = 3.0, 5.0 Hz, 1H), 2.57 (m, 1H), 1.01 (d, *J* = 7 Hz,

3H); ^{13}C NMR (100 MHz, CDCl_3): δ 137.6, 131.1, 131.0, 129.9, 129.4, 128.6, 128.2, 127.1, 64.0, 62.8, 58.5, 54.2, 51.7, 48.2, 16.48; IR (thin film): 3054, 2986, 2305, 2253, 1421, 1265, 909, 738, 704, 661 cm^{-1} ; HRMS (ESI) m/z calculated for $\text{C}_{19}\text{H}_{22}\text{N}$ (M) $^+$: 264.1752; found 264.1745.

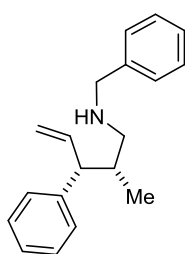


***N*-((1*R*,2*S*)-2-Hydroxy-2,3-dihydro-1*H*-inden-1-yl)-4-(pyrrolidin-1-yl)picolinamide (249)**: This compound was prepared according to literature procedure and matches the characterization data provided in the following the publication: Geherty, M.E.; Dura, R.D.; Nelson, S.G. *J. Am. Chem. Soc.* **2010**, 132, 11875-11877.



(2*R*, 3*R*)-2-Methyl-3-phenylpent-4-enal (250): [$\text{CpRu}(\text{CH}_3\text{CN})_3$] PF_6 (5 mol %, 31 mg, 0.07 mmol), picolinamide **249** (5 mol %, 23 mg, 0.07 mmol) and THF (2.9 mL) were combined in a nitrogen-filled glovebox. The mixture was periodically agitated over 30 min, then transferred to a mixture containing allyl vinyl ether (250 mg, 1.43 mmol), 4Å MS (100% wt/wt, 250 mg) and $\text{B}(\text{OPh})_3$ (5 mol %, 21 mg, 0.07 mmol). Immediately after removal from the glovebox, CH_3CN (20 mol %, 15 μL , 0.3 mmol) was added and the resulting solution was stirred an additional 24 hours at ambient temperature. The resultant solution was concentrated under a stream of N_2 , filtered through a plug of Florisil[®] and concentrated to yield 225 mg (90%) as a mixture of **250** and (*E*)-2-methyl-5-phenylpent-4-enal as the only detectable products. Separating the stereoisomers of **250** by GLC flow rate 1.0 mL/min, method: 90 °C for 10 min, ramp @ 0.7 °C/min to 160 °C, hold for 5 min; Tr (min) = 44.9 [(2*S*, 3*S*)-**250**_{anti}], 45.6 (**250**_{syn1}), 46.9 (**250**_{syn2}), 47.4 [(2*R*, 3*R*)-**250**_{anti}] (ratio = 17.6:11.5:31.8:431) provided the

enantiomer ratio (2*S*, 3*S*)-**250**_{anti}: (2*R*,3*R*)-**250**_{anti} = 3.9:96.1 (92% ee). ¹H NMR (400 MHz, CDCl₃): δ 9.57 (d, *J* = 3 Hz, 1H), 7.35-7.22 (m, 5H), 5.99 (m, 1H), 5.15 (d, *J* = 6.0 Hz, 1H), 3.61 (t, *J* = 9 Hz, 1H), 2.83 (m, 1H), 1.15 (d, *J* = 7 Hz). This compound was prepared according to literature procedure and matches the characterization data provided in the following the publication: Geherty, M.E.; Dura, R.D.; Nelson, S.G. *J. Am. Chem. Soc.* **2010**, 132, 11875-11877.

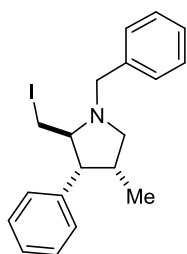


(2*R*,3*R*)-N-Benzyl-2-methyl-3-phenylpent-4-en-1-amine (252): General

procedure D was followed employing 200 mg of aldehyde **250** (1.14 mmol), 480 mg of NaHB(OAc)₃ (2.3 mmol), 0.25 mL of benzylamine (2.3 mmol), and

66 μL of acetic acid (1.14 mmol) in 12 mL of CH₂Cl₂. The crude product was

purified by flash chromatography (70% diethyl ether in hexanes) to afford 181 mg of the title compound (60%) as a colorless oil. $[\alpha]_{\text{D}}^{23} + 38$ (*c* 2.0, CHCl₃); ¹H NMR (400 MHz, CDCl₃): δ 7.31-7.17 (m, 10H), 6.01 (m, 1H), 5.04 (m, 2H), 3.65 (d, *J* = 11.0 Hz, 2H), 3.19 (t, *J* = 9.0 Hz, 1H), 2.52 (dd, *J* = 5.0, 7.0 Hz, 1H), 2.33 (dd, *J* = 4.5, 7.0 Hz, 1H), 2.05 (m, 1H), 0.98 (d, *J* = 6.5 Hz, 3H); ¹³C NMR (100 MHz, CDCl₃): δ 143.9, 139.9, 128.4, 128.3, 128.0, 127.8, 126.8, 126.1, 115.7, 54.4, 54.0, 53.7, 38.0, 16.0; IR (thin film): 3835, 3027, 2959, 2926, 1638, 1493, 1453, 1116, 912, 735, 699 cm⁻¹; HRMS (ESI) *m/z* calcd for C₁₉H₂₄N (M + H)⁺: 266.1909; found 266.1904.



(2*S*,3*R*,4*R*)-1-Benzyl-2-(iodomethyl)-4-methyl-3-phenylpyrrolidine (253):

General procedure E was followed employing 150 mg of pentamine **252** (0.57 mmol), and 140 mg of NIS (0.63 mmol) in 2 mL of THF. The resulting mixture was purified by flash chromatography (10% diethyl ether in hexanes) to afford 63 mg of an inseparable mixture of the title compound **253**, and 1-benzyl-3-iodo-5-methyl-4-phenylpiperidine as a light yellow oil. ¹H NMR (400 MHz, CDCl₃): δ 7.40-7.10 (m, 10H), 4.67 (dt, 4.5, 7.0 Hz, 1H), 3.55 (d, *J* = 5 Hz, 2H), 3.25 (dd, *J* = 3.0, 7.0 Hz, 1H), 3.12 (dd, *J* = 4.5, 8.0 Hz, 1H), 2.87 (m, 3H), 2.02 (m, 1H), 0.54 (d, 7.0 Hz, 3H).

¹ Characterization data obtained for ¹H NMR only. Compound not utilized in final route.

² Characterization data obtained for ¹H and ¹³C NMR only. Compound not utilized in final route.

APPENDIX A

X-RAY CRYSTAL DATA FOR (S,E)-6-METHYL-8-((1-(TRIISOPROPYLSILYL)-1H-PYRROL-2-YL)METHYLENE)-6,7,8,9-TETRAHYDRO-5H-PYRROLO[1,2-A]AZEPIN-5-ONE 89

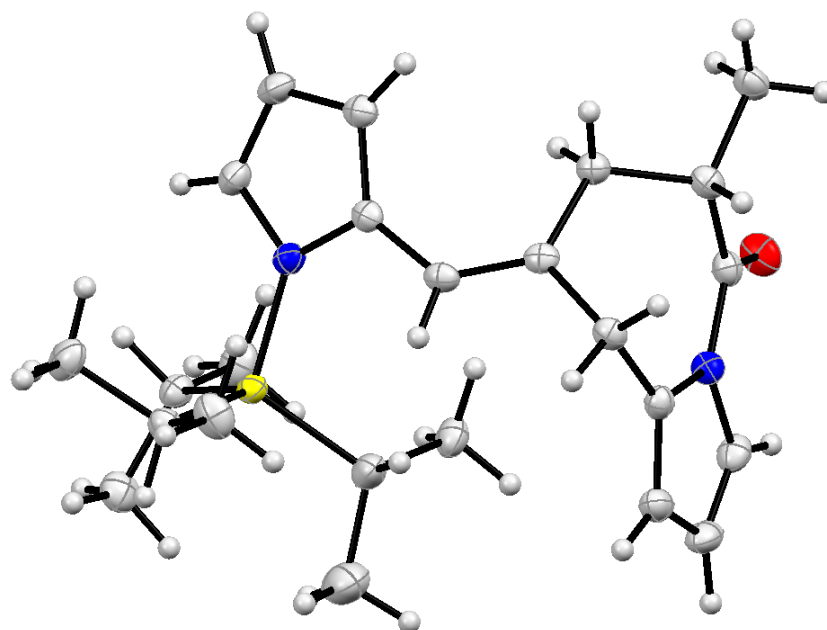


Figure 14. X-ray crystal structure of 89

ORTEP structure of (S,E)-6-methyl-8-((1-(triisopropylsilyl)-1H-pyrrol-2-yl)methylene)-6,7,8,9-tetrahydro-5H-pyrrolo[1,2-a]azepin-5-one. The molecular structure is drawn with 50% probability displacement ellipsoids; hydrogen atoms are drawn with an artificial radius.

Table 7. Crystallographic Information for Compound **89**

Identification code	perez1		
Chemical formula	C ₂₄ H ₃₆ N ₂ OSi		
Formula weight	396.64		
Temperature	100(2) K		
Wavelength	1.54178 Å		
Crystal size	0.020 x 0.140 x 0.200 mm		
Crystal habit	clear green plate		
Crystal system	triclinic		
Space group	P -1		
Unit cell dimensions	a = 7.3821(3) Å	α = 100.975(3)°	
	b = 11.1160(5) Å	β = 99.125(2)°	
	c = 15.2794(7) Å	γ = 108.084(2)°	
Volume	1137.81(9) Å ³		
Z	2		
Density (calculated)	1.158 g/cm ³		
Absorption coefficient	1.020 mm ⁻¹		
F(000)	432		

Table 8. Atomic coordinates and equivalent isotropic displacement parameters (Å²) for **89**

	x/a	y/b	z/c	U(eq)
Si1	0.05288(6)	0.20810(4)	0.86395(3)	0.01729(19)
O1	0.77490(18)	0.40359(14)	0.61921(9)	0.0283(3)
C1	0.7814(3)	0.16723(17)	0.85265(13)	0.0204(4)
N1	0.0849(2)	0.08457(14)	0.77980(10)	0.0193(3)
N2	0.5123(2)	0.46806(14)	0.61705(10)	0.0189(3)
C2	0.6719(3)	0.1662(2)	0.75851(14)	0.0294(5)
C3	0.6899(3)	0.03516(19)	0.87475(15)	0.0292(5)
C4	0.1625(3)	0.18985(17)	0.97931(12)	0.0206(4)
C5	0.3854(3)	0.2208(2)	0.99879(14)	0.0284(5)
C6	0.1096(3)	0.2684(2)	0.05917(13)	0.0294(5)
C7	0.1692(3)	0.37321(18)	0.84274(15)	0.0299(5)
C8	0.3838(3)	0.40516(18)	0.83567(13)	0.0262(4)
C9	0.1370(4)	0.4826(2)	0.90539(19)	0.0451(6)
C10	0.1033(3)	0.97052(17)	0.79822(13)	0.0218(4)
C11	0.1175(3)	0.89215(17)	0.72201(14)	0.0236(4)
C12	0.1077(3)	0.95680(17)	0.65140(13)	0.0210(4)

	x/a	y/b	z/c	U(eq)
C13	0.0873(2)	0.07420(16)	0.68731(12)	0.0179(4)
C14	0.0714(2)	0.17646(17)	0.64175(12)	0.0185(4)
C15	0.1710(2)	0.21673(16)	0.58035(12)	0.0173(4)
C16	0.1498(2)	0.33110(17)	0.54477(12)	0.0188(4)
C17	0.3135(2)	0.45528(17)	0.59844(12)	0.0186(4)
C18	0.3008(3)	0.56714(18)	0.64568(13)	0.0237(4)
C19	0.4937(3)	0.65324(18)	0.69464(14)	0.0271(4)
C20	0.6195(3)	0.59132(18)	0.67709(13)	0.0239(4)
C21	0.6025(3)	0.37823(17)	0.58713(12)	0.0199(4)
C22	0.4768(2)	0.25459(17)	0.51322(12)	0.0191(4)
C23	0.3167(2)	0.16149(17)	0.54753(12)	0.0183(4)
C24	0.6033(3)	0.18226(18)	0.47554(13)	0.0234(4)

Table 9. Bond lengths [\AA] and angles [$^\circ$] for **89**

Si1-N1	1.7947(16)	Si1-C7	1.8834(19)
Si1-C1	1.8833(18)	Si1-C4	1.8944(18)
O1-C21	1.211(2)	C1-C2	1.531(2)
C1-C3	1.540(2)	C1-H1A	1.0
N1-C10	1.391(2)	N1-C13	1.399(2)
N2-C20	1.401(2)	N2-C17	1.406(2)
N2-C21	1.409(2)	C2-H2A	0.98
C2-H2B	0.98	C2-H2C	0.98
C3-H3A	0.98	C3-H3B	0.98
C3-H3C	0.98	C4-C5	1.539(2)
C4-C6	1.536(3)	C4-H4A	1.0
C5-H5A	0.98	C5-H5B	0.98
C5-H5C	0.98	C6-H6A	0.98
C6-H6B	0.98	C6-H6C	0.98
C7-C9	1.504(3)	C7-C8	1.539(3)
C7-H7A	1.0	C8-H8A	0.98
C8-H8B	0.98	C8-H8C	0.98
C9-H9A	0.98	C9-H9B	0.98
C9-H9C	0.98	C10-C11	1.355(3)
C10-H10	0.86(2)	C11-C12	1.410(3)
C11-H11	0.92(3)	C12-C13	1.379(3)
C12-H12	0.96(2)	C13-C14	1.466(2)

C14-C15	1.340(3)	C14-H14	0.94(2)
C15-C23	1.500(2)	C15-C16	1.515(2)
C16-C17	1.502(2)	C16-H16A	1.00(2)
C16-H16B	0.96(2)	C17-C18	1.352(3)
C18-C19	1.431(3)	C18-H18	0.96(2)
C19-C20	1.347(3)	C19-H19	0.92(3)
C20-H20	0.96(3)	C21-C22	1.520(2)
C22-C24	1.520(2)	C22-C23	1.545(2)
C22-H22	1.00(2)	C23-H23A	0.96(2)
C23-H23B	0.95(2)	C24-H24A	0.98
C24-H24B	0.98	C24-H24C	0.98
N1-Si1-C7	109.31(8)	N1-Si1-C1	107.35(8)
C7-Si1-C1	111.20(8)	N1-Si1-C4	105.81(8)
C7-Si1-C4	114.55(9)	C1-Si1-C4	108.26(8)
C2-C1-C3	109.99(16)	C2-C1-Si1	113.49(13)
C3-C1-Si1	110.69(12)	C2-C1-H1A	107.5
C3-C1-H1A	107.5	Si1-C1-H1A	107.5
C10-N1-C13	106.19(15)	C10-N1-Si1	122.52(13)
C13-N1-Si1	131.21(12)	C20-N2-C17	108.04(15)
C20-N2-C21	121.93(15)	C17-N2-C21	130.00(15)
C1-C2-H2A	109.5	C1-C2-H2B	109.5
H2A-C2-H2B	109.5	C1-C2-H2C	109.5
H2A-C2-H2C	109.5	H2B-C2-H2C	109.5
C1-C3-H3A	109.5	C1-C3-H3B	109.5
H3A-C3-H3B	109.5	C1-C3-H3C	109.5
H3A-C3-H3C	109.5	H3B-C3-H3C	109.5
C5-C4-C6	110.11(15)	C5-C4-Si1	114.34(13)
C6-C4-Si1	112.65(12)	C5-C4-H4A	106.4
C6-C4-H4A	106.4	Si1-C4-H4A	106.4
C4-C5-H5A	109.5	C4-C5-H5B	109.5
H5A-C5-H5B	109.5	C4-C5-H5C	109.5
H5A-C5-H5C	109.5	H5B-C5-H5C	109.5
C4-C6-H6A	109.5	C4-C6-H6B	109.5
H6A-C6-H6B	109.5	C4-C6-H6C	109.5
H6A-C6-H6C	109.5	H6B-C6-H6C	109.5
C9-C7-C8	113.02(18)	C9-C7-Si1	113.46(15)
C8-C7-Si1	114.58(13)	C9-C7-H7A	104.8
C8-C7-H7A	104.8	Si1-C7-H7A	104.8

C7-C8-H8A	109.5	C7-C8-H8B	109.5
H8A-C8-H8B	109.5	C7-C8-H8C	109.5
H8A-C8-H8C	109.5	H8B-C8-H8C	109.5
C7-C9-H9A	109.5	C7-C9-H9B	109.5
H9A-C9-H9B	109.5	C7-C9-H9C	109.5
H9A-C9-H9C	109.5	H9B-C9-H9C	109.5
C11-C10-N1	110.33(17)	C11-C10-H10	125.1(14)
N1-C10-H10	124.4(14)	C10-C11-C12	107.20(16)
C10-C11-H11	129.3(16)	C12-C11-H11	123.5(17)
C13-C12-C11	107.75(17)	C13-C12-H12	125.3(13)
C11-C12-H12	126.9(13)	C12-C13-N1	108.53(15)
C12-C13-C14	128.83(17)	N1-C13-C14	122.64(15)
C15-C14-C13	126.13(16)	C15-C14-H14	116.6(12)
C13-C14-H14	117.2(12)	C14-C15-C23	124.17(16)
C14-C15-C16	119.82(16)	C23-C15-C16	115.88(15)
C17-C16-C15	110.02(14)	C17-C16-H16A	104.2(11)
C15-C16-H16A	112.6(11)	C17-C16-H16B	112.5(14)
C15-C16-H16B	116.1(14)	H16A-C16-H16B	100.5(17)
C18-C17-N2	107.41(15)	C18-C17-C16	128.28(16)
N2-C17-C16	123.91(15)	C17-C18-C19	108.51(17)
C17-C18-H18	126.3(15)	C19-C18-H18	124.9(15)
C20-C19-C18	107.80(17)	C20-C19-H19	125.5(15)
C18-C19-H19	126.6(15)	C19-C20-N2	108.25(17)
C19-C20-H20	131.8(14)	N2-C20-H20	119.9(14)
O1-C21-N2	119.36(16)	O1-C21-C22	123.24(17)
N2-C21-C22	117.39(15)	C24-C22-C21	110.65(15)
C24-C22-C23	109.58(14)	C21-C22-C23	112.66(15)
C24-C22-H22	110.2(11)	C21-C22-H22	106.1(12)
C23-C22-H22	107.5(12)	C15-C23-C22	115.55(14)
C15-C23-H23A	109.3(12)	C22-C23-H23A	106.1(12)
C15-C23-H23B	110.0(13)	C22-C23-H23B	109.8(13)
H23A-C23-H23B	105.5(16)	C22-C24-H24A	109.5
C22-C24-H24B	109.5	H24A-C24-H24B	109.5
C22-C24-H24C	109.5	H24A-C24-H24C	109.5
H24B-C24-H24C	109.5		

Table 10. Anisotropic atomic displacement parameters (\AA^2) for **89**

The anisotropic atomic displacement factor exponent takes the form: $-2\pi^2 [h^2 a^{*2} U_{11} + \dots + 2 h k a^* b^* U_{12}]$

U_{11}	U_{22}	U_{33}	U_{23}	U_{13}	U_{12}	
Si1	0.0165(3)	0.0150(3)	0.0192(3)	0.0037(2)	0.0039(2)	0.0045(2)
O1	0.0158(7)	0.0358(8)	0.0295(7)	0.0043(6)	0.0013(5)	0.0082(6)
C1	0.0188(9)	0.0210(9)	0.0223(9)	0.0056(7)	0.0052(7)	0.0080(7)
N1	0.0172(7)	0.0175(7)	0.0228(8)	0.0049(6)	0.0045(6)	0.0058(6)
N2	0.0162(7)	0.0200(7)	0.0172(7)	0.0025(6)	0.0015(6)	0.0042(6)
C2	0.0190(9)	0.0413(11)	0.0270(10)	0.0085(9)	0.0026(7)	0.0109(8)
C3	0.0191(9)	0.0249(10)	0.0424(12)	0.0118(9)	0.0066(8)	0.0043(7)
C4	0.0196(9)	0.0190(8)	0.0200(9)	0.0037(7)	0.0019(7)	0.0046(7)
C5	0.0194(10)	0.0295(10)	0.0309(11)	0.0101(9)	-0.0011(8)	0.0033(8)
C6	0.0324(11)	0.0324(10)	0.0215(10)	0.0062(8)	0.0044(8)	0.0102(9)
C7	0.0316(11)	0.0207(9)	0.0412(12)	0.0101(9)	0.0171(9)	0.0088(8)
C8	0.0246(10)	0.0219(9)	0.0272(10)	0.0072(8)	0.0058(8)	0.0009(7)
C9	0.0479(14)	0.0277(11)	0.0569(15)	0.0069(11)	0.0166(12)	0.0097(10)
C10	0.0223(9)	0.0183(9)	0.0252(10)	0.0081(8)	0.0053(7)	0.0065(7)
C11	0.0214(9)	0.0160(9)	0.0326(11)	0.0051(8)	0.0049(7)	0.0069(7)
C12	0.0159(9)	0.0195(8)	0.0244(10)	0.0015(7)	0.0040(7)	0.0046(7)
C13	0.0128(8)	0.0184(8)	0.0190(8)	0.0016(7)	0.0023(6)	0.0033(6)
C14	0.0147(8)	0.0185(8)	0.0205(9)	0.0013(7)	0.0015(7)	0.0069(7)
C15	0.0135(8)	0.0170(8)	0.0169(8)	0.0000(7)	-0.0017(6)	0.0043(6)
C16	0.0153(9)	0.0218(9)	0.0197(9)	0.0047(7)	0.0025(7)	0.0081(7)
C17	0.0177(9)	0.0197(8)	0.0196(9)	0.0074(7)	0.0045(7)	0.0067(7)
C18	0.0292(10)	0.0225(9)	0.0232(10)	0.0072(8)	0.0089(8)	0.0120(8)
C19	0.0373(11)	0.0173(9)	0.0241(10)	0.0025(8)	0.0074(8)	0.0073(8)
C20	0.0236(10)	0.0203(9)	0.0205(9)	0.0033(7)	0.0016(7)	0.0006(7)
C21	0.0175(9)	0.0231(9)	0.0191(9)	0.0062(7)	0.0045(7)	0.0062(7)
C22	0.0168(9)	0.0228(9)	0.0179(9)	0.0041(7)	0.0029(7)	0.0083(7)
C23	0.0168(9)	0.0189(9)	0.0183(9)	0.0038(7)	0.0021(7)	0.0065(7)
C24	0.0217(9)	0.0264(9)	0.0262(10)	0.0071(8)	0.0091(7)	0.0121(8)

Table 11. Hydrogen atomic coordinates and isotropic atomic displacement parameters (\AA^2) for **89**

	x/a	y/b	z/c	U(eq)
H1A	-0.2368	0.2363	0.8992	0.024
H2A	-0.4679	0.1447	0.7571	0.044
H2B	-0.3109	0.1006	0.7110	0.044
H2C	-0.2757	0.2528	0.7471	0.044
H3A	-0.4511	0.0158	0.8687	0.044
H3B	-0.2486	0.0398	0.9376	0.044
H3C	-0.2890	-0.0342	0.8320	0.044
H4A	0.1017	0.0955	0.9782	0.025
H5A	0.4308	0.2090	1.0593	0.043
H5B	0.4515	0.3115	0.9975	0.043
H5C	0.4158	0.1615	0.9519	0.043
H6A	0.1696	0.2558	1.1171	0.044
H6B	-0.0331	0.2379	1.0509	0.044
H6C	0.1585	0.3615	1.0605	0.044
H7A	0.0957	0.3673	0.7803	0.036
H8A	0.4333	0.4924	0.8249	0.039
H8B	0.3916	0.3400	0.7847	0.039
H8C	0.4632	0.4035	0.8930	0.039
H9A	0.2009	0.5655	0.8910	0.068
H9B	0.1929	0.4878	0.9692	0.068
H9C	-0.0039	0.4658	0.8968	0.068
H10	0.099(3)	-0.049(2)	0.8499(15)	0.021(5)
H11	0.134(4)	-0.188(3)	0.7145(18)	0.045(7)
H12	0.112(3)	-0.075(2)	0.5890(16)	0.023(5)
H14	-0.013(3)	0.2203(18)	0.6587(13)	0.012(4)
H16A	0.029(3)	0.3483(19)	0.5541(13)	0.017(5)
H16B	0.132(3)	0.320(2)	0.4796(16)	0.029(6)
H18	0.182(4)	0.584(2)	0.6508(16)	0.034(6)
H19	0.527(3)	0.735(2)	0.7340(17)	0.034(6)
H20	0.760(4)	0.619(2)	0.6954(16)	0.036(6)
H22	0.409(3)	0.284(2)	0.4637(14)	0.017(5)
H23A	0.250(3)	0.0863(19)	0.4972(14)	0.013(5)
H23B	0.376(3)	0.130(2)	0.5943(15)	0.020(5)
H24A	0.7052	0.2416	0.4541	0.035
H24B	0.5215	0.1074	0.4243	0.035
H24C	0.6646	0.1511	0.5239	0.035

APPENDIX B

X-RAY CRYSTAL DATA FOR RAC-(3S, 4R)-1-BENZYL-3-METHYL-4-PHENYL-1-ANONIABICYCLO[3.1.0]HEXANE HEXAFLUOROANTIMONATE (V) 194

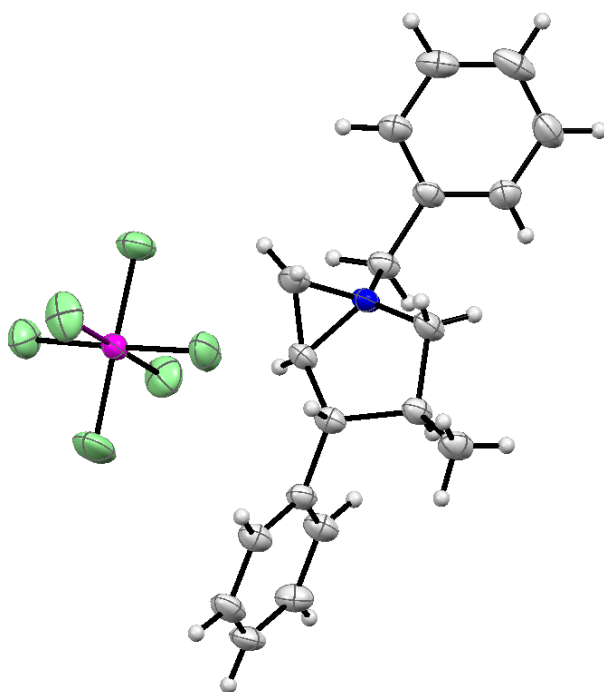


Figure 15. X-ray crystal structure of **194**

ORTEP structure of *rac*-(3S,4R)-1-benzyl-3-methyl-4-phenyl-1-azoniabicyclo[3.1.0]hexane hexafluoroantimonate (V). The molecular structure is drawn with 50% probability displacement ellipsoids; hydrogen atoms are drawn with an artificial radius.

Table 12. Crystallographic Information for Compound **194**

Identification code	perez2
Chemical formula	C ₁₉ H ₂₂ F ₆ NSb
Formula weight	500.12
Temperature	150(2) K
Wavelength	1.54178 Å
Crystal size	0.020 x 0.080 x 0.180 mm
Crystal habit	translucent colourless plate
Crystal system	triclinic
Space group	P -1
Unit cell dimensions	a = 10.3372(2) Å α = 62.3680(7)° b = 10.4889(2) Å β = 78.1060(7)° c = 10.5185(2) Å γ = 81.1370(8)°
Volume	986.45(3) Å ³
Z	2
Density (calculated)	1.684 g/cm ³
Absorption coefficient	11.634 mm ⁻¹
F(000)	496
Diffractometer	Bruker Apex II CCD
Radiation source	IMuS micro-focus, Cu
Theta range for data collection	4.38 to 68.23°
Index ranges	-12<=h<=12, -12<=k<=11, -12<=l<=12
Reflections collected	18064
Independent reflections	3519 [R(int) = 0.0208]
Coverage of independent reflections	97.3%
Absorption correction	multi-scan
Max. and min. transmission	0.8010 and 0.2290
Refinement method	Full-matrix least-squares on F ²
Refinement program	SHELXL-2013 (Sheldrick, 2013)
Function minimized	Σ w(F _o ² - F _c ²) ²
Data / restraints / parameters	3519 / 0 / 332
Goodness-of-fit on F ²	0.828
Δ/σ _{max}	0.002
Final R indices	3438 data; R1 = 0.0185, wR2 = I > 2σ(I) 0.0588 all data R1 = 0.0189, wR2 =

	0.0596
Weighting scheme	$w=1/[\sigma^2(F_o^2)+(0.0680P)^2]$ where $P=(F_o^2+2F_c^2)/3$
Largest diff. peak and hole	0.772 and -0.331 eÅ ⁻³
R.M.S. deviation from mean	0.057 eÅ ⁻³

Table 13. Atomic coordinates and equivalent isotropic displacement parameters (Å²) for **194**

	x/a	y/b	z/c	U(eq)
Sb1	0.76125(2)	0.74101(2)	0.54529(2)	0.02610(7)
F1	0.87160(16)	0.87272(19)	0.5333(2)	0.0559(4)
N1	0.72392(16)	0.31645(18)	0.38418(17)	0.0266(3)
C1	0.7429(3)	0.4648(2)	0.3614(2)	0.0383(5)
F2	0.81830(16)	0.78801(18)	0.34871(15)	0.0472(3)
C2	0.6479(2)	0.3751(2)	0.4864(2)	0.0298(4)
F3	0.62455(15)	0.88699(17)	0.49326(18)	0.0480(3)
C3	0.6930(2)	0.2843(2)	0.6344(2)	0.0280(4)
F4	0.64894(16)	0.61089(17)	0.55656(19)	0.0511(4)
C4	0.75965(19)	0.1454(2)	0.6243(2)	0.0280(4)
F5	0.70185(19)	0.6912(2)	0.74115(17)	0.0599(4)
C5	0.8210(2)	0.1989(3)	0.4649(2)	0.0321(5)
F6	0.89949(16)	0.59694(17)	0.59171(17)	0.0495(4)
C6	0.8590(2)	0.0652(3)	0.7289(2)	0.0365(4)
C7	0.5856(2)	0.3127(2)	0.8579(2)	0.0325(4)
C8	0.4827(2)	0.2912(3)	0.9732(2)	0.0366(5)
C9	0.3766(2)	0.2152(2)	0.9931(2)	0.0364(4)
C10	0.3714(2)	0.1608(2)	0.8964(2)	0.0365(4)
C11	0.4739(2)	0.1831(2)	0.7805(2)	0.0336(4)
C12	0.58089(18)	0.2589(2)	0.76029(19)	0.0282(4)
C13	0.65653(19)	0.2998(2)	0.2808(2)	0.0303(4)
C14	0.7907(2)	0.1563(2)	0.1585(2)	0.0347(4)
C15	0.8851(2)	0.1435(3)	0.0498(3)	0.0411(5)
C16	0.9458(2)	0.2646(3)	0.9397(3)	0.0454(6)
C17	0.9100(2)	0.3973(3)	0.9393(2)	0.0424(5)
C18	0.8150(2)	0.4099(2)	0.0480(2)	0.0351(4)
C19	0.75597(18)	0.2890(2)	0.15932(19)	0.0280(4)

Table 14. Bond lengths [Å] and angles [°] for **194**

Sb1-F5	1.8637(15)
Sb1-F6	1.8712(14)
Sb1-F2	1.8728(14)
N1-C13	1.492(2)
N1-C1	1.499(3)
C1-C2	1.477(3)
C1-H1A	0.99(3)
C2-H2	0.93(2)
C3-C4	1.553(3)
C4-C6	1.521(3)
C4-H4	0.93(2)
C5-H5B	1.02(3)
C6-H6B	0.91(3)
C7-C8	1.393(3)
C7-H7	0.98(2)
C8-H8	0.95(3)
C9-H9	0.95(2)
C10-H10	0.99(3)
C11-H11	0.98(3)
C13-H13A	0.93(2)
C14-C19	1.387(3)
C14-H14	0.85(3)
C15-H15	0.94(3)
C16-H16	0.93(3)
C17-H17	0.95(3)
C18-H18	0.94(3)
Sb1-F1	1.8683(15)
Sb1-F4	1.8725(14)
Sb1-F3	1.8750(14)
N1-C5	1.499(3)
N1-C2	1.506(2)
C1-H1B	0.92(3)
C2-C3	1.528(3)
C3-C12	1.518(3)
C3-H3	0.92(2)

C4-C5	1.525(3)
C5-H5A	0.92(3)
C6-H6A	0.96(3)
C6-H6C	0.97(3)
C7-C12	1.393(3)
C8-C9	1.379(3)
C9-C10	1.391(3)
C10-C11	1.394(3)
C11-C12	1.385(3)
C13-C19	1.503(3)
C13-H13B	1.00(2)
C14-C15	1.385(3)
C15-C16	1.389(4)
C16-C17	1.381(4)
C17-C18	1.389(3)
C18-C19	1.385(3)
F5-Sb1-F1	90.87(9)
F1-Sb1-F6	90.03(8)
F1-Sb1-F4	179.27(5)
F5-Sb1-F2	178.66(6)
F6-Sb1-F2	88.85(7)
F5-Sb1-F3	90.42(8)
F6-Sb1-F3	178.40(5)
F2-Sb1-F3	89.56(7)
C13-N1-C1	119.34(16)
C13-N1-C2	120.78(16)
C1-N1-C2	58.92(13)
C2-C1-H1B	118.8(16)
C2-C1-H1A	118.5(15)
H1B-C1-H1A	116.(2)
C1-C2-C3	119.52(19)
C1-C2-H2	118.0(13)
C3-C2-H2	120.5(14)
C12-C3-C4	114.77(17)
C12-C3-H3	109.6(15)
C4-C3-H3	110.9(15)
C6-C4-C3	113.13(17)
C6-C4-H4	112.2(15)

C3-C4-H4	106.2(14)
N1-C5-H5A	109.4(17)
N1-C5-H5B	106.8(15)
H5A-C5-H5B	114.(2)
C4-C6-H6B	110.4(18)
C4-C6-H6C	111.3(15)
H6B-C6-H6C	107.(2)
C8-C7-H7	120.3(14)
C9-C8-C7	120.67(19)
C7-C8-H8	116.2(16)
C8-C9-H9	122.6(13)
C9-C10-C11	119.61(19)
C11-C10-H10	118.2(15)
C12-C11-H11	120.1(14)
C11-C12-C7	119.19(17)
C7-C12-C3	119.42(17)
N1-C13-H13A	104.6(15)
N1-C13-H13B	103.8(13)
H13A-C13-H13B	108.(2)
C19-C14-H14	119.(2)
C14-C15-C16	120.0(2)
C16-C15-H15	119.5(16)
C17-C16-H16	120.6(18)
C16-C17-C18	120.6(2)
C18-C17-H17	115.8(18)
C19-C18-H18	120.6(18)
C14-C19-C18	119.10(18)
C18-C19-C13	120.95(18)
F5-Sb1-F6	91.18(7)
F5-Sb1-F4	89.15(8)
F6-Sb1-F4	90.70(8)
F1-Sb1-F2	90.47(8)
F4-Sb1-F2	89.51(8)
F1-Sb1-F3	89.86(7)
F4-Sb1-F3	89.41(7)
C13-N1-C5	119.34(16)
C5-N1-C1	116.07(17)
C5-N1-C2	107.47(15)

C2-C1-N1	60.78(13)
N1-C1-H1B	114.9(15)
N1-C1-H1A	115.9(15)
C1-C2-N1	60.30(13)
N1-C2-C3	107.75(17)
N1-C2-H2	112.6(14)
C12-C3-C2	112.96(17)
C2-C3-C4	103.24(16)
C2-C3-H3	104.8(14)
C6-C4-C5	113.60(16)
C5-C4-C3	103.85(16)
C5-C4-H4	107.2(14)
N1-C5-C4	104.42(15)
C4-C5-H5A	112.4(17)
C4-C5-H5B	109.6(15)
C4-C6-H6A	113.2(16)
H6A-C6-H6B	110.(2)
H6A-C6-H6C	105.(2)
C8-C7-C12	119.92(19)
C12-C7-H7	119.8(14)
C9-C8-H8	123.1(16)
C8-C9-C10	119.76(18)
C10-C9-H9	117.6(13)
C9-C10-H10	122.2(15)
C12-C11-C10	120.85(18)
C10-C11-H11	119.0(14)
C11-C12-C3	121.40(17)
N1-C13-C19	110.67(15)
C19-C13-H13A	113.9(15)
C19-C13-H13B	114.8(13)
C19-C14-C15	120.8(2)
C15-C14-H14	120.(2)
C14-C15-H15	120.4(16)
C17-C16-C15	119.4(2)
C15-C16-H16	120.0(18)
C16-C17-H17	123.6(18)
C19-C18-C17	120.2(2)
C17-C18-H18	119.1(18)

Table 15. Anisotropic atomic displacement parameters (\AA^2) for **194**

The anisotropic atomic displacement factor exponent takes the form: $-2\pi^2 [h^2 a^{*2} U_{11} + \dots + 2 h k a^* b^* U_{12}]$

	U_{11}	U_{22}	U_{33}	U_{23}	U_{13}	U_{12}
Sb1	0.02633(10)	0.02878(10)	0.02405(10)	-0.01374(7)	-0.00199(6)	-0.00028(6)
F1	0.0438(8)	0.0568(10)	0.0858(12)	-0.0444(9)	-0.0128(8)	-0.0095(7)
N1	0.0277(8)	0.0315(8)	0.0191(7)	-0.0122(6)	-0.0004(6)	0.0007(6)
C1	0.0551(13)	0.0333(11)	0.0247(10)	-0.0139(9)	0.0031(9)	-0.0075(9)
F2	0.0513(9)	0.0566(9)	0.0267(6)	-0.0166(6)	0.0005(6)	0.0004(7)
C2	0.0335(11)	0.0323(10)	0.0245(9)	-0.0165(8)	0.0006(8)	0.0013(7)
F3	0.0364(7)	0.0456(8)	0.0552(9)	-0.0209(7)	-0.0064(6)	0.0103(6)
C3	0.0281(10)	0.0336(11)	0.0235(10)	-0.0146(8)	-0.0008(8)	-0.0037(8)
F4	0.0523(9)	0.0443(8)	0.0629(10)	-0.0271(7)	-0.0038(7)	-0.0169(7)
C4	0.0275(9)	0.0338(10)	0.0227(9)	-0.0135(8)	-0.0033(7)	-0.0002(8)
F5	0.0738(11)	0.0751(12)	0.0289(7)	-0.0284(7)	-0.0001(7)	0.0073(9)
C5	0.0292(11)	0.0427(13)	0.0254(11)	-0.0183(9)	-0.0060(8)	0.0076(9)
F6	0.0507(8)	0.0482(9)	0.0458(8)	-0.0222(7)	-0.0140(7)	0.0205(7)
C6	0.0352(11)	0.0455(13)	0.0251(11)	-0.0134(9)	-0.0082(8)	0.0042(9)
C7	0.0317(10)	0.0405(12)	0.0269(10)	-0.0166(8)	-0.0035(8)	-0.0031(8)
C8	0.0414(12)	0.0485(13)	0.0238(10)	-0.0212(9)	-0.0037(8)	0.0012(9)
C9	0.0332(10)	0.0474(12)	0.0215(9)	-0.0131(8)	0.0042(8)	-0.0014(8)
C10	0.0339(10)	0.0456(12)	0.0269(10)	-0.0136(8)	0.0005(8)	-0.0095(9)
C11	0.0341(10)	0.0426(11)	0.0261(9)	-0.0175(8)	-0.0021(8)	-0.0039(8)
C12	0.0297(9)	0.0324(10)	0.0201(8)	-0.0108(7)	-0.0031(7)	0.0004(7)
C13	0.0287(9)	0.0385(11)	0.0228(9)	-0.0137(8)	-0.0048(8)	0.0012(8)
C14	0.0414(11)	0.0346(11)	0.0258(9)	-0.0117(8)	-0.0075(8)	0.0016(8)
C15	0.0445(12)	0.0478(14)	0.0368(11)	-0.0266(10)	-0.0102(9)	0.0117(10)
C16	0.0337(11)	0.0763(18)	0.0315(11)	-0.0321(11)	-0.0011(9)	0.0032(11)
C17	0.0412(12)	0.0568(14)	0.0255(10)	-0.0155(9)	0.0017(9)	-0.0118(10)
C18	0.0417(11)	0.0391(12)	0.0243(9)	-0.0147(8)	-0.0037(8)	-0.0022(8)
C19	0.0279(9)	0.0372(10)	0.0198(8)	-0.0137(7)	-0.0069(7)	0.0025(7)

Table 16. Hydrogen atomic coordinates and isotropic atomic displacement parameters (\AA^2) for **194**

x/a	y/b	z/c	U(eq)	
H1B	0.711(2)	0.539(3)	0.282(3)	0.036(6)
H1A	0.829(3)	0.478(3)	0.380(3)	0.042(7)
H2	0.558(2)	0.394(2)	0.479(2)	0.025(5)
H3	0.755(2)	0.337(2)	0.637(2)	0.025(5)
H4	0.691(2)	0.089(3)	0.641(2)	0.030(5)
H5A	0.831(3)	0.128(3)	0.435(3)	0.033(7)
H5B	0.906(3)	0.246(3)	0.446(3)	0.041(6)
H6A	0.934(3)	0.119(3)	0.709(3)	0.043(7)
H6B	0.887(3)	-0.021(3)	0.729(3)	0.049(7)
H6C	0.819(2)	0.045(3)	0.828(3)	0.037(6)
H7	0.662(2)	0.366(2)	0.845(3)	0.031(6)
H8	0.491(3)	0.331(3)	1.036(3)	0.044(7)
H9	0.303(2)	0.202(2)	1.068(2)	0.031(5)
H10	0.297(3)	0.106(3)	0.907(3)	0.038(6)
H11	0.470(2)	0.144(3)	0.713(3)	0.035(6)
H13A	0.610(2)	0.218(3)	0.338(3)	0.034(6)
H13B	0.592(2)	0.385(2)	0.250(2)	0.026(5)
H14	0.756(3)	0.082(3)	0.228(3)	0.060(9)
H15	0.906(3)	0.054(3)	0.048(3)	0.046(7)
H16	1.007(3)	0.257(3)	-0.135(3)	0.056(8)
H17	0.946(3)	0.484(3)	-0.134(3)	0.052(7)
H18	0.793(3)	0.501(3)	0.046(3)	0.053(8)

BIBLIOGRAPHY

1. Zotchev, S. B., "Marine Actinomycetes as an Emerging Resource for the Drug Development Pipelines," *J. Biotech.* **2012**, *158*, 168-175.
2. Fenical, W.; Jensen, P., "Developing a New Resource for Drug Discovery: Marine Actinomycete Bacteria," *Nat. Chem. Biol.* **2006**, *2*, 666-673.
3. Kwon, H. C.; Kauffman, C. A.; Jensen, P. R.; Fenical, W., "Marinomycins A–D, Antitumor-Antibiotics of a New Structure Class from a Marine Actinomycete of the Recently Discovered Genus *Marinispora*," *J. Am. Chem. Soc.* **2006**, *128*, 1622-1632.
4. Pathirana, C.; Jensen, P. R.; Fenical, W., "Marinone and Debromomarinone: Antibiotic Sesquiterpenoid Naphthoquinones of a New Structure Class from a Marine Bacterium," *Tetrahedron Lett.* **1992**, *33*, 7663-7666.
5. Williams, P. G.; Buchanan, G. O.; Feling, R. H.; Kauffman, C. A.; Jensen, P. R.; Fenical, W., "New Cytotoxic Salinosporamides from the Marine Actinomycete *Salinispora Tropicana*," *J. Org. Chem.* **2005**, *70*, 6196-6203.
6. Boonlarpgradab, C.; Kauffman, C. A.; Jensen, P. R.; Fenical, W., "Marineosins A and B, Cytotoxic Spiroaminals from a Marine-Derived Actinomycete," *Org. Lett.* **2008**, *10*, 5505-5508.
7. Furstner, A., "Chemistry and Biology of Roseophilin and the Prodigiosin Alkaloids: A Survey of the Last 2500 Years," *Angew. Chem. Int. Ed.* **2003**, *42*, 3582-3603.
8. Aldrich, L. N.; Dawson, E. S.; Lindsley, C. W., "Evaluation of the Biosynthetic Proposal for the Synthesis of Marineosins A and B," *Org. Lett.* **2010**, *12*, 1048-1051.
9. Cai, X.-C.; Wu, X.; Snider, B. B., "Synthesis of the Spiroimino Moiety of Marineosins A and B," *Org. Lett.* **2010**, *12*, 1600-1603.
10. Mo, S.; Sydor, P. K.; Corre, C.; Alhamadsheh, M. M.; Stanley, A. E.; Haynes, Stuart W.; Song, L.; Reynolds, K. A.; Challis, G. L., "Elucidation of the *Streptomyces Coelicolor* Pathway to 2-Undecylpyrrole, a Key Intermediate in Undecylprodiginine and Streptorubin B Biosynthesis," *Chem. Bio.* **2008**, *15*, 137-148.

11. Panarese, J. D.; Konkol, L. C.; Berry, C. B.; Bates, B. S.; Aldrich, L. N.; Lindsley, C. W., "Spiroaminal Model Systems of the Marineosins with Final Step Pyrrole Incorporation," *Tetrahedron Lett.* **2013**, *54*, 2231-2234.
12. Aldrich, L. N.; Berry, C. B.; Bates, B. S.; Konkol, L. C.; So, M.; Lindsley, C. W., "Towards the Total Synthesis of Marineosin A: Construction of the Macrocyclic Pyrrole and an Advanced, Functionalized Spiroaminal Model," *Eur. J. Org. Chem.* **2013**, *2013*, 4215-4218.
13. Li, G.; Zhang, X.; Li, Q.; Feng, P.; Shi, Y., "A Concise Approach to the Spiroaminal Fragment of Marineosins," *Org. Biomol. Chem.* **2013**, *11*, 2936-2938.
14. Pinkerton, D. M.; Banwell, M. G.; Willis, A. C., "Total Syntheses of Tambjamines C, E, F, G, H, I and J, BE-18591, and a Related Alkaloid from the Marine Bacterium *Pseudoalteromonas Tunicata*," *Org. Lett.* **2007**, *9*, 5127-5130.
15. Daïri, K.; Yao, Y.; Faley, M.; Tripathy, S.; Rioux, E.; Billot, X.; Rabouin, D.; Gonzalez, G.; Lavallée, J.-F.; Attardo, G., "A Scalable Process for the Synthesis of the Bcl Inhibitor Obatoclox," *Org. Process Res. Dev.* **2007**, *11*, 1051-1054.
16. Greenhouse, R.; Ramirez, C.; Muchowski, J. M., "Synthesis of Alkylpyrroles by the Sodium Borohydride Reduction of Acylpyrroles," *J. Org. Chem.* **1985**, *50*, 2961-2965.
17. Geherty, M. E. Catalytic Asymmetric Claisen Rearrangements. The Development of Ru(II)-Catalyzed Formal [3,3] Sigmatropic Rearrangements and Related Enolate Allylation Reactions. Ph.D. Thesis [Online], University of Pittsburgh, Pittsburgh, PA, December 2012. d-scholarship.pitt.edu/16662/ (accessed Dec 28, 2014).
18. Davenport, A. J.; Davies, D. L.; Fawcett, J.; Russell, D. R., "Chiral Pyridylimidazolines: Synthesis, Arene Ruthenium Complexes and Application in Asymmetric Catalysis," *J. Chem. Soc. Perk. T 1* **2001**, 1500-1503.
19. Muchowski, J. M.; Hess, P., "Lithiation of the 6-Dimethylamino-1-Azafulvene Dimer. A Versatile Synthesis of 5-Substituted Pyrrole-2 Carboxaldehydes," *Tetrahedron Lett.* **1988**, *29*, 777-780.
20. Kawai, T.; Komaki, M.; Iyoda, T., "Cross-Metathesis of Vinyl Aromatic Heterocycles with 1-Octene in the Presence of a Schrock Catalyst," *J. Mol. Catal. A - Chemical* **2002**, *190*, 45-53.
21. Hoye, T. R.; Jeffrey, C. S.; Tennakoon, M. A.; Wang, J.; Zhao, H., "Relay Ring-Closing Metathesis (RRCM): A Strategy for Directing Metal Movement throughout Olefin Metathesis Sequences," *J. Am. Chem. Soc.* **2004**, *126*, 10210-10211.
22. Clark, J. R.; French, J. M.; Jecs, E.; Diver, S. T., "Geminal Alkene-Alkyne Cross Metathesis Using a Relay Strategy," *Org. Lett.* **2012**, *14*, 4178-4181.

23. Donohoe, T. J.; Bower, J. F., "An Expedient Route to Substituted Furans via Olefin Cross-Metathesis,"*Proc. Natl. Acad. Sci. U.S.A.* **2010**, *107*, 3373-3376.
24. Johnson, D. K.; Donohoe, J.; Kang, J., "Dilithium Tetrachlorocuprate Catalyzed Coupling of Allylmagnesium Bromide with α,ω -Dihaloalkanes,"*Synthetic Commun.* **1994**, *24*, 1557-1564.
25. Ghosh, S.; Ghosh, S.; Sarkar, N., "Factors Influencing Ring Closure through Olefin Metathesis – A Perspective,"*J. Chem. Sci.* **2006**, *118*, 223-235.
26. Spandl, R. J.; Thomas, G.; Diaz-Gavilan, M.; O'Connell, K. M. G.; Spring, D. R., Wiley: Ann Arbor, 2009; p 677.
27. Schreiber, S. L., "Target-Oriented and Diversity-Oriented Organic Synthesis in Drug Discovery,"*Science* **2000**, *287*, 1964-1969.
28. Spandl, R. J.; Bender, A.; Spring, D. R., "Diversity-Oriented Synthesis; A Spectrum of Approaches and Results,"*Org. Biomol. Chem.* **2008**, *6*, 1149-1158.
29. Thomas, G.; Wyatt, E.; Spring, D., "Enriching Chemical Space with Diversity-Oriented Synthesis,"*Curr. Opin. Drug Discov. Devel.* **2006**, *9*, 700 - 712.
30. Ding, K.; Lu, Y.; Nikolovska-Coleska, Z.; Qiu, S.; Ding, Y.; Gao, W.; Stuckey, J.; Krajewski, K.; Roller, P. P.; Tomita, Y.; Parrish, D. A.; Deschamps, J. R.; Wang, S., "Structure-Based Design of Potent Non-Peptide MDM2 Inhibitors,"*J. Am. Chem. Soc.* **2005**, *127*, 10130-10131.
31. Kobayashi, H.; Shin-ya, K.; Furihata, K.; Hayakawa, Y.; Seto, H., "Absolute Configuration of a Novel Glutamate Receptor Antagonist Kaitocephalin,"*Tetrahedron Lett.* **2001**, *42*, 4021-4023.
32. Burton, G.; Ku, T. W.; Carr, T. J.; Kiesow, T.; Sarisky, R. T.; Lin-Goerke, J.; Baker, A.; Earnshaw, D. L.; Hofmann, G. A.; Keenan, R. M.; Dhanak, D., "Identification of Small Molecule Inhibitors of the Hepatitis C Virus RNA-Dependent RNA Polymerase from a Pyrrolidine Combinatorial Mixture,"*Bioorg. Med. Chem. Lett.* **2005**, *15*, 1553-1556.
33. Kati, W. M.; Montgomery, D.; Carrick, R.; Gubareva, L.; Maring, C.; McDaniel, K.; Steffy, K.; Molla, A.; Hayden, F.; Kempf, D.; Kohlbrenner, W., "In Vitro Characterization of A-315675, a Highly Potent Inhibitor of A and B Strain Influenza Virus Neuraminidases and Influenza Virus Replication,"*Antimicrob. Agents Chemother.* **2002**, *46*, 1014-1021.
34. Scott, J. D.; Williams, R. M., "Chemistry and Biology of the Tetrahydroisoquinoline Antitumor Antibiotics,"*Chem. Rev.* **2002**, *102*, 1669-1730.

35. Gothelf, A. S.; Gothelf, K. V.; Hazell, R. G.; Jørgensen, K. A., "Catalytic Asymmetric 1,3-Dipolar Cycloaddition Reactions of Azomethine Ylides—A Simple Approach to Optically Active Highly Functionalized Proline Derivatives," *Angew. Chem. Int. Ed.* **2002**, *41*, 4236-4238.
36. (a) Gothelf, K. V.; Jørgensen, K. A., "Asymmetric 1,3-Dipolar Cycloaddition Reactions," *Chem. Rev.* **1998**, *98*, 863-910; (b) Kumar, A.; Gupta, G.; Srivastava, S., "Diversity-Oriented Synthesis of Pyrrolidines via Natural Carbohydrate Solid Acid Catalyst," *J. Comb. Chem.* **2010**, *12*, 458-462; (c) Grigg, R.; Gunaratne, H. Q. N.; Sridharan, V., "X=Y-ZH Systems as Potential 1,3-Dipoles : Part 14. Bronsted and Lewis Acid Catalysis of Cycloadditions of Arylidene Imines of α -Amino Acid Esters," *Tetrahedron* **1987**, *43*, 5887-5898; (d) Li, G.-Y.; Chen, J.; Yu, W.-Y.; Hong, W.; Che, C. M., "Stereoselective Synthesis of Functionalized Pyrrolidines by Ruthenium Porphyrin-Catalyzed Decomposition of α -Diazo Esters and Cascade Azomethine Ylide Formation/1,3-Dipolar Cycloaddition Reactions," *Org. Lett.* **2003**, *5*, 2153-2156; (e) Galliford, C. V.; Beenen, M. A.; Nguyen, S. T.; Scheidt, K. A., "Catalytic, Three-Component Assembly Reaction for the Synthesis of Pyrrolidines," *Org. Lett.* **2003**, *5*, 3487-3490; (f) Alemparte, C.; Blay, G.; Jørgensen, K. A., "A Convenient Procedure for the Catalytic Asymmetric 1,3-Dipolar Cycloaddition of Azomethine Ylides and Alkenes," *Org. Lett.* **2005**, *7*, 4569-4572; (g) Garner, P.; Kaniskan, H. Ü.; Hu, J.; Youngs, W. J.; Panzner, M., "Asymmetric Multicomponent [C+NC+CC] Synthesis of Highly Functionalized Pyrrolidines Catalyzed by Silver(I)," *Org. Lett.* **2006**, *8*, 3647-3650; (h) Annunziata, R.; Cinquini, M.; Cozzi, F.; Raimondi, L.; Pilati, T., "1,3-Dipolar Cycloaddition Reactions of Azomethine Ylides on Enantiomerically Pure (*E*)- $[\gamma]$ -Alkoxy- $[\alpha]$, $[\beta]$ -Unsaturated Esters," *Tetrahedron: Asymm.* **1991**, *2*, 1329-1342.
37. (a) Barr, D. A.; Dorrity, M. J.; Grigg, R.; Hargreaves, S.; Malone, J. F.; Montgomery, J.; Redpath, J.; Stevenson, P.; Thornton-Pett, M., "X=Y-ZH Compounds as Potential 1,3-Dipoles. Part 43. Metal Ion Catalyzed Asymmetric 1,3-Dipolar Cycloaddition Reactions of Imines and Methyl Acrylate," *Tetrahedron* **1995**, *51*, 273-294; (b) Galley, G.; Liebscher, J.; Paetzel, M., "Polyfunctionalized Pyrrolidines by Stereoselective 1,3-Dipolar Cycloaddition of Azomethine Ylides to Chiral Enones," *J. Org. Chem.* **1995**, *60*, 5005-5010; (c) Nyerges, M.; Rudas, M.; Tóth, G.; Herényi, B.; Kádas, I.; Bitter, I.; Töke, L., "Influence of Ag(I) and Li(I) Catalysts for 1,3-Dipolar Cycloaddition Reactions of Azomethine Ylides. Reversal of the Stereochemistry," *Tetrahedron* **1995**, *51*, 13321-13330; (d) Barr, D. A.; Grigg, R.; Gunaratne, H. Q. N.; Kemp, J.; McMeekin, P.; Sridharan, V., "X-Y-ZH Systems as Potential 1,3-Dipoles : Part 15. Amine Generated Azaallyl Anions versus Metallo-1,3-dipoles in Cycloadditions of $[\alpha]$ -Amino Acid Esters. Facile Regio- and Stereo-Specific Formation of Pyrrolidines," *Tetrahedron* **1988**, *44*, 557-570.
38. Allway, P.; Grigg, R., "Chiral Co(II) and Mn(II) catalysts for the 1,3-Dipolar Cycloaddition Reactions of Azomethine Ylides Derived from Arylidene Imines of Glycine," *Tetrahedron Lett.* **1991**, *32*, 5817-5820.
39. Grigg, R., "Asymmetric Cascade 1,3-Dipolar Cycloaddition Reactions of Imines," *Tetrahedron: Asymm.* **1995**, *6*, 2475-2486.
40. Longmire, J. M.; Wang, B.; Zhang, X., "Highly Enantioselective Ag(I)-Catalyzed [3 + 2] Cycloaddition of Azomethine Ylides," *J. Am. Chem. Soc.* **2002**, *124*, 13400-13401.

41. Longmire, J. M. W., B; Zhang, X., "Highly Efficient Kinetic Resolution of 2-Cyclohexenyl Acetate in Pd-Catalyzed Allylic Alkylation," *Tetrahedron Lett.* **2000**, *41*, 5435.
42. Chen, C.; Li, X.; Schreiber, S. L., "Catalytic Asymmetric [3+2] Cycloaddition of Azomethine Ylides. Development of a Versatile Stepwise, Three-Component Reaction for Diversity-Oriented Synthesis," *J. Am. Chem. Soc.* **2003**, *125*, 10174-10175.
43. Chuo, C.; Xiaodong, L.; Neumann, C. S.; M.-C Lo, M.; Schreiber, S. L., "Convergent Diversity-Oriented Synthesis of Small-Molecule Hybrids," *Angew. Chem. Int. Ed.* **2005**, *44*, 2249-2252.
44. Clemons, P.; Koehler, A.; Wagner, B.; Springings, T.; Spring, D.; King, R.; Schreiber, S.; Foley, M., "A One-Bead, One-Stock Solution Approach to Chemical Genetics: Part 2," *Chem. Bio.* **2001**, *8*, 1183-1195.
45. Gilchrest, B.; Eller, M.; Koehler, A.; McPherson, O.; Neumann, C.; Lewis, T. Therapeutic Methods using WRN Binding Molecules. U.S. Patent 2,008,027,990, August 29, 2007.
46. Nelson, S.; Bungard, C.; Wang, K., "Catalyzed Olefin Isomerization Leading to Highly Stereoselective Claisen Rearrangements of Aliphatic Allyl Vinyl Ethers," *J. Am. Chem. Soc.* **2003**, *125*, 13000-13001.
47. Geherty, M. E.; Dura, R. D.; Nelson, S. G., "Catalytic Asymmetric Claisen Rearrangement of Unactivated Allyl Vinyl Ethers," *J. Am. Chem. Soc.* **2010**, *132*, 11875-11877.
48. Metro, T.-X.; Duthion, B.; Gomez Pardo, D.; Cossy, J., "Rearrangement of β -Amino Alcohols via Aziridiniums: A Review," *Chem. Soc. Rev.* **2010**, *39*, 89-102.
49. Hammer, C. F.; Heller, S. R.; Craig, J. H., "Reactions of β -Substituted Amines—II: Nucleophilic Displacement Reactions on 3-Chloro-1-Ethylpiperidine," *Tetrahedron* **1972**, *28*, 239-253.
50. Verhelst, S. H. L.; Paez Martinez, B.; Timmer, M. S. M.; Lodder, G.; van der Marel, G. A.; Overkleeft, H. S.; van Boom, J. H., "A Short Route toward Chiral, Polyhydroxylated Indolizidines and Quinolizidines," *J. Org. Chem.* **2003**, *68*, 9598-9603.
51. Claisen, L., "Über Umlagerung von Phenol-Allylathern in C-Allyl Phenole," *Ber. Dtsch. Chem. Ges.* **1912**, *45*, 3157-3166.
52. Martín Castro, A. M., "Claisen Rearrangement Over the Past Nine Decades," *Chem. Rev.* **2004**, *104*, 2939-3002.
53. Bal, B. S.; Childers Jr, W. E.; Pinnick, H. W., "Oxidation of α,β -Unsaturated Aldehydes," *Tetrahedron* **1981**, *37*, 2091-2096.

54. Bannasar, M. L.; Zulaica, E.; Alonso, S., "Preparation of RCM Substrates for Azepinoindole Synthesis: Reductive Amination versus Tetrahydro- γ -Carboline Formation,"*Tetrahedron Lett.* **2005**, *46*, 7881-7884.
55. Shiro, Y.; Kato, K.; Fujii, M.; Ida, Y.; Akita, H., "First Synthesis of Polyoxin M,"*Tetrahedron* **2006**, *62*, 8687-8695.
56. Hu, X. E., "Nucleophilic Ring Opening of Aziridines,"*Tetrahedron* **2004**, *60*, 2701-2743.
57. Boga, C. F., Claudio; Savoia, Diego, "Stereoselective Synthesis of 3,6-Disubstituted 1,2-Diaminocyclohexanes through Ring-Closing Metathesis of 4,5-Diamino-1,7-Octadiene Derivatives,"*Synthesis* **2006**, *2*, 285-292.
58. Bray, B. L.; Mathies, P. H.; Naef, R.; Solas, D. R.; Tidwell, T. T.; Artis, D. R.; Muchowski, J. M., "N-(Triisopropylsilyl)pyrrole. A Progenitor "Par Excellence" of 3-Substituted Pyrroles,"*J. Org. Chem.* **1990**, *55*, 6317-6328.
59. Bannasar, M. L.; Zulaica, E.; Alonso, S., "Preparation of RCM Substrates for Azepinoindole Synthesis: Reductive Amination versus Tetrahydro-[γ]-Carboline Formation,"*Tetrahedron Lett.* **2005**, *46*, 7881-7884.
60. Davies, S. N., R; Price, P; Roberts, P; Russell, A; Savory, E.; Smith, A; Thomson, J., "Iodine-Mediated Ring-Closing Iodoamination with Concomitant N-debenzylation for the Asymmetric Synthesis of Polyhydroxylated Pyrrolidines,"*Tetrahedron: Asymm.* **2009**, *20*, 758-772.